

ESD RECORD COPY

RETURN TO
SCIENTIFIC & TECHNICAL INFORMATION DIVISION
(ESTI), BUILDING 1211

143

COPY NR. _____ OF _____ COPIES

HYPERSONIC AXISYMMETRIC WAKES INCLUDING EFFECTS OF RATE CHEMISTRY

GASL Report TR-180

by

M. H. Bloom and M. H. Steiger

ESTI PROCESSED

DDC TAB PROJ OFFICER

ACCESSION MASTER FILE

DATE _____

ESTI CONTROL NR. AL-40797



CY NR. 1 OF 1 CY#

September 12, 1960

Reissued September 18, 1962

*SD TR-180 (4-41) * 64-417
ARE Related to the same
W/STN 6/17/61*

The work reported in this document was performed at General Applied Science Laboratory, Inc. for M. I. T. Lincoln Laboratory under Subcontract No. 226; this work was supported by the U.S. Advanced Research Projects Agency under Air Force Contract AF 19(604)-4559.



Publication of this technical documentary report does not constitute Air Force approval of the report's findings or conclusions. It is published only for the exchange and stimulation of ideas.

Appendix C ----- Supplement and Errata Added.

HYPERSONIC AXISYMMETRIC
WAKES INCLUDING EFFECTS
OF RATE CHEMISTRY

TECHNICAL REPORT NO. 180

By M. H. Bloom and M. H. Steiger

SUBCONTRACT NO. 226

Prepared For

ed by: Antonio Ferri
Antonio Ferri
Technical Director

TABLE OF CONTENTS

<u>Section</u>	<u>Title</u>	<u>Page</u>
I	Introduction	1
II	Analysis	9
III	Calculations	34
	References	38
	Notations	40
	Appendix A	44
	Appendix B	48
	Table I	51
	Figures 1 through 16	52
	Supplement - 1/19/61	1 - 4
	Errata Sheet - 4/11/61	1

HYPERSONIC AXISYMMETRIC WAKES
INCLUDING EFFECTS OF RATE CHEMISTRY

by M.H. Bloom and M.H. Steiger

I INTRODUCTION

A wake is the flow field downstream of a body, and is characterized by disturbed properties which eventually return to ambient atmospheric conditions. Wake characteristics, such as velocity defects, may be generated by the boundary layer shed by the body under subsonic or supersonic conditions, or may be generated by the bow shock under supersonic conditions, or by the combined effects of boundary layer and shock. Evidently the relative importance of the boundary layer and shock, insofar as wake properties are concerned, depends on the body shape and flight conditions.

For blunt bodies at hypersonic speeds, boundary layer mixing and the disturbed pressure field are the dominant influences in the base region near the body and immediately downstream, say for distances up to the order of 10 body diameters. In the far field beyond this, the elevated pressures induced by the shock system of the body decay to the level of the ambient pressure, and the shock-induced disturbances which persist far downstream are the primary factors. The order of the distance in which the pressure downstream of a blunt axisymmetric nose reaches the ambient level may be

estimated from blast-theory¹, which yields roughly $x/D \approx 0.07M_{\infty}^2 / (p/p_{\infty} - 0.4)$, or for return to ambient pressure, $x/D \approx M_{\infty}^2 / 10$. Therefore, for Mach numbers on the order of 20, downstream positions beyond 40 or 50 body diameters, measured from the nose, may be considered to constitute the far field of the wake and may be treated as a uniform-pressure field. Changes in the remaining disturbed properties can be treated only by considering diffusive processes such as those of viscosity, thermal conductivity and mass diffusion. Moreover, under hypersonic conditions, it may be necessary to take into account the effects of chemical rate processes.

Basic discussions of constant-pressure viscous flows of wake or jet type are given, for example, by Schlichting (Reference 2) for constant-density, and Pai (References 3 and 4) for compressible flow. Some discussions or analyses with more direct bearing on hypersonic axisymmetric wakes are contained in the recent works of Feldman (Reference 5), Lew and Langeló (Reference 6), Ting and Libby (Reference 7), M. and R. Goulard (Reference 8) and Bloom and Steiger (Reference 9). Laminar flows which are chemically in equilibrium or frozen are considered in References 5-8. Ting and Libby (Reference 7) also treat turbulent flows. Bloom and Steiger (Reference 9) deal with two-dimensional symmetric and asymmetric cases as well as axially symmetric flow, considering both laminar and turbulent conditions, and considering chemical rate processes.

The present work deals with the behavior of the uniform-pressure far field wake. The flow is treated as a continuum, by the boundary-layer approximations, utilizing integral method techniques according to the approach developed in Reference 9. Chemical rate processes of air relative to atom-molecule dissociation and to ionization are taken into account.

A pertinent general discussion of the nonequilibrium thermochemistry of air has been given by Bloom (Reference 10). Experimental rate constants for the important processes cited by Bloom were those summarized by Wray, Teare, Kivel and Hammerling (Reference 11) and by Teare and Dreiss (Reference 12).

Although the analysis to be presented holds in general for flows which are non-isoenergetic, that is, of non-uniform stagnation enthalpy, the far field wake may be treated as approximately isoenergetic at its initial station since the fraction of energy absorbed upstream by the body is negligible. In effect this approximation implies the neglect of upstream heat transfer to the body and of deviations of the Prandtl number from unity upstream. In contrast, wakes stemming primarily from non-adiabatic boundary layers over the body or with Prandtl numbers different from unity must be considered as non-isoenergetic initially.

Other approximations concerning the transport properties of the flow will be specified in the course of the analysis. In particular, the approximations made in dealing with mass diffusion in a multicomponent mixture are

given in Appendix A.

The governing equations in the wake are of boundary layer type and therefore are parabolic in their mathematical structure. As a result, the flow field downstream of a given initial section, designated say as $x = 0$, is fully determined once the flow properties at $x = 0$ are specified. Thus the downstream flow depends upon the upstream flow only insofar as the upstream flow establishes the initial conditions at $x = 0$. It is believed that the wake properties will not be strongly dependent upon the detailed aberrations of the profiles of the variables specified at $x = 0$. Therefore the initial profiles will be represented in a smooth simplified form expressible in terms of a polynomial consistent with the polynomial profiles utilized in the integral method. Conditions furnished by estimates of the upstream flow are matched at the central axis and at the outer edge of the wake. This approach is considered satisfactory also because the upstream conditions are not known with accuracy sufficient to warrant a more complex calculation at this time. It may be deemed desirable to make a more accurate wake calculation when more accurate upstream properties become available.

The general features of hypersonic flow around blunt bodies with regard to the properties of the shock layer, shock-shape, and near-field wake are reasonably well-known, at least for the purpose of providing initial data for the far-field wake. One approximate method for obtaining the required initial data consists of estimating a reasonable shock shape for a

given body, and determining the conditions in the region directly behind the shock, assuming that chemical equilibrium is closely achieved near the shock. The subsequent properties within stream tubes are then estimated by neglecting transport effects and assuming isentropic expansion to a given pressure, say the ambient pressure of the far-field wake. Isentropic expansion occurs in the limiting cases for which the thermodynamic processes are not rate-dependent, that is, for thermodynamic and chemical equilibrium or frozen conditions. This point of view is supported by the work of Bloom and Steiger (Reference 13) who demonstrated that the flow in the inviscid supersonic region of hypersonic blunt bodies will be frozen with respect to atom-molecule composition for flight velocities between 15,000 and 25,000 fps at altitudes between 150,000 and 250,000 feet.

Typical profiles of such initial data obtained by Ting and Libby (Reference 7) for a body-size and flight condition different from that to be considered here are reproduced in Figure 2 for illustration. Velocity profiles obtained for equilibrium and frozen expansions are shown together with third-degree polynomial representations of the initial data. In these curve-fits the method of least squares was used to establish the value of the velocity at the axis and to give a value for the radial extent of the profile, that is, the initial boundary layer thickness. The initial profiles of atom and electron concentrations obtained by Ting and Libby, assuming that the concentrations

of species per unit mass remain constant (frozen) in the expansion, also are reproduced in Figure 2 together with curve-fits of these profiles.

Reasoning is presented whereby the effect of turbulence in the wake may be estimated. Of course, this procedure is semi-empirical. It hinges on the introduction of the turbulent eddy transport parameters for shear, heat flux and mass - diffusion. Furthermore, the assumption is made that the turbulent Prandtl number and Lewis number are roughly equal in magnitude to their counterparts in laminar flow. Thus, only the eddy viscosity μ_t must be estimated explicitly. In the integral method, it develops that μ_t is required to be evaluated only at the symmetry axis, where it is designated as μ_{t0} . It has been well established that the turbulent eddy viscosity μ_t is much larger than its laminar counterpart μ , at least in incompressible flow. In fact, the ratio μ_t/μ may be as large as several hundred in incompressible flow. There is no reason to expect this order of magnitude to change radically in compressible flow.

Based on reasoning of Mager (Reference 16) for surface boundary layers and Ting and Libby (Reference 7) for axisymmetric wakes, a somewhat rational estimate of the effect of compressibility on μ_t can be made. In the wake case, experimental checks of this procedure have yet to be made; therefore the procedure must be considered arbitrary at this time. However, it is reasonable and thus warrants consideration. In any event, this estimate of the

effect of compressibility on μ_t does not show a change in the order of magnitude of μ_t / μ from that of incompressible flow.

It will be seen that the effect of turbulence appears in two major ways. First, the streamwise length of the wake is inversely proportional to the molecular viscosity μ_o at the axis in laminar flow, and is inversely proportional to the eddy viscosity μ_{to} at the axis in turbulent flow. Therefore the streamwise extent of the wake with respect to the velocity field, state variables and concentration of major components, is diminished roughly in the ratio μ_o / μ_{to} due to turbulence. That is, the turbulent wake may be several hundred times shorter than the comparable laminar wake.

Secondly, in the equation governing species concentrations, the ratio of the chemical production rate term to the diffusion term is inversely proportional to μ_o in laminar flow and inversely proportional to μ_{to} in turbulent flow. Therefore, the importance of chemical rate processes relative to mass diffusion is diminished by orders of magnitude in turbulent flow.

For the altitudes (150,000 - 250,000 ft.) and flight velocities (18,900 - 20,400 fps) of direct interest here, it will be seen that the chemical rate effects are negligible with respect to mass-diffusion effects even in laminar flow for the primary air components, but not for the electron-producing process. That is, the flow will be chemically frozen for the main air species under these conditions, although it will not be frozen in this manner at sufficiently low altitudes.

The necessity of using a chemical rate process for calculating electron densities in a hypersonic flow field is fully brought out by the present investigation. The results indicate that the ion species (α_{NO^+}) is definitely in a nonequilibrium state for both the supersonic expansion region and the wake, for flight velocities of about 20,000 fps and altitudes between 150,000 and 250,000 feet.

Very recently Rosenbaum and Bloom (Reference 17) completed an investigation of the inviscid nonequilibrium molecular dissociation and ionization flow about a body with a 6 inch hemispherical nose radius for free stream flight conditions of 200,000 feet and 20,200 fps. Their results show that for these flight conditions (1) all species (α_{O} , α_{N} , α_{NO^+}) attain equilibrium in a relatively close distance behind the bow shock, (2) the main species (α_{N} , α_{O}) are frozen in the supersonic expansion region and (3) the ion species (α_{NO^+}) is in a nonequilibrium state which remains closer to equilibrium than the frozen values. The electron distribution about the body is presented in Figure 16.

II ANALYSIS

The following system of equations is assumed to govern the flow in an axially-symmetric laminar wake, shown schematically in Figure 1. The assumptions utilized in representing mass diffusion in the multicomponent reacting air mixture, are discussed in more detail in Appendix A.

Overall mass conservation:

$$(\rho u)_x + (\rho v)_y = 0 \quad (1)$$

Momentum:

$$(\rho u^2)_x + (\rho uv)_y = (\mu y u_y)_y \quad (2a)$$

$$p_y = 0 \quad (2b)$$

Energy:

$$\begin{aligned} (\rho u H)_x + (\rho v H)_y &= \left[(\mu/P) y H_y \right]_y + \left[(P-1)(\mu/P) y u u_y \right]_y + \\ &+ \left[(Le-1)(\mu/P) y \sum_i h_i a_{iy} \right]_y \end{aligned} \quad (3)$$

Mass conservation of species i:

$$(\rho y a_i)_x + (\rho v y a_i)_y = \left[(Le \mu/P) y a_{iy} \right]_y + \rho y w_i \quad (4)$$

Notation not defined in the text is given in an attached list.

Before the supplementary thermodynamic and chemical relations are discussed the boundary conditions will be stated and some results not dependent upon thermochemistry derived. The minimum number of

independent boundary conditions is shown enclosed in square brackets. The remaining boundary conditions are derived from the differential equations or are prescribed on physical grounds in the usual manner of the integral method.

Boundary Conditions:

$$\text{at } y = 0: \quad [v = 0], \quad [u_y = 0], \quad [H_y = 0], \quad [a_{iy} = 0] \quad (5a)$$

$$(\rho u/2) u_x = (\mu u_y)_y \quad (5b)$$

$$\begin{aligned} (\rho u/2) H_x = & \left[(\mu/P) H_y \right]_y + \left[(P-1)(\mu/P) u u_y \right]_y + \\ & + \left[(Le-1)(\mu/P) \sum_i h_i a_{iy} \right]_y \end{aligned} \quad (5c)$$

$$(\rho u/2) a_{ix} = \left[(Le\mu/P) a_{iy} \right]_y + \rho w_i/2 \quad (5d)$$

$$u = u_0(x), \quad H = H_0(x), \quad a_i = a_{i0}(x) \quad (5e)$$

$$\text{at } y \rightarrow \delta: \quad [u = u_e], \quad [H = H_e], \quad [a_i = a_{ie}] \quad (5f)$$

$$u_y = u_{yy} = 0, \quad H_y = H_{yy} = 0, \quad a_{iy} = a_{iyy} = 0$$

Integral Equations:

The integral equations following from (1) - (5) are:

$$\theta_x = 0 \text{ or } \theta = \theta_c(\text{constant}); \quad \theta = \int_0^\delta \bar{\rho} \bar{u} (1 - \bar{u}) y \, dy \quad (6a)$$

$$(\theta_E)_x = 0 \text{ or } \theta_E = \theta_{Ec}(\text{constant}); \quad \theta_E = \int_0^\delta \bar{\rho} \bar{u} (1 - \bar{H}) y \, dy \quad (6b)$$

$$(\theta_i)_x = (1/u_e) \int_0^\delta \bar{\rho} w_i y \, dy; \quad \theta_i = \int_0^\delta \bar{\rho} \bar{u} (a_{ie} - a_i) y \, dy \quad (6c)$$

Transformations:

The following transformations are now introduced into the integral equations (6) and boundary conditions (5):

$$mdm = \bar{\rho} y dy, \quad m = \delta_m N; \quad \delta_m^2 / 2 = \int_0^{\delta_m} (1/\bar{\rho}) m dm \quad (7)$$

$$ds = \bar{\mu}_o dx / (\rho_e u_e \theta_c / \mu_e), \quad s - s_c = \left(\int_{x_c}^x \bar{\mu}_o dx \right) / (\rho_e u_e \theta_c / \mu_e)$$

It is observed that θ , θ_E and θ_i have the dimension of (length)²; m , δ , and δ_m have the dimension of (length); while s and N are dimensionless.

The following working forms are derived from (6) and (5b-d):

$$\delta_m^2 \int_0^1 \bar{u}(1-\bar{u}) N dN = \theta_c \quad (8a)$$

$$(\delta_m^2 / \theta_c) \bar{u}_o \bar{u}_{os} = 2\bar{u}_{NNo} \quad (8b)$$

$$\delta_m^2 \int_0^1 \bar{u}(1-\bar{H}) N dN = \theta_{EC} \quad (9a)$$

$$\begin{aligned} (\delta_m^2 / \theta_c) \bar{u}_o \bar{H}_{os} &= (2/P_o) \bar{H}_{NNo} + (4/P_o)(P_o - 1)(u_e^2 / 2H_e) \bar{u}_o \bar{u}_{NNo} \\ &+ (2/P_o)(Le_o - 1) \sum_i \bar{h}_{io} a_{iNNo} \end{aligned} \quad (9b)$$

$$\theta_{is} = (\rho_e u_e \theta_c / \mu_e) (1/\bar{\mu}_o) (\delta_m^2 / u_e) \int_0^1 \bar{\rho} w_1 N dN \quad (10a)$$

$$\begin{aligned} (\delta_m^2 / \theta_c) \bar{u}_o a_{ios} &= (2Le_o / P_o) a_{iNNo} + (1/\bar{\mu}_o u_e) (\rho_e u_e \theta_c / \mu_e) \cdot \\ &\cdot (\delta_m^2 / \theta_c) w_{io} \end{aligned} \quad (10b)$$

Direct consideration of the original differential equations shows that for the approximation $Le = 1$, the energy equation (3) becomes independent of concentrations except indirectly through μ and P . This simplification carries over to the energy boundary condition (9b), where, in addition, the explicit appearance of μ has been eliminated by the transformation of x . For the further approximation $P = 1$, the Crocco integral relation $H = A + Bu$, where A and B are constants, is applicable in view of the axial symmetry. By satisfying the relations $H = H_{oc}$ and H_e when $u = u_{oc}$ and u_e , this relation may be expressed in the form:

$$\frac{H_e - H}{H_e - H_{oc}} = \frac{u_e - u}{u_e - u_{oc}} \quad (11)$$

Likewise, when the effects of chemical rates are negligible and the term involving w_i in (4) is dropped, and moreover $Le/P = 1$, the following integral of (4) is derived:

$$\frac{a_{ie} - a_i}{a_{ie} - a_{ioc}} = \frac{u_e - u}{u_e - u_{oc}} \quad (12)$$

This relation is comparable to (11) and satisfies the conditions $a_i = a_{ioc}$ and a_{ie} when $u = u_{oc}$ and u_e .

It is recalled that the integral method for solving partial differential equations is an approximate method which is used in cases where more exact calculations are difficult to obtain, or where a moderate sacrifice in accuracy is permissible in the interest of simplicity. It involves the assumption of functional forms of the dependent variables. These forms are chosen in a reasonable fashion to satisfy a number of boundary conditions, but are permitted to retain undetermined parameters, which are then utilized to satisfy the integral equations and/or additional boundary conditions, or other conditions derivable from the differential equations. These other conditions may be derived, for example, by requiring that the differential equations be satisfied at certain interior points or regions away from the boundaries. On the other hand they may take the form of additional integral equations derived by piecewise integration of the differential equations over one of the variables (in boundary-layer problems usually the coordinate normal to the main stream), or by applying weighing factors to the original differential equations prior to integration. The weighing functions may be powers of the normal coordinate or of the streamwise velocity, for example. Clearly, the larger the number of independent conditions which are satisfied by the assumed functions, the greater will be the accuracy of the solution. A compromise between simplicity and accuracy influences the choice of the specific procedure to be employed in

a given problem; this choice usually involves a degree of judgment based upon experience. More accurate test calculations, limiting cases, special cases whose mathematically exact solutions are known, and experimental results provide yardsticks for evaluating the accuracy or reasonableness of a solution obtained by the integral method.

In the present analysis it is assumed that the overall behavior of the profiles of velocity, stagnation enthalpy and species concentration can be depicted adequately by fourth-degree polynomials in the normalized, transformed radial coordinate N , and that only one undetermined parameter included explicitly in each profile is sufficient to represent the effect of streamwise variations. Another undetermined parameter, the wake-thickness δ , assumed to be the same for all flow variables, is included implicitly through the definition of N .

This selection of the profile-forms implies that the initial data for each variable can be represented with sufficient accuracy by a fourth-degree polynomial with one constant, aside from the wake-thickness common to all variables, available for adjustment. In practice, for a symmetric wake, the adjustable quantity in each profile will be the value of the variable evaluated at the center axis. For additional accuracy in fitting the initial data or in representing the flow field, additional parameters may be included in the profile representation. Beyond the initial station these may be evaluated in the manner outlined above.

Assumed Profiles:

The assumed profiles, which satisfy boundary conditions (5a), (5f) and definitions (5e) are seen to be the same for u , H and a_i , namely:

$$\frac{u - u_o}{u_e - u_o} = \frac{H - H_o}{H_e - H_o} = \frac{a_i - a_{io}}{a_{ie} - a_{io}} = 6N^2 - 8N^3 + 3N^4 \quad (13a)$$

or in another form,

$$\frac{u_e - u}{u_e - u_o} = \frac{H_e - H}{H_e - H_o} = \frac{a_{ie} - a_i}{a_{ie} - a_{io}} = 1 - 6N^2 + 8N^3 - 3N^4 \quad (13b)$$

The profile forms (13a) are plotted in Figure 3.

The relations in (13) should not be confused with the special integrals (11) and (12). However, they do lead to the following relations based on the definitions of θ , θ_E and θ_i given in (6):

$$\theta = \left(\frac{1 - \bar{u}_o}{1 - \bar{H}_o} \right) \theta_E = \left(\frac{1 - \bar{u}_o}{a_{ie} - a_{io}} \right) \theta_i \quad (14)$$

Now if we choose to satisfy the momentum and energy integral equations (8a) and (9a), which state that both θ and θ_E are constants along the flow, we derive:

$$\frac{1 - \bar{u}_o}{1 - \bar{H}_o} = \frac{\theta}{\theta_E} = \frac{\theta_c}{\theta_{Ec}} = \frac{1 - \bar{u}_{oc}}{1 - \bar{H}_{oc}} \quad (15)$$

which, with assumption (13b), yields (11). Thus it is seen that the assumption that the velocity and stagnation enthalpy profiles are of the same form, and the satisfaction of the momentum and energy integral relations, lead to the special relation (11), but without any assumptions concerning the transport properties Le and P .

Likewise, for the case of negligible chemical rate effects, the assumption that the velocity and species concentration profiles are of the same form, and the satisfaction of the momentum and concentration integral relations yields (12) but without any assumptions concerning Le/P .

Viewed in another way, it is seen that the approximate relations assumed between velocity, enthalpy and concentrations become exact in the special cases cited.

The polynomial in N assumed in (13a) varies monotonically from zero at the axis to unity at the edge of the wake. This is consistent with the initial conditions with which we wish to deal here. As a consequence of this assumption it is seen from (6) that if $u_o = u_e$ or $H_o = H_e$ at any one streamwise station, it is required that $\theta \equiv 0$ or $\theta_E \equiv 0$ throughout the flow. The condition $\theta \equiv 0$ is satisfied only in the trivial case of uniform flow. However, $\theta_E \equiv 0$ implies a flow with uniform stagnation enthalpy, which is quite possible in view of the adiabatic condition of the wake with respect to its surroundings. Analogous considerations hold for the distributions of species - concentration when chemical rate effects are negligible.

Integral method solutions: velocity and wake-thickness parameters:

We choose to satisfy the momentum integral equation (8a) and the momentum condition along the axis (8b) in order to determine the transformed wake thickness δ_m and the velocity parameter $\bar{u}_o(s)$. Substitution of the assumed profile (13) into (8) yields:

$$\theta_c / \delta_m^2 = (1 - \bar{u}_o)(10 + 11\bar{u}_o)/210 \quad (16)$$

$$\bar{u}_o \bar{u}_{os} = (4/35)(1 - \bar{u}_o)^2 (10 + 11\bar{u}_o) \quad (17a)$$

A plot of (16) is shown in Figure 4.

Equation (17a) is separable and its integration yields an equation of the form:

$$s = f(\bar{u}_o) + \text{constant} \quad (17b)$$

where

$$f(\bar{u}_o) \equiv (5/12)(1/1 - \bar{u}_o) - (25/126) \ln \left[(10 + 11\bar{u}_o)(1 - \bar{u}_o) \right] \quad (17c)$$

Since the absolute origin of the axial coordinate x or s is arbitrary within an additive constant, we may define the position $x = 0$ or $s = 0$ to be the location at which a given initial value of \bar{u}_o exists. With this initial value denoted as \bar{u}_{oc} , (17b) can be expressed as

$$s = f(\bar{u}_o) - f(\bar{u}_{oc}) \quad (17d)$$

Equation (17d) is plotted in Figure 5 for $\bar{u}_{oc} = 0$. This curve is general in the sense that if we consider a particular value, say \bar{u}_{oa} , which corresponds to a coordinate value s_a , the curve gives the subsequent or

prior values of \bar{u}_o which correspond to coordinate increments $s - s_a$, regardless of the absolute location of s_a . As $s \rightarrow \infty$, $\bar{u}_o \rightarrow 1$.

Stagnation enthalpy parameter:

Now if we choose to determine $\bar{H}_o(s)$ by satisfying the energy integral equation (9a) we derive (15) as previously mentioned. That is

$$(1 - \bar{H}_o)/(1 - \bar{H}_{oc}) = (1 - \bar{u}_o)/(1 - \bar{u}_{oc}) \quad (18)$$

where \bar{H}_{oc} may be specified independently. Of course, when $\bar{H}_{oc} = 1$ it is required that $\bar{H}_o = 1$ in accordance with the previous discussion of flow with uniform H. This solution for H_o , derived from the integral equation which essentially expresses an average across the flow, does not depend upon P or Le. On the other hand, an idea of the Prandtl number - Lewis number influence can be obtained by alternately satisfying the energy differential equation along the center axis. For this purpose (9b) may be combined with (16), (17a) and the results of (13) to yield the following expression:

$$\frac{d\bar{H}_o}{d\bar{u}_o} = - \frac{1}{P_o} \frac{\bar{H}_{NNo}}{2(1 - \bar{u}_o)} + \frac{2(P_o - 1)}{P_o} \frac{u_e^2}{2H_e} \bar{u}_o + \frac{(Le_o - 1)}{P_o} \frac{\sum_i h_{io} a_{iNNo}}{12(1 - \bar{u}_o)} \quad (19a)$$

$$= - \frac{1}{P_o} \frac{(1 - \bar{H}_o)}{(1 - \bar{u}_o)} + \frac{2(P_o - 1)}{P_o} \frac{u_e^2}{2H_e} \bar{u}_o + \frac{(Le_o - 1)}{P_o} \frac{\sum_i \bar{h}_{io} (a_{ie} - a_{io})}{(1 - \bar{u}_o)} \quad (19b)$$

$$= \frac{1 - \bar{H}_o}{1 - \bar{u}_o} + \frac{1 - P_o}{P_o} \left[\frac{1 - \bar{H}_o}{1 - \bar{u}_o} - \frac{u_e^2}{H_e} \bar{u}_o \right] + \frac{(Le_o - 1)}{P_o} \frac{\sum_i \bar{h}_{io} (a_{ie} - a_{io})}{1 - \bar{u}_o} \quad (19c)$$

For $P_o = 1$ and $Le_o = 1$, this equation yields (18). A rough estimate of the effects of deviations of P_o and Le_o from unity can be obtained by making an a priori estimate of the order of magnitude of the two additional terms on the right hand side of (19c), and then integrating (19c) as a linear equation. This is equivalent to forming an integral equation from (19c) and obtaining a first iterative solution. The procedure is shown in Appendix A.

The considerations in Appendix A show that, for constant average values of the second and third right hand terms in (19c), whose sum is denoted by B, (19c) may be integrated to yield

$$\frac{1 - \bar{H}_o}{1 - \bar{u}_o} = \frac{1 - \bar{H}_{oc}}{1 - \bar{u}_{oc}} + |B| \ln \left(\frac{1 - \bar{u}_{oc}}{1 - \bar{u}_o} \right) \quad (20)$$

where B is a negative quantity whose magnitude is on the order of $(1 - P_o) / P_o$ for hypersonic conditions in the far-field wake and $Le_o - 1 \approx 1 - P_o$.

Representative values of \bar{H}_o as a function of \bar{u}_o , calculated from (20), are shown in Figure 6 for $B = 0$, corresponding to $P_o = Le_o = 1$, and the typical value $|B| = 0.3$. Cases are shown for an initial stagnation enthalpy equal to that of the free stream, i. e., $\bar{H}_{oc} = 1$, and for a small initial deviation in \bar{H}_o , i. e. $\bar{H}_{oc} = 1 - 0.2(1 - \bar{u}_{oc})$. The effect of $P_o \neq 1$ and $Le_o \neq 1$ is to encourage decreases in H_o below H_e . The order of these additional decreases is about 5 per cent of H_e .

Species concentration for negligible chemical rates (frozen) :

It is possible to show that for a class of technically-important wake flows including those of direct interest here, certain chemical processes occur with sufficient slowness that the rate effects are negligible with respect to the corresponding diffusion effects. Such flows are termed "frozen" with respect to these particular processes. Specifically, the processes involving the dissociation of O_2 and N_2 and recombination into O_2 and N_2 will be frozen at the altitudes and flow velocities of special interest here. This is not necessarily the case for trace components such as NO or for the electron-producing processes. However, the O_2 and N_2 processes are particularly important since they dominate the state variables, such as density and temperature, of the air mixture.

Solutions for the concentrations of the frozen species under the influence of mass diffusion can be pursued without a discussion of the thermochemical processes of air components. Therefore the discussion of the thermochemistry will be given later.

With the w_i terms neglected, (10a) and (10b) take the form:

$$\theta_i = \theta_{ic} \text{ (constant)} \quad (21a)$$

$$\left(\frac{\delta}{m} \right) \frac{u}{c} \alpha_{ios} = \left(2 \frac{Le}{P} \right) \alpha_{iNNo} \quad (21b)$$

The solution of these equations bears a strong resemblance to those governing the stagnation enthalpy parameter H_o and discussed previously. For example, when $Le/P = 1$, (12) follows from the differential equations. Likewise, with the assumed profiles (13), satisfaction of the integral equation (21a) above yields (12) with no specification of Le/P . Furthermore, the alternate satisfaction of the differential equation along the axis may be accomplished by the use of (21b) coupled with (16), (17a) and (13), which yields

$$\frac{da_{io}}{d\bar{u}_o} = \frac{Le_o (a_{ie} - a_{io})}{P_o (1 - \bar{u}_o)} \quad (21c)$$

Integration of (21c), assuming $Le_o/P_o = \text{constant}$, yields

$$\frac{a_{ie} - a_{io}}{a_{ie} - a_{ioc}} = \left(\frac{1 - \bar{u}_o}{1 - \bar{u}_{oc}} \right)^{Le_o/P_o} \quad (22)$$

and clearly shows the order of the effect of $Le_o/P_o \neq 1$. Since $Le_o/P_o \approx 2$ in high temperature air, its effect on the diffusion-controlled species concentrations can be appreciable. Eq. (22) is shown plotted in Figure 7a for $Le_o/P_o = 1$ and 2. Corresponding plots in terms of the streamwise coordinate are shown in Figure 7b.

Species concentration for very rapid chemical rates (equilibrium):

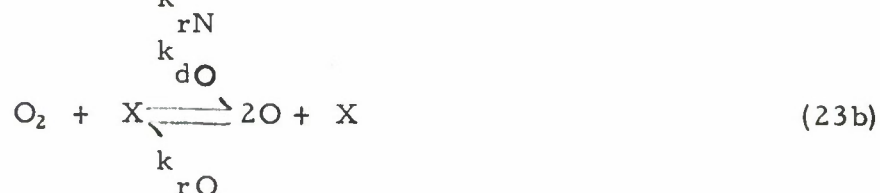
In the limiting case in which the rate parameters of the chemical processes are very large, the species concentrations are uniquely determined by the usual relations governing equilibrium thermodynamics (mass-action law for each reaction; equation of state; relation between enthalpy, concentrations, and temperature; conservation of atoms in the course of the reaction) once the pressure and enthalpy are specified. In this case the quantity w_i , which represents the local rate of change of concentration of a given species due to chemical change alone, becomes an indeterminate form formed by the product of a very large rate parameter and the difference between the forward and reverse process terms which approaches zero. There is no need to evaluate w_i directly, since in this case, the species conservation equation (4) simply expresses the fact that if we consider a mass element in transit, the change in species concentrations within the element is due to the chemical change effect, signified by w_i , plus the diffusion effect. Therefore, when the concentrations are known, as in the case of chemical equilibrium, the convective term and diffusion term in (4) may be evaluated, and thus w_i may be determined from (4) if necessary. In practice (4) may be disregarded in the case of chemical equilibrium, since, in effect it is automatically satisfied.

Thermochemistry of air:

At the energy levels involved in the wake flows under consideration here, the state variables such as density and temperature of the air mixture, are dominated by the primary components O_2 , N_2 , O and N . All other components are expected to be present only as traces whose energy changes are negligibly small with respect to those cited. Of course the trace components are important from the standpoint of their influence on radiation or electron densities. However, the primary processes involving $O_2 \rightleftharpoons 2O$ and $N_2 \rightleftharpoons 2N$ may be considered first, by ignoring the trace components. Then the trace processes can be investigated utilizing the previously-determined state and concentrations of major species as input information.

In the relations to be given, the individual species of the air mixture are assumed to behave as perfect gases. Furthermore the translational rotational and vibrational degrees of freedom of the molecules are assumed to be in equilibrium, despite the fact that dissociation and ionization processes may be rate-dependent.

The principles of chemical kinetics and statistical thermodynamics are applied to the following reactions of three-body collision type:



where X signifies the catalyst, which here is assumed to consist of any other particle contained in the mixture. Refinements of the type which consider the influence of various types of catalysts on the reaction rates are not considered here. This would require consideration of a separate reaction and rate process for each catalyst, and would result in coupling which would complicate the computational procedure considerably.

The following relations corresponding to (23) are derived:

Chemical production rates:

$$w_O = \left(k_{rO} \rho_{dO} / M_O^2 \right) \left(M_{O_2} / \bar{M} \right) \rho \left[a_{O_2} e^{-D_O/RT} - (\rho/\rho_{dO}) a_O^2 \right] \quad (24a)$$

$$w_N = \left(k_{rN} \rho_{dN} / M_N^2 \right) \left(M_{N_2} / \bar{M} \right) \rho \left[a_{N_2} e^{-D_N/RT} - (\rho/\rho_{dN}) a_N^2 \right] \quad (24b)$$

$$w_{O_2} = -w_O \quad ; \quad w_{N_2} = -w_N \quad (24c, d)$$

where

$$1/\bar{M} = \sum_i a_i / M_i \quad (24e)$$

$$\rho_{di} = (m_i/2)(k_{di}/k_{ri}) e^{D_i/RT}$$

$$= (m_i/h_p^3) (\pi m_i kT)^{3/2} \left(T_i^R / T \right) \left(1 - e^{-T_i^V/T} \right) \left(\frac{E_i}{f_i} \right)^2 / f_{i_2}^E$$

$$i = O \text{ or } N \quad (24f)$$

where k_{di} and k_{ri} are the forward and reverse reaction rate parameters shown in (23), M_i denotes molecular mass in mass/mole, m_i denotes particle mass in mass/particle, D_i is the dissociation energy per mole associated with the atomic species, h_p is Planck's constant, k the gas constant per molecule, R the gas constant per mole, T_i^R the characteristic rotational temperature of a species, T_i^V the characteristic vibrational temperature, f_i^E the electronic partition function of atomic species, and $f_{i_2}^E$ the electronic partition function for corresponding molecular species.

Enthalpy of the mixture:

$$h = (RT/2M_O) \left\{ 3.88 + 0.232 \Lambda_{O_2} + 0.875 \Lambda_{N_2} + a_O (1.50 - \Lambda_{O_2}) + a_N (1.14)(1.50 - \Lambda_{N_2}) \right\} + a_{O_2} D_{O_2} / 2M_{O_2} + a_{N_2} D_{N_2} / 2M_{N_2} \quad (25)$$

where

$$\Lambda_i = (T_i^V / T) / (e^{T_i^V / T} - 1) ; \quad i = O_2, N_2$$

Of course the number density of electrons is equal to the number density of ions in the present approximation. Therefore $n^e = n^{NO^+} = (\rho a_{NO^+}) / (m_{NO^+})$, where m_i is the particle mass which is equal to M_i divided by Avogadro's number and n_i has the units particles per unit volume.

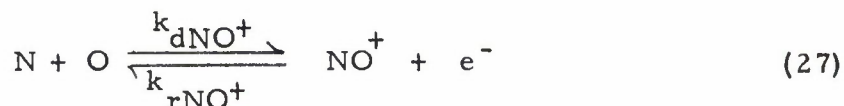
Equation of state:

$$p = \rho RT / \bar{M} \quad (26)$$

Numerical values for use in the above thermochemical relations are given in Reference 10 unless specified elsewhere.

Electron production:

In view of our interest in the electron density distribution in the flow field, we shall consider the following electron-producing reaction which has been found to be of importance in experiments summarized in References 11 and 12:



This leads to

$$w_{NO^+} = (k_{rNO^+}) \rho \left[(M_{NO^+}^2 / M_N M_O) (k_{dNO^+} / k_{rNO^+}) a_N a_O - a_{NO^+}^2 \right] \quad (28a)$$

where, with T in $^{\circ}R$, and I_{NO^+} the ionization energy per mole:

$$k_{dNO^+} / k_{rNO^+} = (1/2) (M_{NO^+} M_{e^-}^{3/2} / M_O M_N) \cdot \left[\frac{(2 + 2e^{-320/T})}{(5 + 3e^{-411/T} + e^{-589/T})} \right] \cdot \left[\frac{(T/8.83)(e^{4100/T})}{(e^{4100/T} - 1)} \right] \cdot e^{- (I_{NO^+} - D_{NO^+}) / RT} \quad (28b)$$

All the information required for making calculations of species concentrations of O, N, O₂, N₂ and subsequently NO⁺ and e⁻ is now at hand. For the calculations to be presented, only the ordinary differential equation obtained from the partial differential equation along the symmetry axis will be employed. The integral equations for stagnation enthalpy and species concentration will be disregarded. This choice is made because the flow field near the axis is believed to be of major importance, because the condition along the axis retains a considerable amount of mathematical exactitude and because Prandtl number and Lewis number effects are retained. In effect then we are simply satisfying the differential equation along the axis, estimating that the second derivatives of the variables are proportional to the difference between the outer values and inner values of the variables, and then using the assumed profiles to interpolate between the values at the axis and the outer values.

Transport properties:

The means for evaluating the transport properties of gas mixtures are now well known, particularly in the case of binary mixtures. Detailed discussions of these calculations are given in References 14 and 15. The expressions for the transport properties will not be repeated here for the following reasons:

The thermal conductivity λ , as well as the mean specific heat \bar{c}_p , a thermodynamic property, appear together with the viscosity coefficient μ in the Prandtl number $P = \mu \bar{c}_p / \lambda$ whereas the mean diffusion coefficient $(D_{ij})_{av}$, which is used here, appears in the Lewis number $Le = \rho (D_{ij})_{av} \bar{c}_p / \lambda$. The parameters P and Le are not evaluated in detail here, since it is well known that they do not exhibit a strong dependence on the state (including the precise composition) of air or of mixtures of its main components. That is, for such mixtures, P takes on values roughly between 0.7 and 1.0, while Le assumes values on the order of 1.4. Along the lines previously discussed, constant average values of P and Le are assumed for the present calculations.

On the other hand, the viscosity coefficient appears explicitly. It has been determined that for air in equilibrium at high temperatures, the viscosity μ is correlated within an accuracy of 10% by the well-known Sutherland relation, which can be written in the following form:

$$\bar{\mu} = \bar{T}^{\frac{1}{2}} \left(\frac{1 + C}{1 + C/\bar{T}} \right) \quad (29)$$

where $\bar{\mu} = \mu/\mu_e$, $\bar{T} = T/T_e$ and $C = 200^\circ R/T_e$. This relation is used in the present calculations.

Turbulent flow:

Methods for treating the turbulent flow of wakes and jets have received considerable treatment in the literature (for example, see Reference 2, Chapter 23). In effect, in turbulent flow, each of the molecular transport

effects such as shear stress, heat flux and mass diffusion velocity, is augmented by an additional quantity due to the turbulent transports associated with the turbulent fluctuations. Based on physical reasoning albeit with a degree of arbitrariness, definitions can be introduced to express the turbulent shear, turbulent heat flux and turbulent mass diffusion in forms analogous to the molecular transports. That is, the shear can be set proportional to the gradient of the mean velocity, the heat flux proportional to the gradient of mean temperature and the mass-diffusion velocity proportional to the gradient of the mean concentration. The proportionality factors are termed eddy-viscosity μ_t , eddy-conductivity λ_t and eddy-diffusivity (D_{ij}) respectively, and are determined by combinations of physical reasoning and experimental observation. The turbulent transports outweigh the molecular transports in importance in flow regions which are not extremely close to solid surfaces, where laminarization takes place. In fact, in free turbulent flows, such as wakes and jets, the molecular transports can usually be neglected with respect to the turbulent contributions throughout the flow.

In practice, the definition of the eddy parameters simply means that in turbulent flows we may utilize the laminar flow equations, with the interpretation that the flow variables signify the corresponding mean quantities of turbulent flow, and that the transport parameters (μ , λ , D_{ij}) in the laminar equations actually denote the sums of the laminar quantities and the

corresponding empirical turbulent eddy-parameters μ_t , λ_t and $(D_{ij})_t$. That is, μ is replaced by $(\mu + \mu_t)$ etc. in the equations stated in (1) to (4). This can be done since the differential equations for the mean turbulent motion are otherwise identical to those for laminar flow provided that the density fluctuations are neglected. As a refinement the density fluctuations can be retained but this is not done usually; their significance has not been established.

An idea of the magnitude of the eddy viscosity in incompressible flow (μ_t^*) can be obtained by means of the following expression which has been found to correlate some experimental data (Reference 2).

$$\mu_t^* = \rho K (2\delta^*)(u_e - u_o) = \text{constant over a section} \quad (30)$$

where K is on the order of 0.02 to 0.005 in axially symmetric and two-dimensional flows, and δ^* is the semi-thickness of the incompressible wake. (It should be noted that in the literature the quantity μ_t/ρ is often described by the terminology "eddy-viscosity", rather than μ_t alone). It has been well established that $\mu_t^* \gg \mu$ in regions away from laminar sub-layers. In fact μ_t^* is on the order of hundreds of times larger than μ^* in wakes. Likewise in compressible flow it is expected that $\mu_t \gg \mu$.

In view of the paucity of information concerning λ_t and $(D_{ij})_t$, it has been considered reasonable to assume $P_t = \mu_t \bar{c}_p / \lambda_t = P(\text{laminar})$
 $Le_t = \rho D_{ij} \bar{c}_p / \lambda_t = Le$, so that only μ_t will require explicit evaluation.

Therefore, in a rough approximation, if turbulent density fluctuations are neglected, if the laminar transports are neglected in comparison with the turbulent values, and if it is assumed that $P_t = P$ (laminar), and $Le_t = Le$ (laminar), the laminar analysis previously given can be carried over directly to the turbulent case with the provision that μ_t must replace μ everywhere except in μ_e , which can remain intact since it is only a reference constant.

It is observed that in the integral method analysis μ appears only as μ_o in the transformed variable s (Eq. 7) and in the chemical rate term in (10b). It has been pointed out that the chemical rate term will be negligible with respect to the diffusion term in (10b) for laminar flow at the altitudes of immediate interest here. Since it is well known that $\mu_t^* \gg \mu^*$ and therefore that $\mu_t \gg \mu$ (perhaps by a factor of several hundred), the chemical processes will be even less important with respect to diffusion under turbulent conditions. This is physically reasonable since mass diffusion would be expected to be enhanced considerably by the effect of turbulence.

Likewise the entire streamwise scale of the wake will be reduced in roughly proportion to $1/\mu_{to}$. This means a streamwise scale reduction by a factor of several hundred. That is, the velocity parameter u_o will approach u_e giving a uniform profile in a much shorter distance in turbulent flow than in laminar flow.

A somewhat rational method for estimating μ_t/μ_t^* can be obtained on the basis of work by Mager (Reference 16) concerning turbulent compressible boundary layers over surfaces, and its extension to the case of axially-symmetric wakes can be obtained on the basis of work by Ting and Libby (Reference 7). This work consists of stating a set of conditions which are sufficient to transform the turbulent compressible equations of momentum and overall-continuity to their incompressible form. The transformation of Mager has been utilized with some success to correlate experimental results in flow over bodies. Its primary conditions are that the Howarth-Dorodnitsyn density-transformation of the normal coordinate can be introduced, that the stream-function remains invariant under the transformation, and that the turbulent shear within a mass-element remains invariant under the transformation. The latter condition, which is by no means obvious, actually stems from a physical interpretation of one of the mathematically required conditions for reduction of the equations. Another aspect of the transformation requires the somewhat arbitrary selection of values for ρ^* and μ_t^* in the incompressible flow.

The same conditions are required for the axially-symmetric wake except that now the invariance of the moment (about the axis) of the turbulent shear within a mass element is required for a reduction of the equations. The validity of the transformation for the axially symmetric wake still awaits experimental check. In this case Ting and Libby have suggested that the

ρ^* and μ_t^* be evaluated at conditions at the outer edge of the wake.

Neither Mager nor Ting and Libby derived the relations required to reduce the energy equation and the species-conservation equations to incompressible form. These would yield relations for λ_t / λ_t^* and $(D_{ij})_t / (D_{ij})_t^*$. It would be interesting to examine the consistency of such relations and the assumptions $P_t = P$ and $Le_t = Le$. This will be left to future work. An assumption in the turbulent energy equation that the turbulent stagnation-enthalpy transport $\overline{v'H'}$ is proportional to the momentum transport $\overline{u'v'}$ (primes denote turbulent fluctuations and bars mean quantities) leads to the isobaric Crocco relation between mean variables. That is, $H = A + Bu$, where A and B are constants. The condition $\overline{v'H'} = \overline{Bu'v'}$ is satisfied when $P_t = 1$ and $H = A + Bu$. The special case for which $B = 0$ corresponds to isoenergetic mean flow.

The following relation was derived by Ting and Libby from the condition of invariance of the turbulent shear-moment:

$$\mu_t / \mu_t^* = (1/\bar{\rho} y^2) \int_0^{y^2} \bar{\rho} dy^2 \quad (31a)$$

It may be assumed from (30) that

$$\mu_t^* = \rho_e K (2\delta_m) (u_e - u_o) \quad (31b)$$

In our integral method analysis μ_t will require evaluation only at the symmetry axis, that is,

$$\text{at } y = 0, \mu_t = \mu_{to} = \mu_t^* = \rho_e K (2\delta_m) (u_e - u_o) \quad (31c)$$

In some cases a constant mean value of μ_t^* may be used with sufficient accuracy.

III CALCULATIONS

Calculations have been made of the far-field laminar wake properties at the following trajectory points of a blunt body:

<u>Code</u>	<u>Altitude (ft)</u>	<u>Velocity (fps)</u>
1	150,000	18,900
2	200,000	20,200
3	250,000	20,400

The corresponding initial conditions at the axis of the wake and other pertinent quantities are shown in Table I. It is recalled that the initial conditions are obtained by assuming that chemical equilibrium is achieved reasonably close behind the bow shock and that the flow then expands in chemically frozen fashion but with vibrational equilibrium until ambient pressure is achieved. This expansion is isentropic. Insofar as electron production is concerned, the same procedure is employed for the NO^+ reaction, utilizing (28) to give the equilibrium values, and then simply multiplying the frozen mass fraction α_{NO^+} by the initial wake-density ρ_{oc} and appropriate conversion factors to get the initial number-density of NO^+ and therefore of e^- .

Consideration of the relations (10b) and (24) for species concentrations of O and N in the wake indicate immediately that the chemical rate production term is negligible with respect to the diffusion term for the flight

conditions listed above. However, this is not the case for the NO^+ and e^- reaction. Initially, the ionization recombination rate term dominates and is shown to cause a rapid decrease in the number-density of electrons. For example, for all flight conditions, the number-density of electrons (particles/cc) decreases by at least a factor of one hundred within a distance of ten feet. This strongly indicates that the electron species is not frozen in the anterior region of the wake, and with the extremely high rate of recombination one should suspect that the electron species in the wake is close to chemical equilibrium.

It should be noted, that for chemical equilibrium of the NO^+ or e^- species the electron density is properly obtained only by setting the bracket in equation (28a) equal to zero.

Figures 8 through 14 present the results of specific calculations. In particular, the variations of quantities along the axis are given, where the independent parameter is in the physical length (feet). For each trajectory point calculations were made under two assumptions $\left[P_o = Le_o = 1 \right]$ and $\left[P_o = 0.71, Le_o = 1.45 \right]$ for the isoenergetic initial conditions $\bar{H}_{oc} = 1$, and for the 200,000 feet, 20,200 fps case calculations were made with $\left[P_o = Le_o = 1 \right]$ for an initial defect in \bar{H}_o , that is, $\bar{H}_{oc} = 0.9$.

The stagnation enthalpy \bar{H} is shown in Figure 8a for the isoenergetic initial condition. It is interesting to note that the maximum defect in \bar{H}_o for the non-isoenergetic wake $\left[P_o = 0.71, Le_o = 1.45, \bar{H}_{oc} = 1 \right]$ is about

7 to 9 percent and agrees closely with the prediction of Appendix B. Shown in Figure 8b is the variation of \bar{H}_o at 200,000 feet as a result of an initial defect in \bar{H}_o , that is, $\bar{H}_{oc} = 0.9$.

The velocity decay along the axis is presented in Figures 9a and 9b for the isoenergetic and non-isoenergetic initial condition respectively. Figures 10a, 11a, 12a respectively illustrate the variations of mass fraction of air (α_{ao}), temperature (\bar{T}_o) and density ($\bar{\rho}_o$) along the axis for the initial isoenergetic condition $\bar{H}_{oc} = 1.0$. The Prandtl-Lewis number effect is clearly illustrated by these curves. Of main importance, is the substantial increase in the maximum value of the temperature for the $\left[P_o = 0.71, \right.$
 $\left. Le_o = 1.45 \right]$ case over the isoenergetic wake; especially if one is interested in the radiation properties of the wake. Analogously, the above variations for an initial defect in \bar{H}_o , that is, $\bar{H}_{oc} = 0.9$ are present in Figures 10b, 11b, 12b for the 200,000 feet, $\left[P_o = Le_o = 1 \right]$ case.

The mass fraction of NO^+ along the axis as calculated from (10b) and (28) is shown in Figures 13a, b, c for the isoenergetic initial conditions $\bar{H}_{oc} = 1$ and Figure 13d presents the variation, for the 200,000 feet, $P_o = Le_o = 1$ case, with an initial defect in \bar{H}_o . The corresponding number-density of electrons (n_o^e) are shown in Figures 14a, b, c, d. From these figures, the effect of an initial defect in \bar{H}_o can be determined. Figure 14b₂ shows that the initial rate of decrease of the number-density is larger for the non-iso-

energetic initial conditions.

Finally, the physical scale x of the streamwise coordinate which is related to s by (7) is shown in Figures 15a and 15b. Notice that the effect of altitude is to increase the physical length at the lower altitudes and decrease it at higher ones. This is due to the dependence of the physical length (x) on the free stream Reynolds number. It can also be seen that Prandtl-Lewis number effect $\left[P_o = 0.71, Le_o = 1.45 \right]$ causes a slight decrease in the physical length over the isoenergetic conditions $\left[P_o = Le_o = 1 \right]$. This is due to the inverse dependence of the physical length (x) on temperature.

For turbulent flow, the following expression may be written from (31c):

$$\frac{\mu_{to}}{\mu_o} = \left(\frac{\rho_e u_e \sqrt{\theta_c}}{\mu_e} \right) \frac{2K}{\bar{\mu}_o} \left(\frac{\delta_m^2}{\theta_c} \right)^{1/2} (1 - \bar{u}_o) \quad (32)$$

In our present calculations, this quantity varies from the order of 10^3 at 250,000 ft. to 10^5 at 150,000 ft. This gives an idea of the substantial relative decrease in the length of the wake in turbulent flow, based on the assumptions previously stated. Under these assumptions, at 250,000 ft. the turbulent wake is on the order of 1000 times shorter than the laminar wake; while at 150,000 ft. the turbulent wake is about 100,000 times shorter than the laminar wake.

REFERENCES

1. Lin, S. C. : Cylindrical Shock Waves Produced by Instantaneous Energy Release, Journal of Applied Physics, Vol. 25, p. 54, 1954.
2. Schlichting, H. : Boundary Layer Theory, McGraw-Hill, 1955.
3. Pai, S. I. : Fluid Dynamics of Jets, Van Nostrand, 1954.
4. Pai, S. I. : Axially-Symmetrical Jet Mixing of a Compressible Fluid, Quarterly of Applied Math., Vol. X, No. 2, p. 141, July 1952.
5. Feldman, S. : Trails of Axi-Symmetric Hypersonic Blunt Bodies Flying Through the Atmosphere, Avco-Everett, RR 82, Dec. 1959.
6. Lew, H. G. and Langelo, V. A. : Plasma Sheath Characteristics About Hypersonic Vehicles, General Electric Space Sciences Lab., R 60 SD 356, April 1960.
7. Ting, L. and Libby, P. A. : Fluid Mechanics of Axisymmetric Wakes Behind Bodies in Hypersonic Flow, General Applied Science Lab., Technical Report 145, March 1960.
8. Goulard, M. and Goulard, R. : The Aerothermodynamics of Reentry Trails, ARS, preprint 1145-60, May 1960.
9. Bloom, M. H. and Steiger, M. : Viscous Reacting Wake Flow : Symmetric and Asymmetric, Polytechnic Institute of Brooklyn, PIBAL 544, 1960.
10. Bloom, M. H. : On the Nonequilibrium Chemistry of Air, General Applied Science Lab., Technical Report 170, May 26, 1960.

11. Wray, K., Teare, J. D., Kivel, B. and Hammerling, P. : Relaxation Processes and Reaction Rates Behind Shock Fronts in Air and Component Gases, Avco-Everett, RR 83, Dec. 1959.
12. Teare, J. D. and Dreiss, G. J. : Theory of the Shock Front, III. Sensitivity to Rate Constants, Avco-Everett, RN 176, Dec., 1959.
13. Bloom, M. H. and Steiger, M. H. : Inviscid Flow with Nonequilibrium Molecular Dissociation for Pressure Distributions Encountered in Hypersonic Flight, IAS Preprint 60-26, Jan. 1960 (to appear in Journal Aero/Space Sciences).
14. Hirschfelder, J. O., Curtiss, C. F., and Bird, R. B. : Molecular Theory of Gases and Liquids, J. Wiley, 1954.
15. Penner, S. S. : Chemistry Problems in Jet Propulsion, Pergamon Press, New York, 1957.
16. Mager, A. : Transformation of the Compressible Turbulent Boundary Layer, Journal Aero. Sciences, Vol. 25, No. 5, p. 305, May 1958.
17. Rosenbaum, H. and Bloom : Rate Chemistry of an Air Like Mixture, Polytechnic Institute of Brooklyn, PIBAL 533.

NOTATIONS

A	constant
B	constant (also see Eq. B1)
C	constant (Eq. 29)
c_p	specific heat ; constant pressure
D	diameter
D_i	dissociation energy per mole associated with atomic species
D_{ij}	binary diffusion coefficient for the interdiffusion of species i and j
f	partition function
f_i^E	electronic partition function of atomic species
$f_{i_2}^E$	electronic partition function of molecular species
h	static enthalpy
h_p	Plank's constant
H	total enthalpy
I_i	ionization energy per mole associated with ionized species
k	thermal conductivity coefficient
k_d	forward reaction rate parameter
k_r	reverse reaction rate parameter
K	defined by eq. 30
Le	Lewis number $Le = \frac{\rho D_{ij} c_p}{k}$

m	transformed normal coordinate
m_i	particle mass
M_i	molecular mass mass/mole
\bar{M}	reduced mass (Eq. 24e)
M_∞	free stream (flight) Mach number
n_i	particle/cc of i^{th} species
N	transformed normal coordinate except where otherwise stated
N_2	molecular nitrogen
O	atomic oxygen
O_2	molecular oxygen
p	pressure
P	Prandtl number $P = \frac{\mu c_p}{k}$
R	gas constant per mole
s	transformed streamwise coordinate (also see Eq. 23a)
T	temperature $^{\circ}\text{R}$
T_i^V	characteristic vibrational temperature
u, v	streamwise and normal velocity component
u_∞	free stream (flight) velocity
\bar{V}	local mean velocity
\bar{V}_i	diffusion velocity of i^{th} species
w_i	net production of i^{th} species (1/sec)

x, y	streamwise and normal coordinate
X	catalyst
α_i	mass fraction of i^{th} species
δ	boundary layer thickness
δ_m	transformed boundary layer thickness
δ^*	semi-thickness of incompressible wake
θ	momentum thickness $\theta = \int_0^\delta \bar{\rho} \bar{u} (1 - \bar{u}) y dy$
θ_E	energy thickness $\theta_E = \int_0^\delta \bar{\rho} \bar{u} (1 - \bar{H}) y dy$
θ_i	i^{th} species thickness $\theta_i = \int_0^\delta \bar{\rho} \bar{u} (\alpha_{ie} - \alpha_i) y dy$
μ	absolute viscosity
ρ	density
ρ_{di}	characteristic density for molecular species (Eq. 24f)
Λ	defined (Eq. 25)

SUBSCRIPTS

c	initial conditions for wake calculations
e	conditions outside viscous layer
e^-	refers to electron
i	refers to i^{th} species
N	refers to atomic nitrogen
N_2	refers to molecular nitrogen
NO^+	refers to ionized nitric oxide

- o values evaluated along axis
- O refers to atomic oxygen
- O₂ refers to molecular oxygen
- s denotes total differentiation with respect to indicated variable
- st stagnation values behind normal shock
- t turbulent
- x, y denotes partial differentiation with respect to indicated variable
- ∞ undisturbed flight conditions

SUPERSCRIPTS

- denotes non-dimensional quantities unless otherwise specified

$$\bar{u} = \frac{u}{u_e}, \quad \bar{\rho} = \frac{\rho}{\rho_e}, \quad \bar{H} = \frac{H}{H_e}, \quad \bar{\mu} = \frac{\mu}{\mu_e}, \quad \bar{h} = \frac{h}{h_e}, \quad \bar{T} = \frac{T}{T_e}$$

- * incompressible

APPENDIX A

The equations governing the flow of multicomponent gas mixtures are discussed in considerable detail by Hirschfelder, Curtiss and Bird (Reference 14; see particularly Chapters 7, 8 and 11). In this appendix we shall pay particular attention to the diffusion velocities V_i of the several species. The diffusion velocity of a given species represents the mass-averaged velocity of the species measured with respect to the mass-averaged velocity of the mixture. Here, the mixture velocity is represented by the components u and v .

The boundary-layer equation of mass conservation of species in the wake is given in terms of V_i as follows:

$$(\rho u a_i)_x + (\rho v a_i)_y = (y \rho a_i V_i)_y + \rho y w_i \quad (\text{A.1})$$

At the symmetry axis, $y = 0$, this equation takes the form

$$u a_{ix} = 2 a_i V_{iy} + \rho w_i \quad (\text{A.2})$$

Contributions to the diffusion velocity are made by several phenomena. Only one class, gradients of the concentration of species, are expected to be significant in the present instance. Their effects are usually termed "mass diffusion". The other processes, such as thermal diffusion, pressure diffusion, external forces, and the Dufour effect, are neglected here. The diffusion velocities in a gas with ν components can be expressed in terms of the binary - diffusion coefficients D_{ij} (not to be confused with the

more artificial "multicomponent diffusion coefficients") by the following set of relations (Reference 14, p. 516):

$$(1/n) \sum_{\substack{j=1 \\ j \neq i}}^v (n_j / D_{ij})(V_j - V_i) = \nabla \ln(n_i / n) \quad (\text{A.3a})$$

$$\sum_i n_i m_i V_i = 0 \quad (\text{A.3b})$$

where n_i is a number density (particles/cc), $n = \sum_i n_i$, $n_i m_i = \rho a_i$, m_i is the particle mass, and $D_{ij} = D_{ji}$.

For a binary mixture (A.3a) yields one relation and (A.3b) another. From these we obtain

$$V_i = -D_{12} \nabla \ln a_i \quad i = 1, 2 \quad (\text{A.4})$$

thus indicating the significance of the binary coefficients D_{ij} . Theoretical and experimental data for estimating the transport properties D_{ij} for a variety of pairs of species are given in Reference 14.

For other than binary mixtures the expressions for the V_i are more complex. In particular we shall be interested here in a quadruple mixture of O, N, O₂ and N₂. In general each V_i is a linear function of the concentration gradients of the several species, the coefficients being functions of the D_{ij} and the species concentrations. However, when the particle weights of the species are not extremely different from each other, the D_{ij} will not

differ substantially in magnitude from each other. Species such as O, N, O₂, N₂ and NO can be considered suitable for approximations involving average particle-weights and average diffusion coefficients. An approximation along these lines will now be suggested for use here.

The quantity $\nabla \ln (n_i / n)$ is re-expressed in terms of the mass fractions a_i as follows:

$$\nabla \ln (n_i / n) = \left(\frac{\rho}{n} \right) \left(\frac{\nabla a_i}{a_i} \right) \left[\sum_{j \neq i}^v \frac{a_j}{m_j} - \left(\frac{a_i}{\nabla a_i} \right) \frac{\nabla a_j}{m_j} \right] \quad (\text{A.5a})$$

For a binary mixture, the term enclosed in square brackets in (A.5a) is equal to $1/m_j$. Likewise, for an average value of the particle weights m_j , but for any number of components, the term in brackets equals $1 / (m_j)_{av}$; in this case,

$$\nabla \ln (n_i / n) \simeq (1/m_j)_{av} (\rho/n) (\nabla a_i / a_i) \quad (\text{A.5b})$$

The left side of (A.3a) can be rewritten as

$$(\rho/n) \sum_{j \neq i}^v (a_j / m_j D_{ij}) (V_j - V_i) \quad (\text{A.5c})$$

For average values $(m_j)_{av}$ and $(D_{ij})_{av}$ this becomes

$$(\rho/n) (1/m_j D_{ij})_{av} (a_i V_i - V_i + a_i V_i) \simeq (\rho/n) (1/m_j D_{ij})_{av} (-V_i) \quad (\text{A.5d})$$

Equation of (A.5b) and (A.5d) yields an approximation to (A.3a) for a multicomponent mixture with particle weights of the same order, namely,

$$V_i \approx - (D_{ij})_{av} \nabla a_i / a_i \quad (\text{A.5e})$$

This is the expression used in (4) with $Le \equiv \rho (D_{ij})_{av} \bar{c}_p / \lambda$,

$P = \mu \bar{c}_p / \lambda$, $\bar{c}_p = \sum_i a_i c_{pi}$. The V_i obtained from this relation automatically satisfy (A.3b).

With (A.5e) the heat flux which appears in the energy equation (3) takes the following form

$$\begin{aligned} q &= -\lambda \nabla T + \rho \sum_i a_i h_i V_i \\ &= -(\mu/P) \nabla h + (\mu/P)(1 - Le) \sum_i h_i \nabla a_i \end{aligned} \quad (\text{A.6})$$

Although there would be no difficulty in principle in obtaining solutions with more exact representations of the multicomponent V_i , the computational program would be substantially longer. Therefore it was considered to be sufficient, at least for initial calculations, to use (A.5e)

APPENDIX BEstimate of Prandtl number - Lewis number effects on the stagnation enthalpy parameter.

Consider (19c) in the following form, with $H \equiv \bar{H}_O$ and $u \equiv \bar{u}_O$:

$$dH/du = (1 - H)/(1 - u) + B \quad (B.1)$$

where

$$B \equiv \frac{1 - P_O}{P_O} \left[\frac{1 - H}{1 - u} - \frac{u_e^2}{H_e} u \right] + \frac{(Le_O - 1)}{P_O} \frac{\sum_i h_{iO} (a_{ie} - a_{iO})}{H_e (1 - u)}$$

The summation of static enthalpy in B may be treated as follows :

$$\sum_i h_{iO} (a_{ie} - a_{iO}) = \sum_i h_{iO} a_{ie} - h_O = \sum_i h_{iO} a_{ie} - \left(H_O - \frac{u_O^2}{2} \right) \quad (B.2)$$

In the air-wakes under consideration here, it is assumed that the atomic species in the outer flow are negligible. Hence the a_{ie} terms represent only molecular species. According to the conventions of statistical thermodynamics, the dissociation energies do not appear in the expressions for the enthalpies of the molecular species. Hence, for the molecular species treated as perfect gases

$$h_i = \int_0^T c_{P_i} (T) dT \quad (B.3)$$

where c_{P_i} takes into account the translational and vibrational degrees of freedom. For O_2 and N_2 , c_{P_i} has a value on the order of $8000 \text{ ft}^2 / \text{sec}^2 \text{ } ^\circ\text{R}$

at elevated temperatures. In this estimate we need not distinguish between O_2 and N_2 in view of their similar molecular weights. Hence we may consider $\alpha_{ie} = 1$ and $h_i \simeq (8000 \text{ ft}^2/\text{sec}^2 \text{ } ^\circ\text{R}) T$, and (B.2) becomes

$$(8000 \text{ ft}^2/\text{sec}^2 \text{ } ^\circ\text{R}) T_o \simeq (H_o - u_o^2/2) \quad (\text{B.3})$$

At hypersonic speeds, $H_e \simeq u_e^2/2$, and division of (B.3) by H_e yields

$$(8000 \text{ ft}^2/\text{sec}^2 \text{ } ^\circ\text{R}) T_o / (u_e^2/2) \simeq (H - u^2) \quad (\text{B.4})$$

For u_e on the order of 20,000 ft/sec (B.4) becomes

$$0.04 (T/1000 \text{ } ^\circ\text{R}) \simeq H - u^2 \quad (\text{B.5})$$

In the far-field wake H is expected to have values on the order of unity, u varies between approximately 0.5 and 1.0, and temperatures on the order of several thousand $^\circ\text{R}$ may be expected. Hence the factor in (B.5) will be a negative fraction, and the corresponding coefficient of $(Le_o - 1)/P_o$ in the definition of B will be a negative quantity on the order of unity. This estimate probably is valid even as $u \rightarrow 1$, since the numerator of the coefficient as represented by (B.5) becomes very small in this regime.

The coefficient of $(1 - P_o)/P_o$ in the definition of B may be assumed with the use of (18) under hypersonic conditions as follows:

$$(1-H)/(1-u) - (u_e^2/H_e)u \simeq (1-H_c)/(1-u_c) - 2u \simeq -2u \quad (\text{B.6})$$

Therefore

$$B \approx - \left[\frac{(1 - P_o)}{P_o} (2u) + \frac{(Le_o - 1)}{P_o} \psi \right] \quad (B.7)$$

where ψ is a positive quantity on the order of unity. Since, for air $1 - P_o \approx Le_o - 1$, it is seen that for the present conditions of interest, B is a negative quantity whose magnitude is on the order of $(1 - P_o) / P_o$.

For a constant average value of B , Eq. (B.1) may be integrated to yield

$$\frac{1 - H}{1 - u} = \frac{1 - H_c}{1 - u_c} + /B/ \ln \left(\frac{1 - u_c}{1 - u} \right) \quad (B.8)$$

where the integration constant has been evaluated at the initial station where values are designated by the subscript c .

Thus it is seen that the Prandtl number - Lewis number term has the effect of delaying the approach of H to unity as $u \rightarrow 1$.

TABLE I

FLIGHT CONDITION		150,000' 18,900'/sec	200,000' 20,200'/sec	250,000' 20,400'/sec
P_{∞}	#/sq ft	2.940	0.460	0.040
ρ_{∞}	slug/ft ³	3.39×10^{-6}	5.88×10^{-7}	6.55×10^{-8}
T_{∞}	^o R	504	454	354
μ_{∞}	# sec/ft ²	35.8×10^{-8}	33.8×10^{-8}	27.1×10^{-8}
M_{∞}		17.2	19.3	22.3
$H_e = h_{st}$	ft ² /sec ²	1.81×10^8	2.07×10^8	2.10×10^8
P_{st}	#/sq ft	1210.0	240.0	27.30
ρ_{st}	slug/ft ³	4.67×10^{-5}	9.26×10^{-6}	1.11×10^{-6}
T_{st}	^o R	11,000	10,400	9,700
a_{st}	mass fraction	0.365	0.445	0.475
a_{st}^o	mass fraction	0.232	0.232	0.232
a_{st}^N	mass fraction	0.133	0.213	0.245
$a_{st}^{NO^+}$	mass fraction	0.563×10^{-3}	0.566×10^{-3}	0.485×10^{-3}
$n_{st}^{NO^+}$	$\frac{\text{particles}}{\text{cc}}$	2.73×10^{14}	5.45×10^{13}	5.60×10^{12}
ρ_{co}	slug/ft ³	7.42×10^{-7}	1.35×10^{-7}	1.49×10^{-8}
T_{co}	^o R	1672.0	1352.0	1125.0
$n_{co}^{NO^+}$	$\frac{\text{particles}}{\text{cc}}$	4.44×10^{12}	8.13×10^{11}	6.89×10^{10}
\bar{H}_{co}		1.0	1.0 0.9	1.0
\bar{u}_{co}		0.692	0.656 0.574	0.634
θ_{co}		0.0065	0.0071 0.0083	0.0074
$C = \frac{198.6}{T_{\infty}}$		0.394	0.437	0.564
I_{NO^+}	electron volt	9.258	9.258	9.258
D_{NO}	electron volt	6.42	6.42	6.42
D_{O_2}	electron volt	5.1155	5.1155	5.1155
D_{N_2}	electron volt	9.756	9.756	9.756

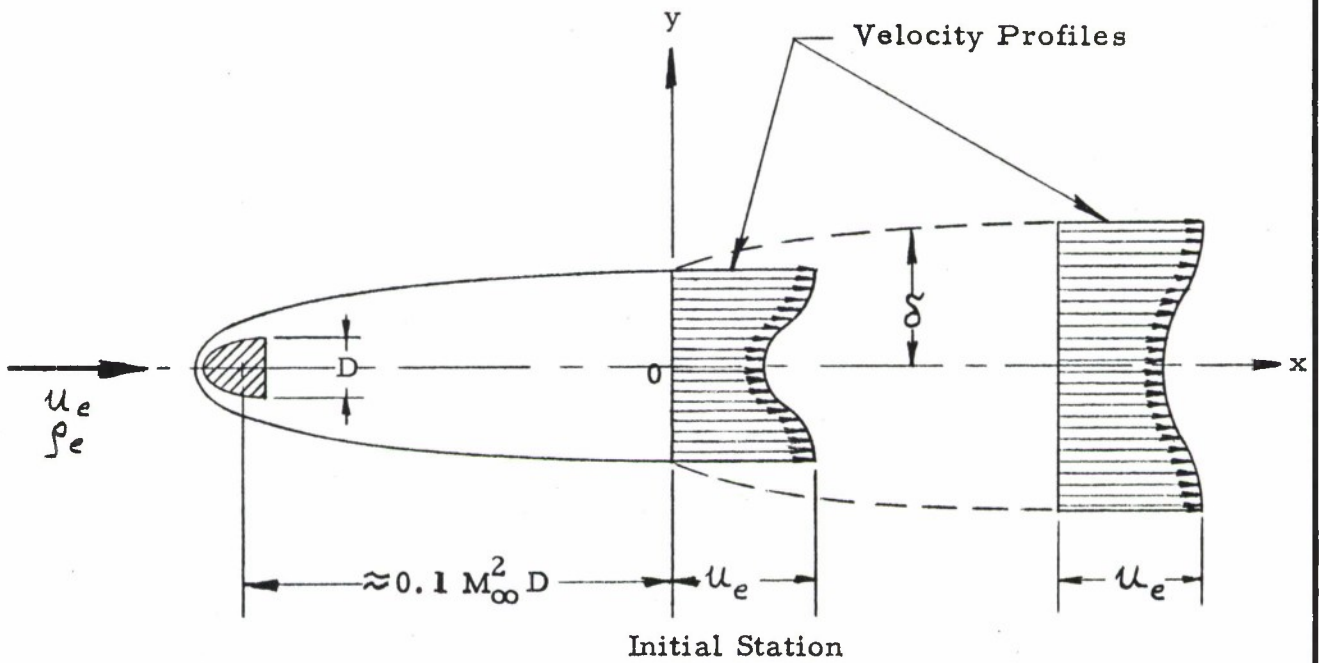


Figure 1. Schematic Diagram of Far-Field Wake

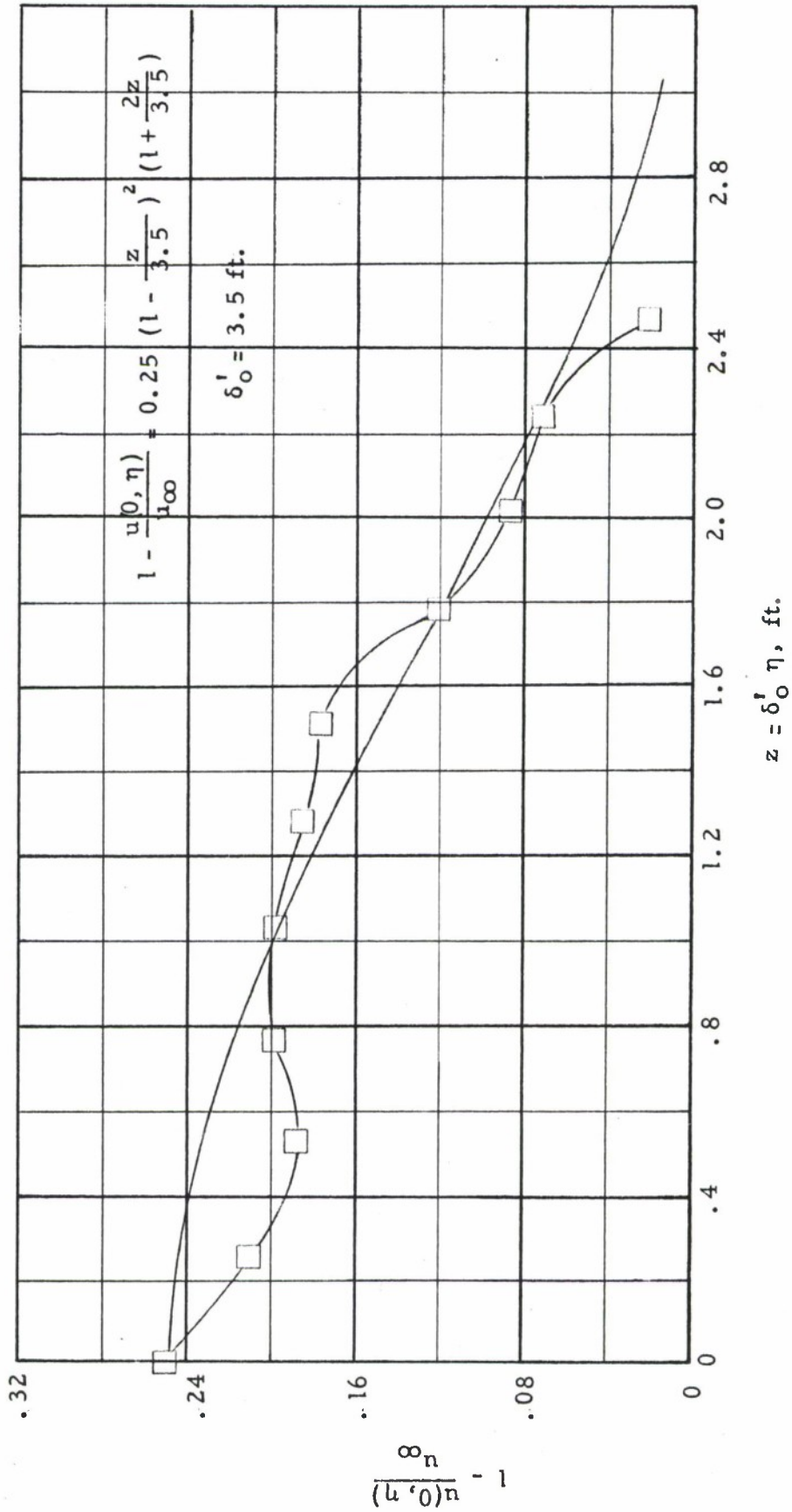


Figure 2a- Initial Velocity Profile for Equilibrium Flow

Figures and Notations are from Reference 7.

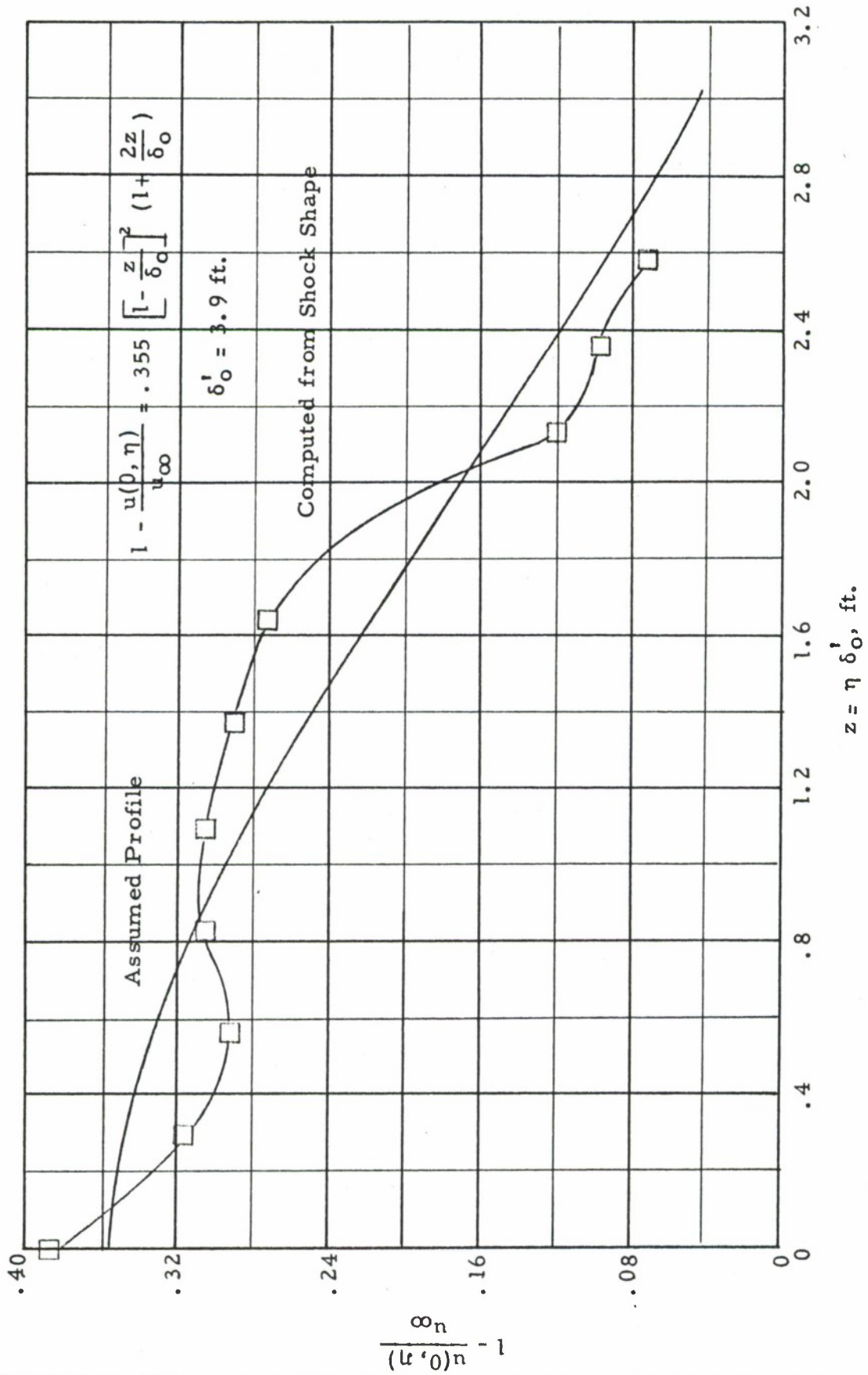


Figure 2b-Initial Velocity Profile for Frozen Flow

Figures and Notations are from Reference 7.

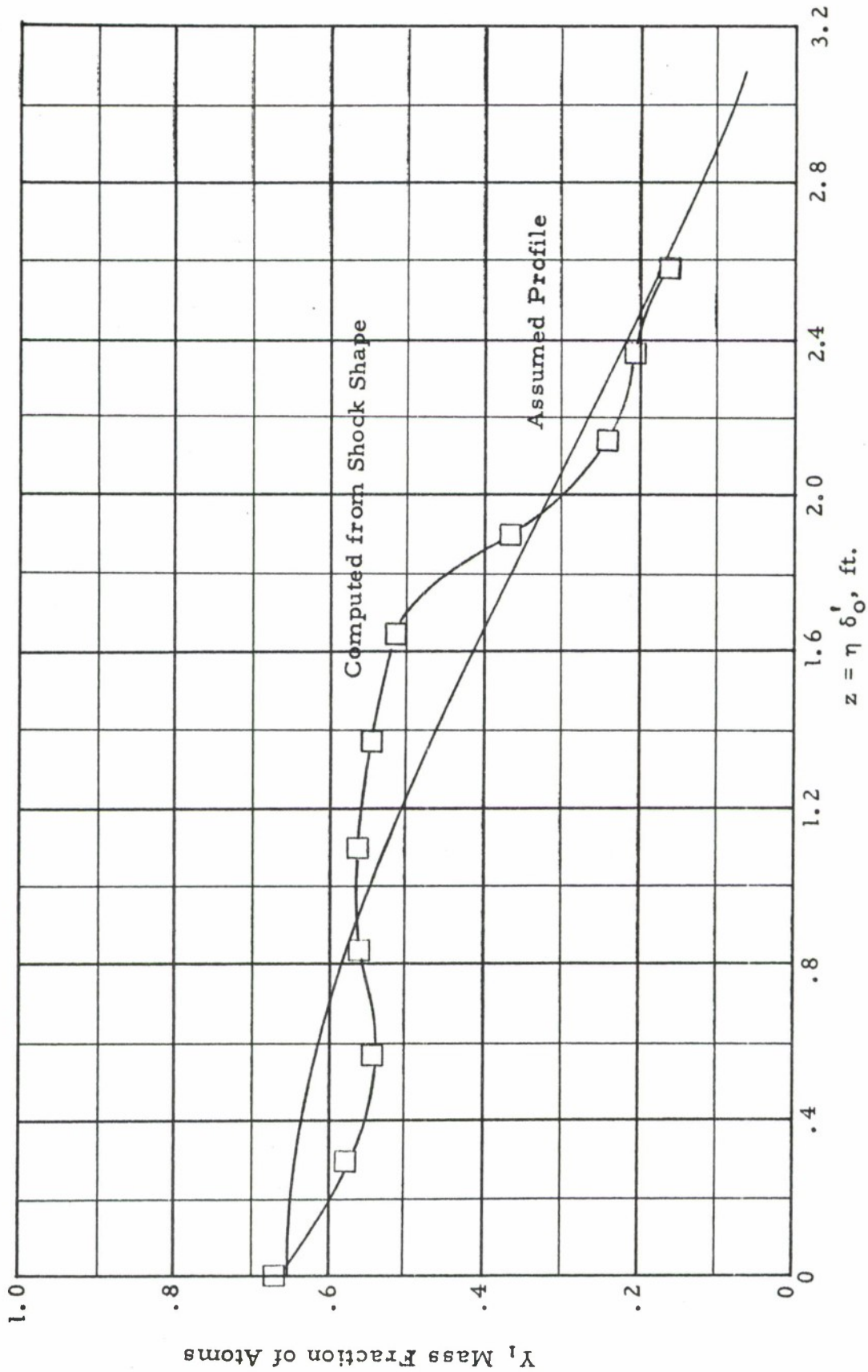


Figure 2c- Initial Mass Fraction of Atoms for Frozen Flow

Figures and Notations are from Reference 7.

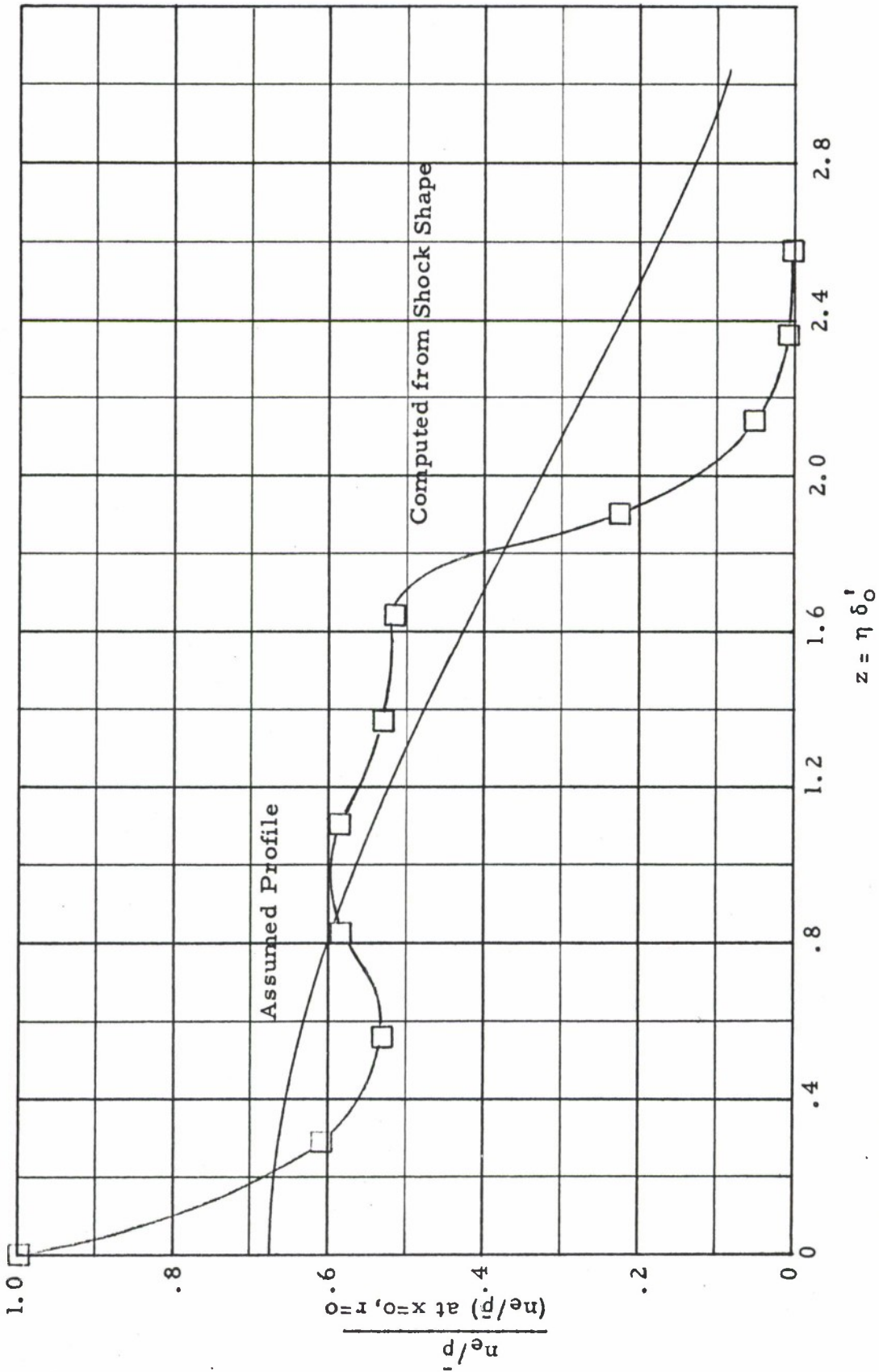


Figure 2d- Initial Profile of Electrons per Unit Mass for Frozen Flow, Initial Data

Figures and Notations are from Reference 7.

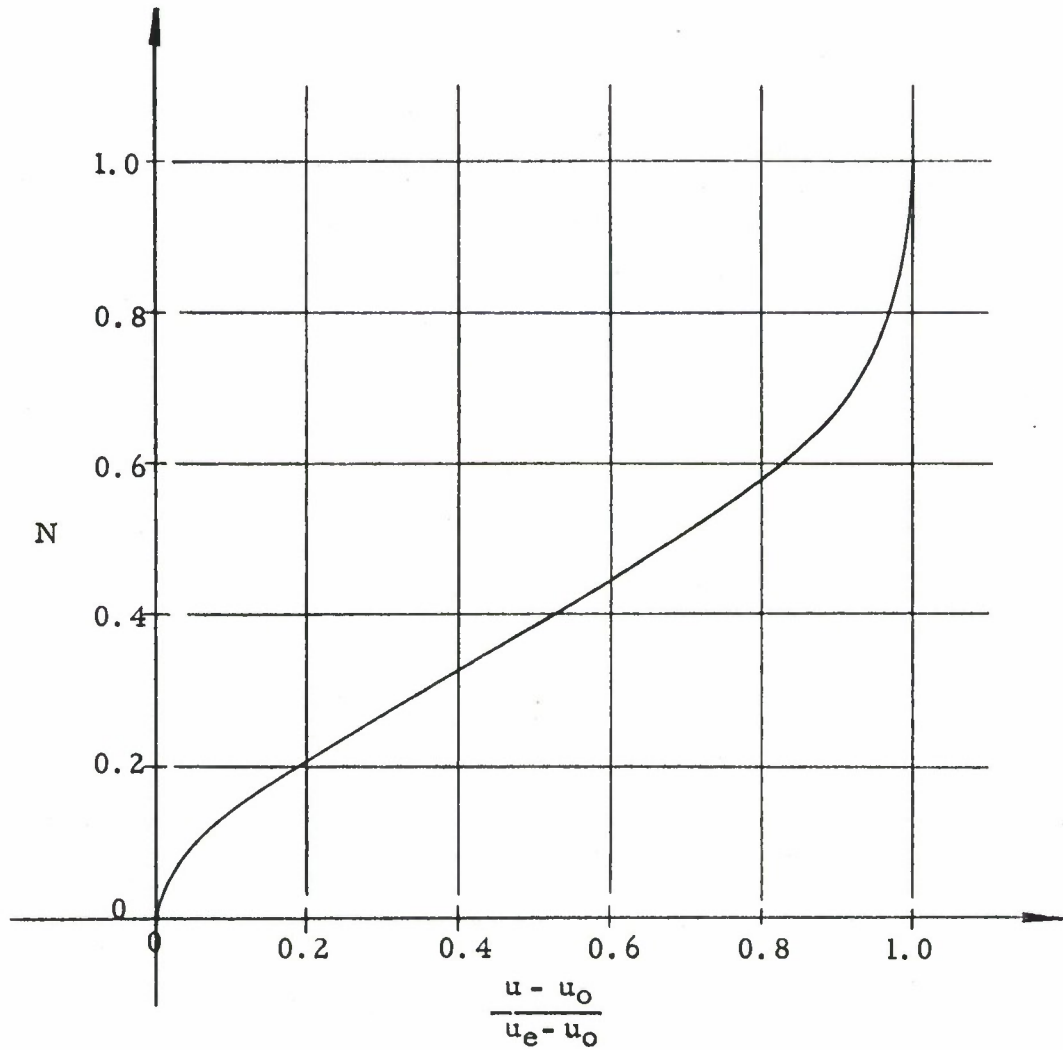


Figure 3. Quadratic Velocity Profile (Eq. 13a)

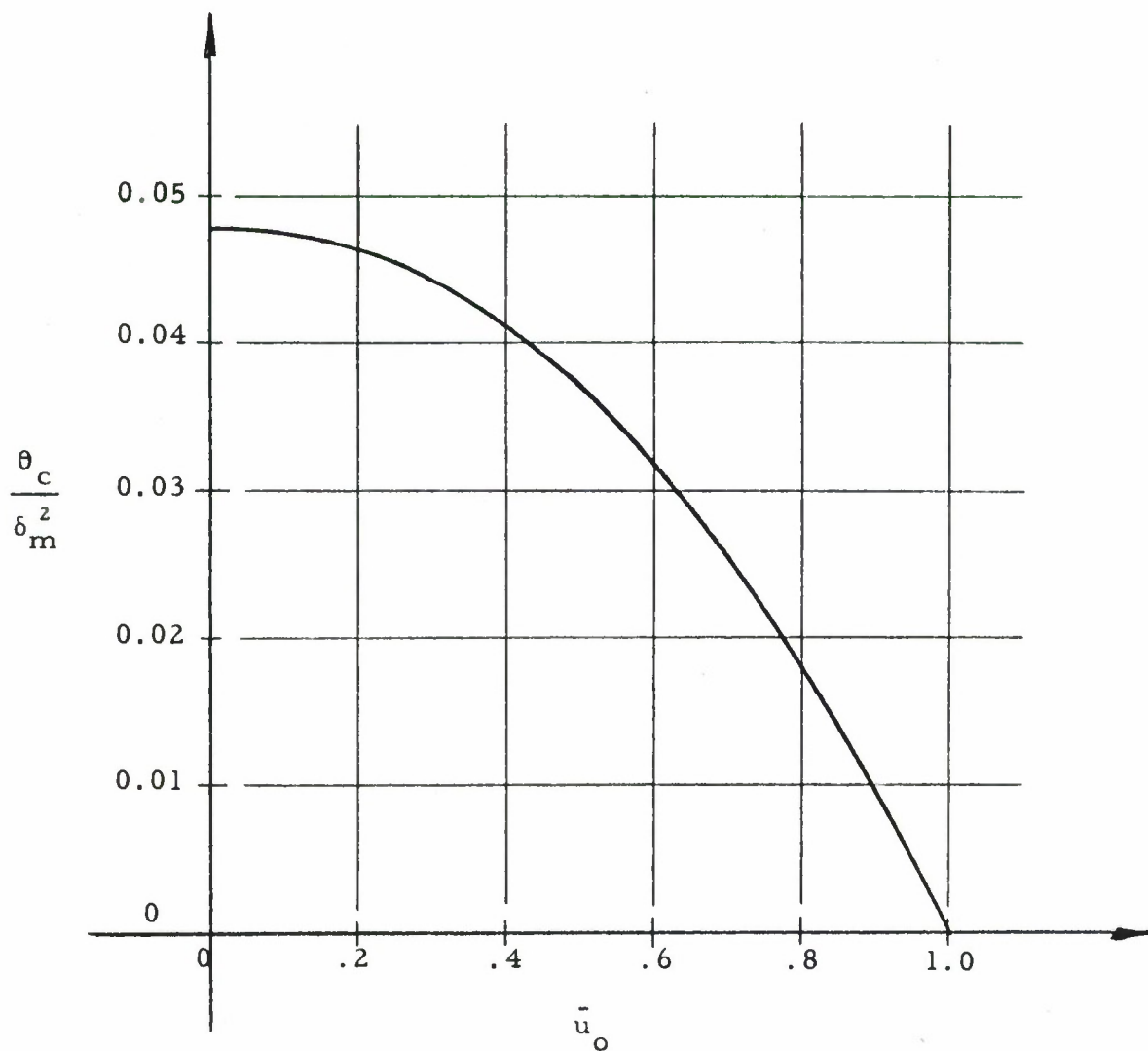
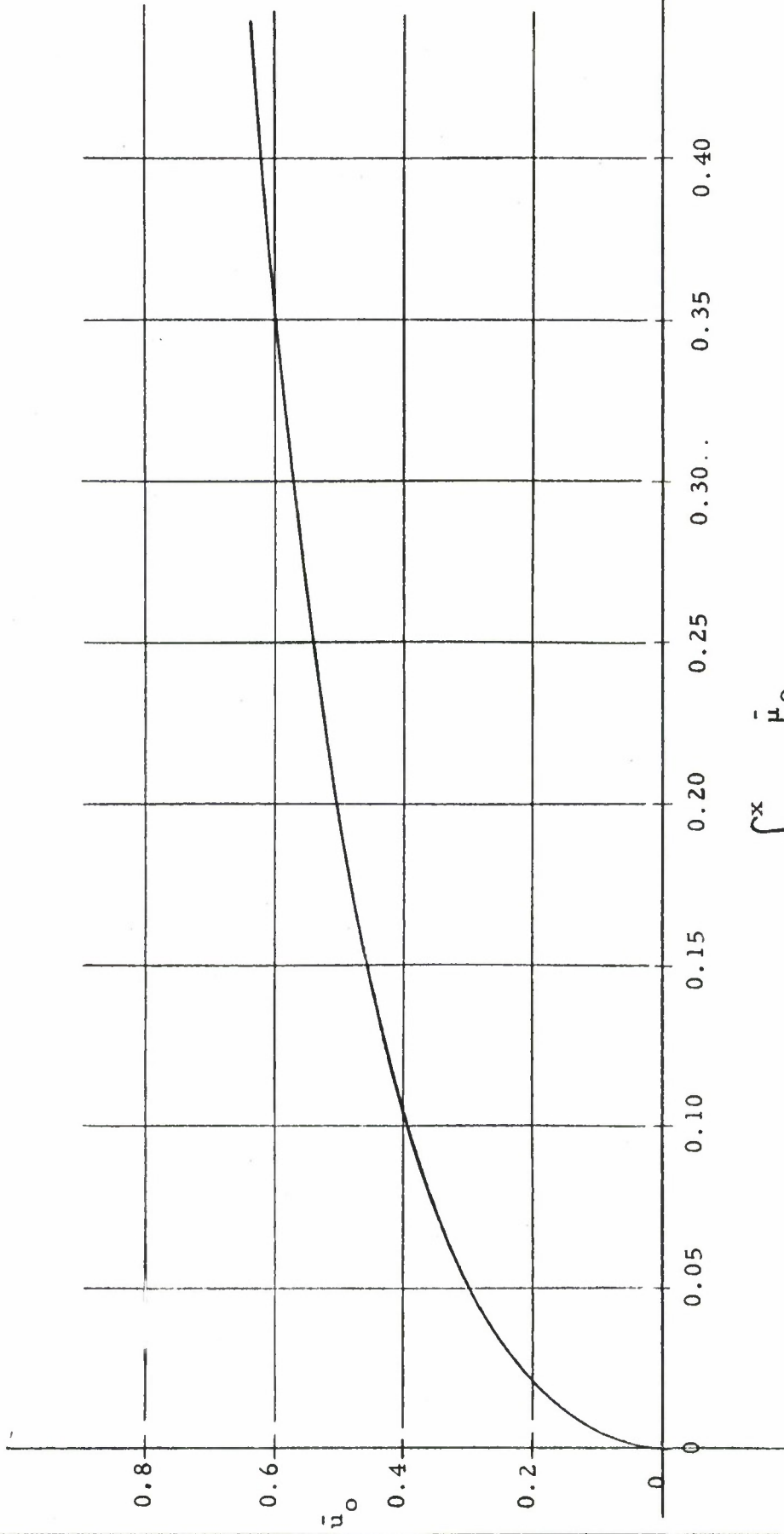


Figure 4. Plot of $\frac{\theta_c}{\delta_m^2}$ versus \bar{u}_o (Eq. 16)



$$s-s_c = \int_{x_c}^x \frac{\bar{\mu}_0}{\rho_e u_e \theta_{oc}} dx$$

$$\frac{\mu_e}{\mu_e}$$

Figure 5a. Velocity parameter versus streamwise coordinate s (Eq. 17)

5b

$$s - s_c = \int_{x_c}^x \frac{\bar{\mu}_o}{\frac{\rho_e u_e \theta}{\mu_e} \frac{dx}{oc}} dx$$

10¹

10⁰

10⁻¹

10⁻²

10⁻³

0 0.2 0.4 0.6 0.8 1.0

u_o

Figure 5b. Velocity parameter versus streamwise coordinate s (Eq. 17)

$$\frac{1 - \bar{H}_O}{1 - \bar{u}_{Oc}} = \left(\frac{1 - \bar{u}_O}{1 - \bar{u}_{Oc}} \right) \left[\frac{1 - \bar{H}_{Oc}}{1 - \bar{u}_{Oc}} + |B| \ln \left(\frac{1 - \bar{u}_{Oc}}{1 - \bar{u}_O} \right) \right]$$

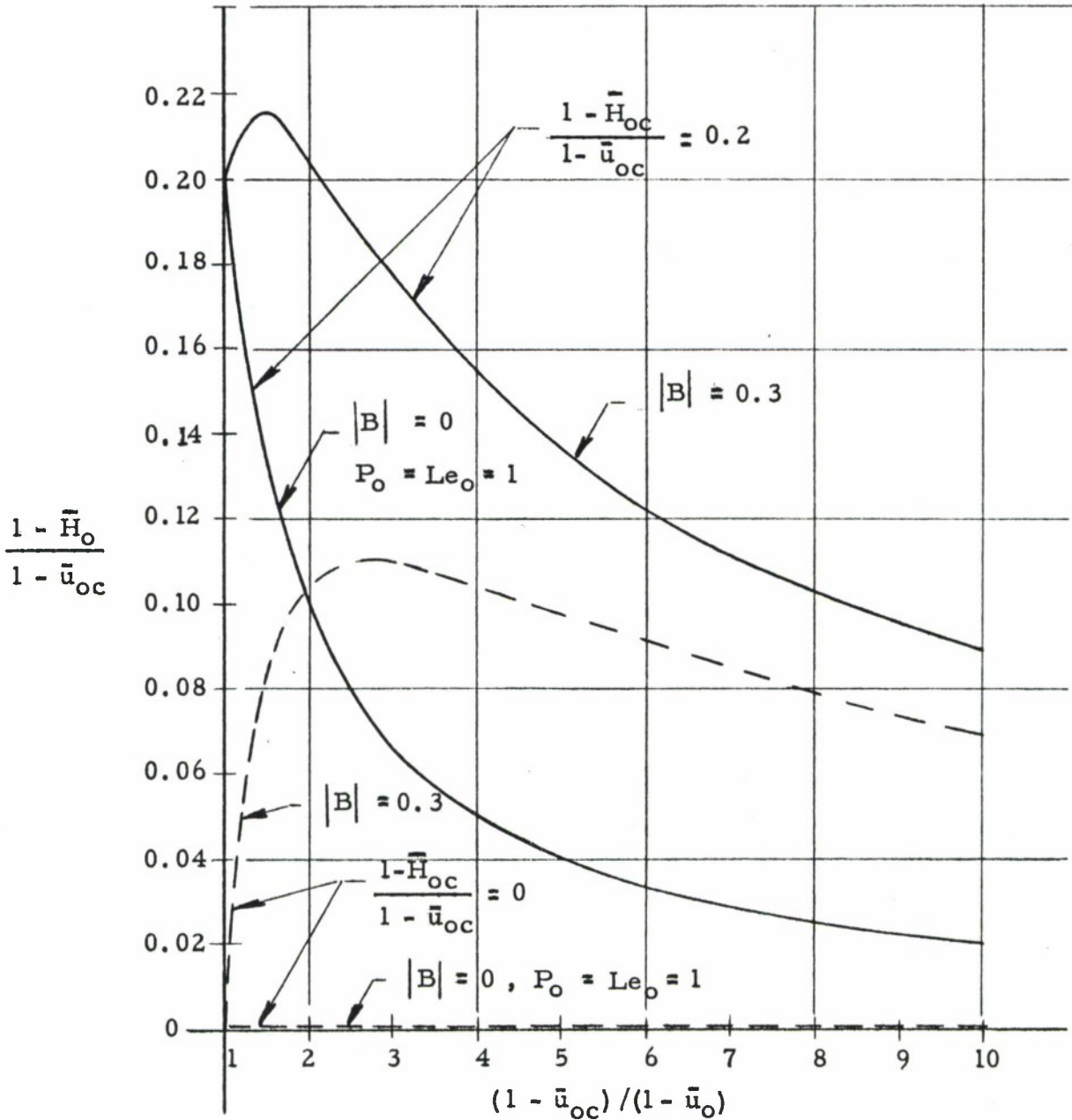


Figure 6. Rough Estimate of Effects of Prandtl Number and Lewis Number Deviations from Unity on the Stagnation Enthalpy-Velocity Relation.

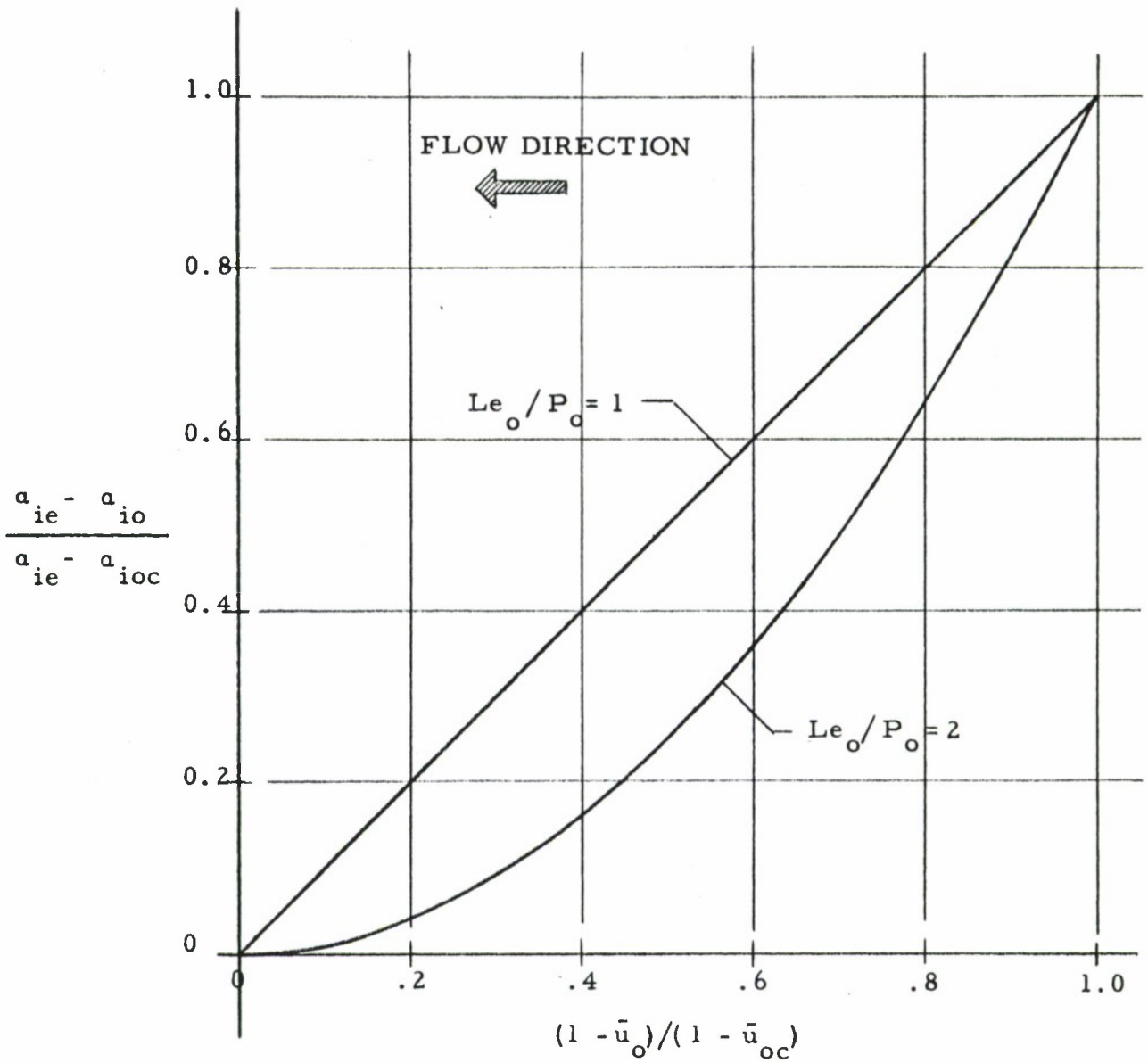


Figure 7a. Concentration parameter versus velocity for diffusion-controlled species with $Le_o/P_o = 1$ and 2.

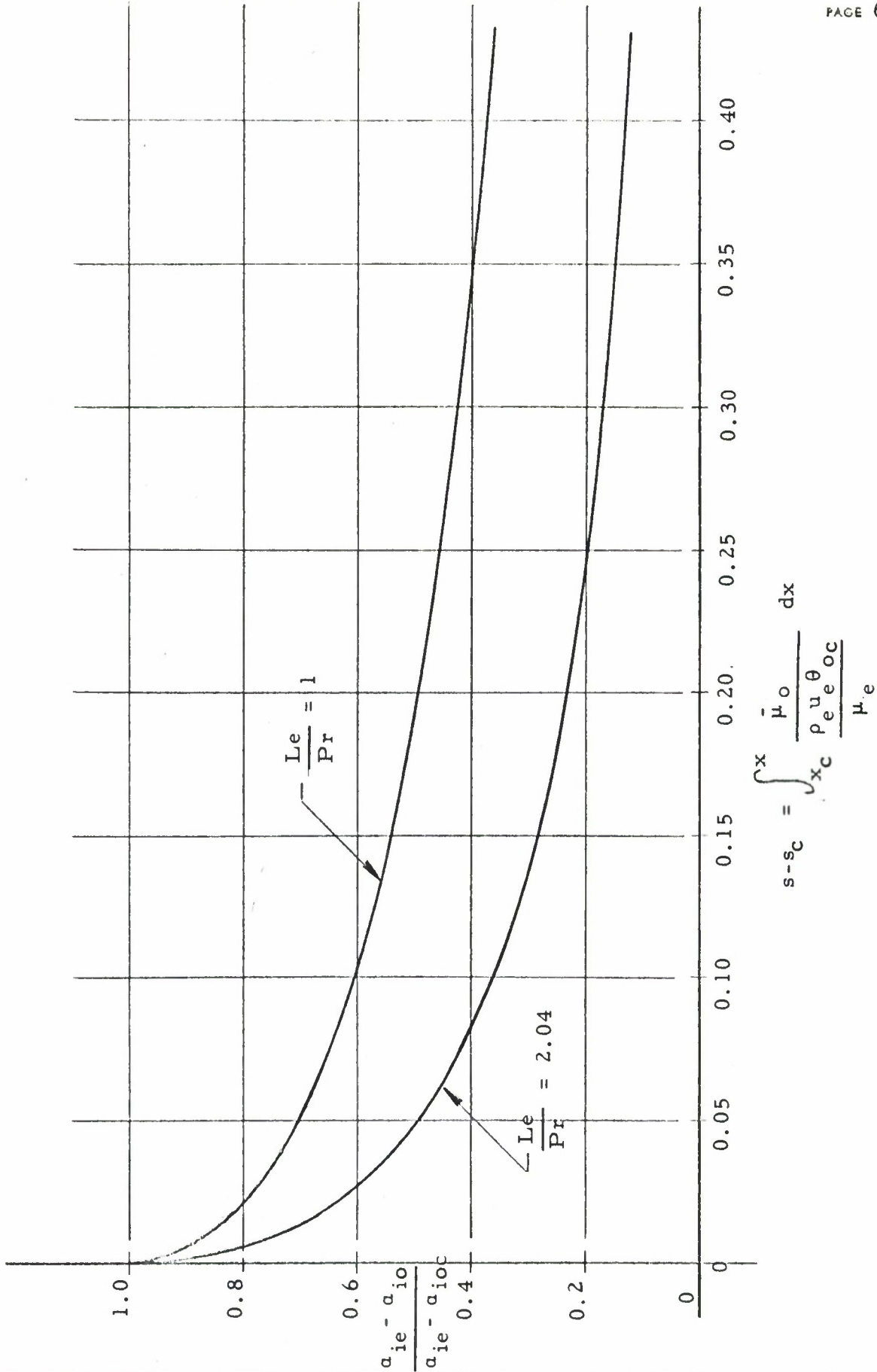


Figure 7b. Concentration parameter versus streamwise coordinate for diffusion-controlled species with $Le_o/P_o = 1$ and 2.04.

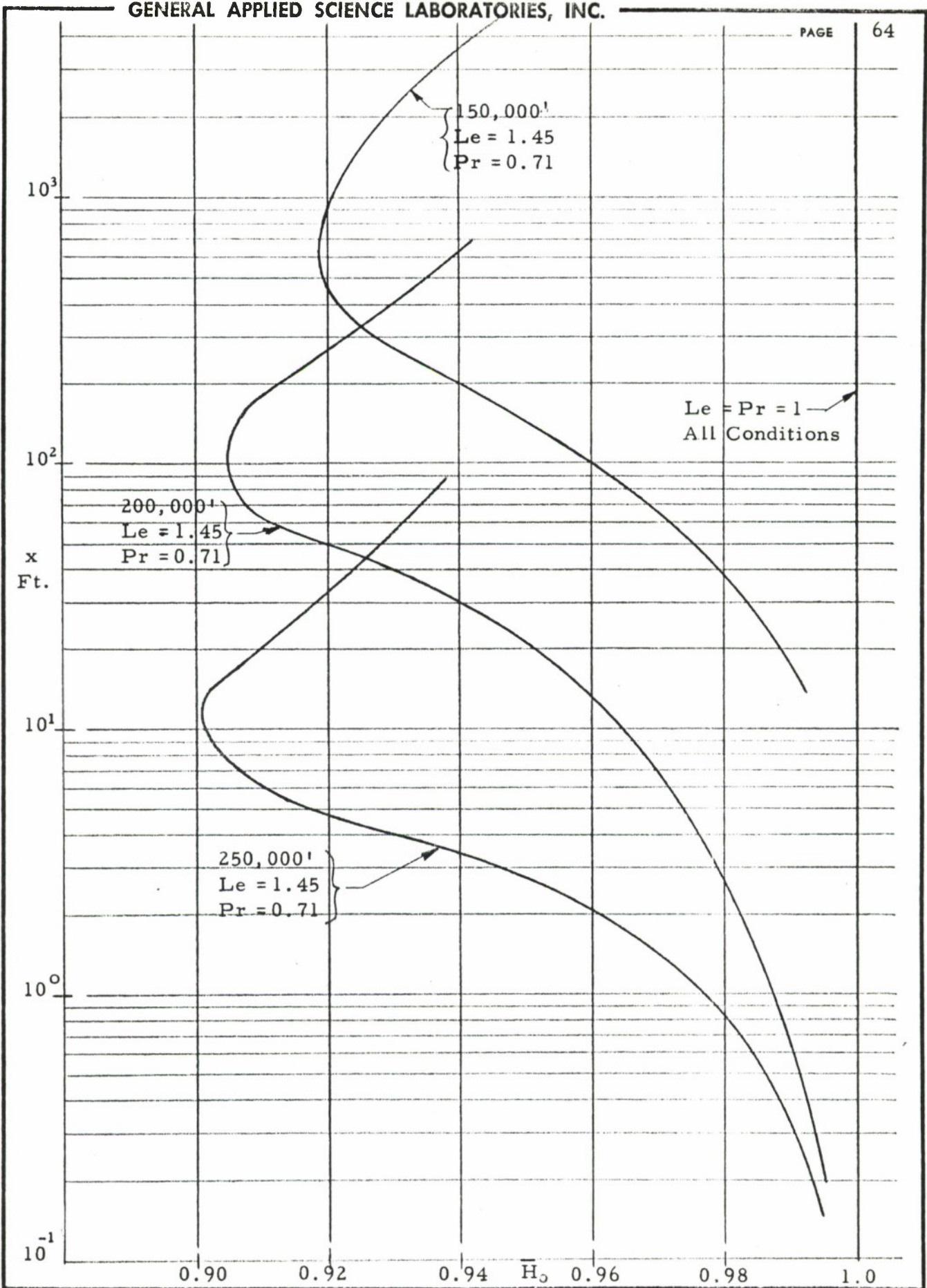


Figure 8a. Stagnation enthalpy variation along the axis $\left[\bar{H}_{0c} = 1 \right]$

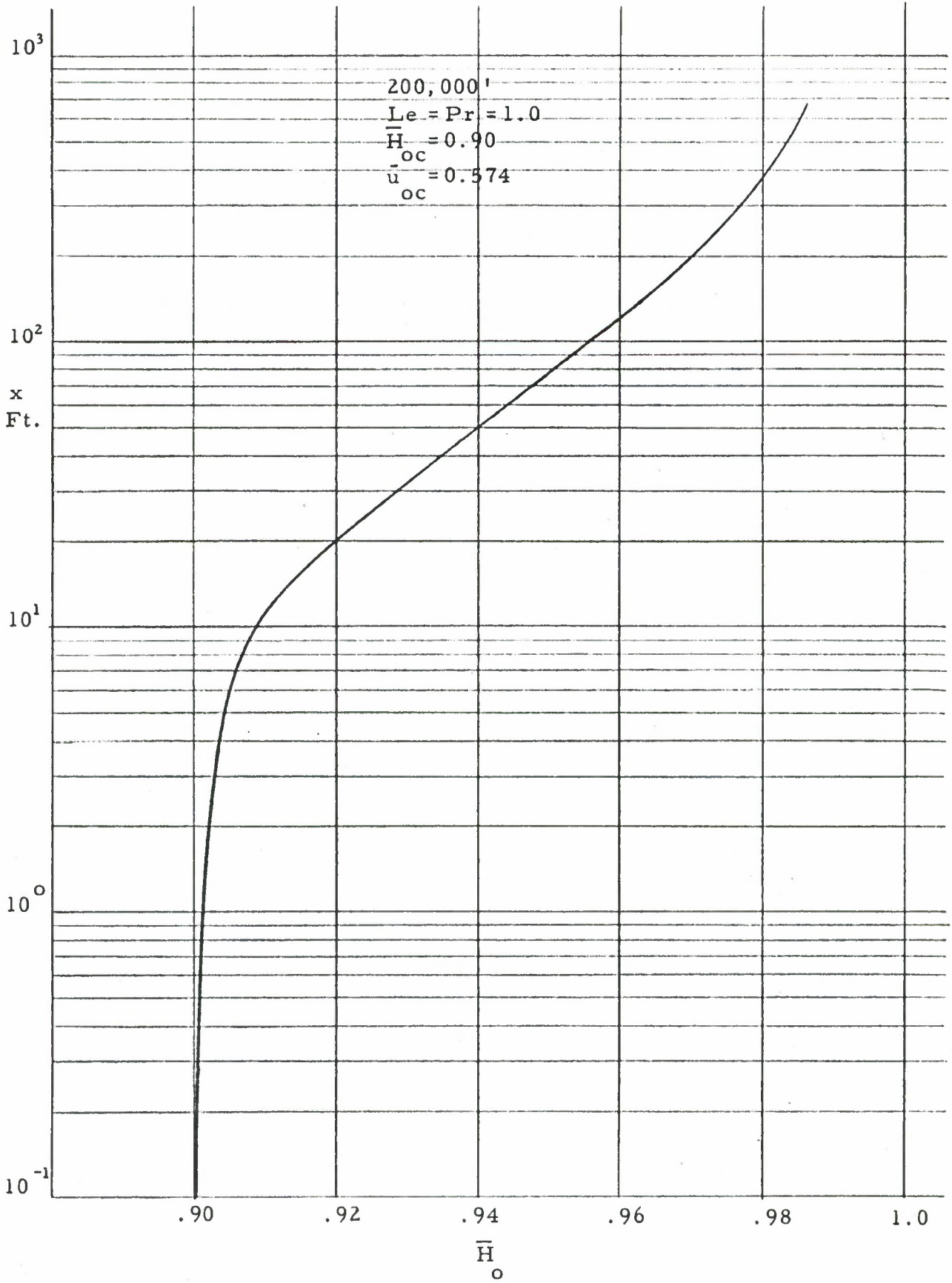


Figure 8b. Stagnation enthalpy variation along the axis.

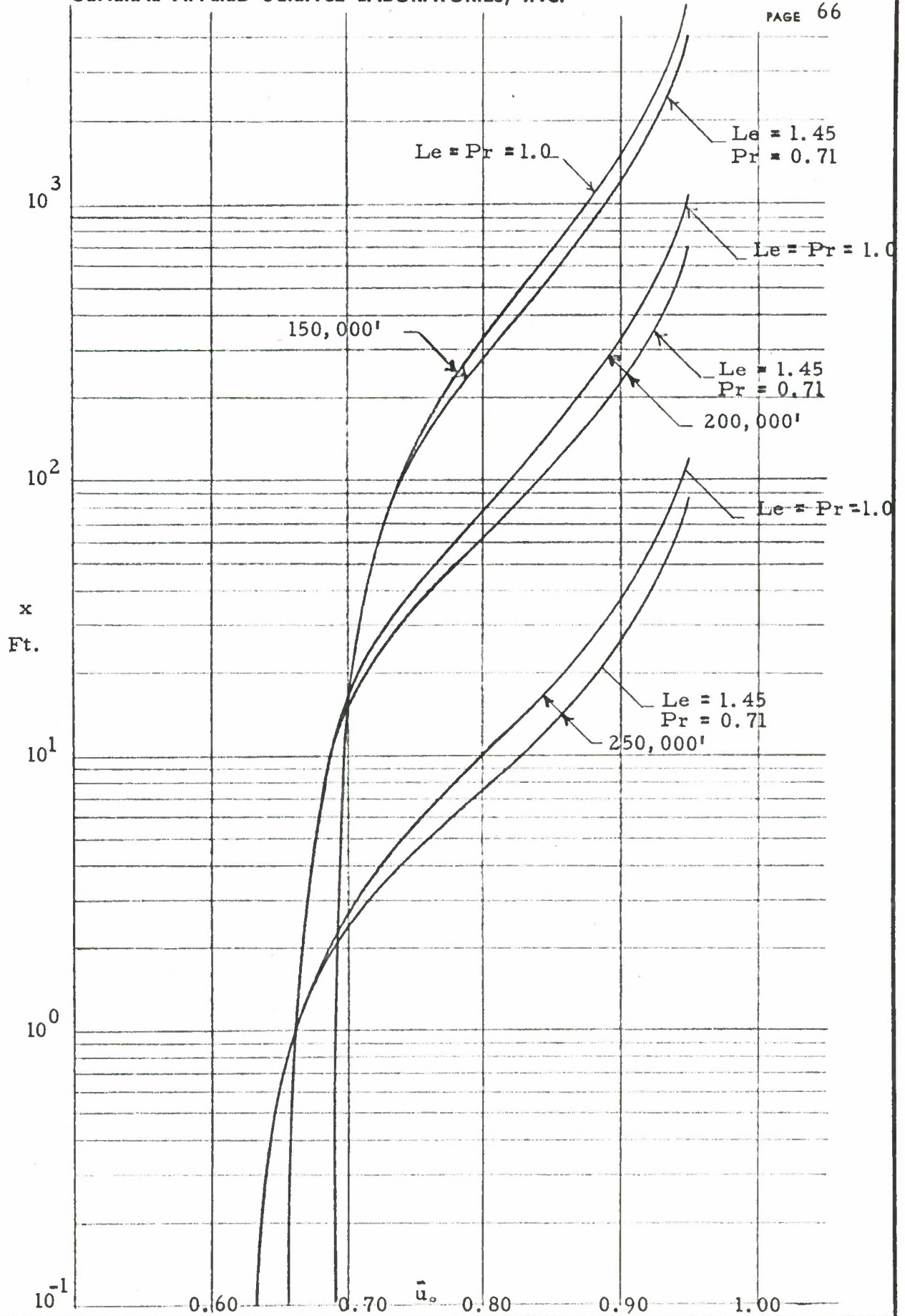


Figure 9a. Velocity Decay Along the Axis $[\bar{H}_{oc} = 1]$

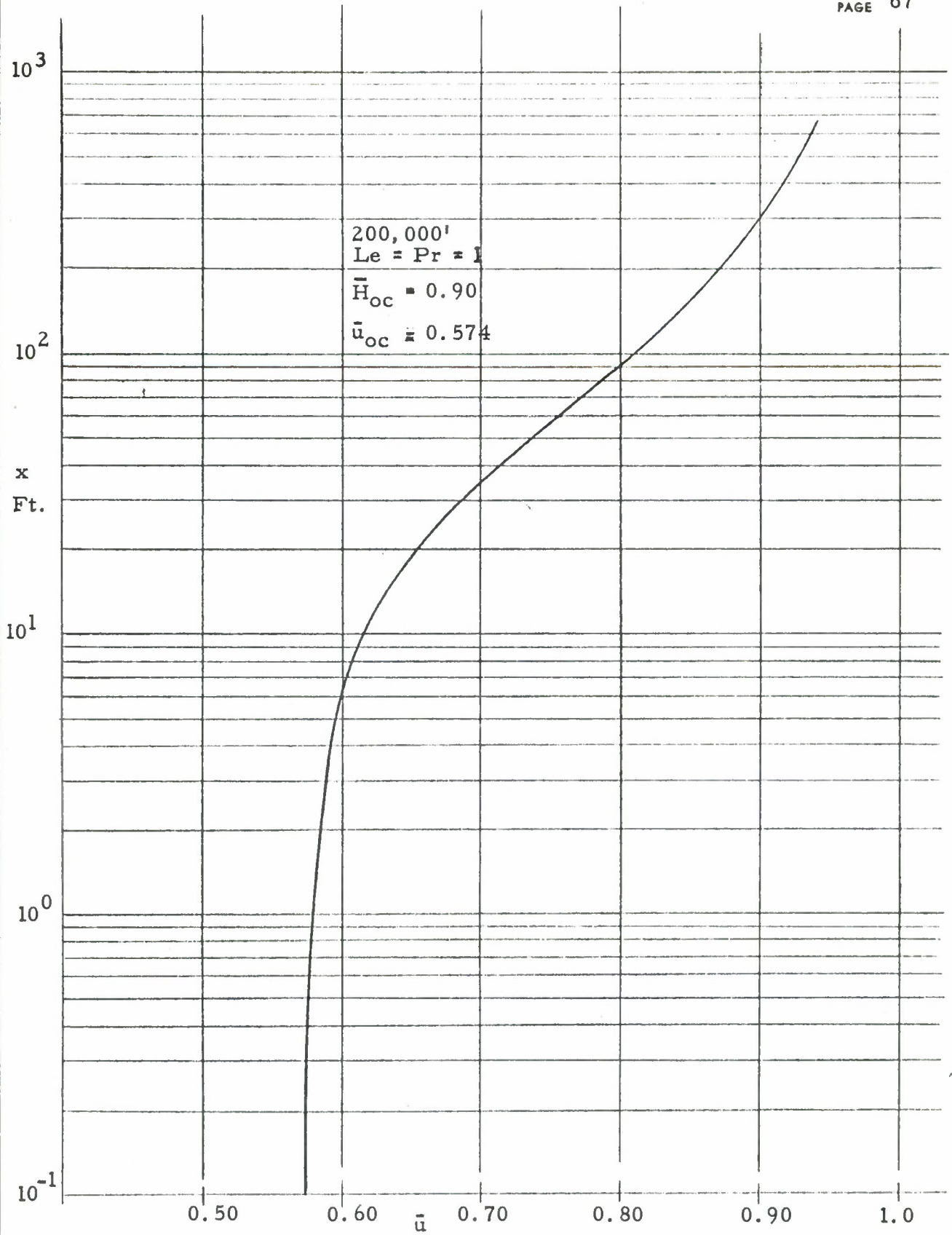


Figure 9b. Velocity Decay Along the Axis

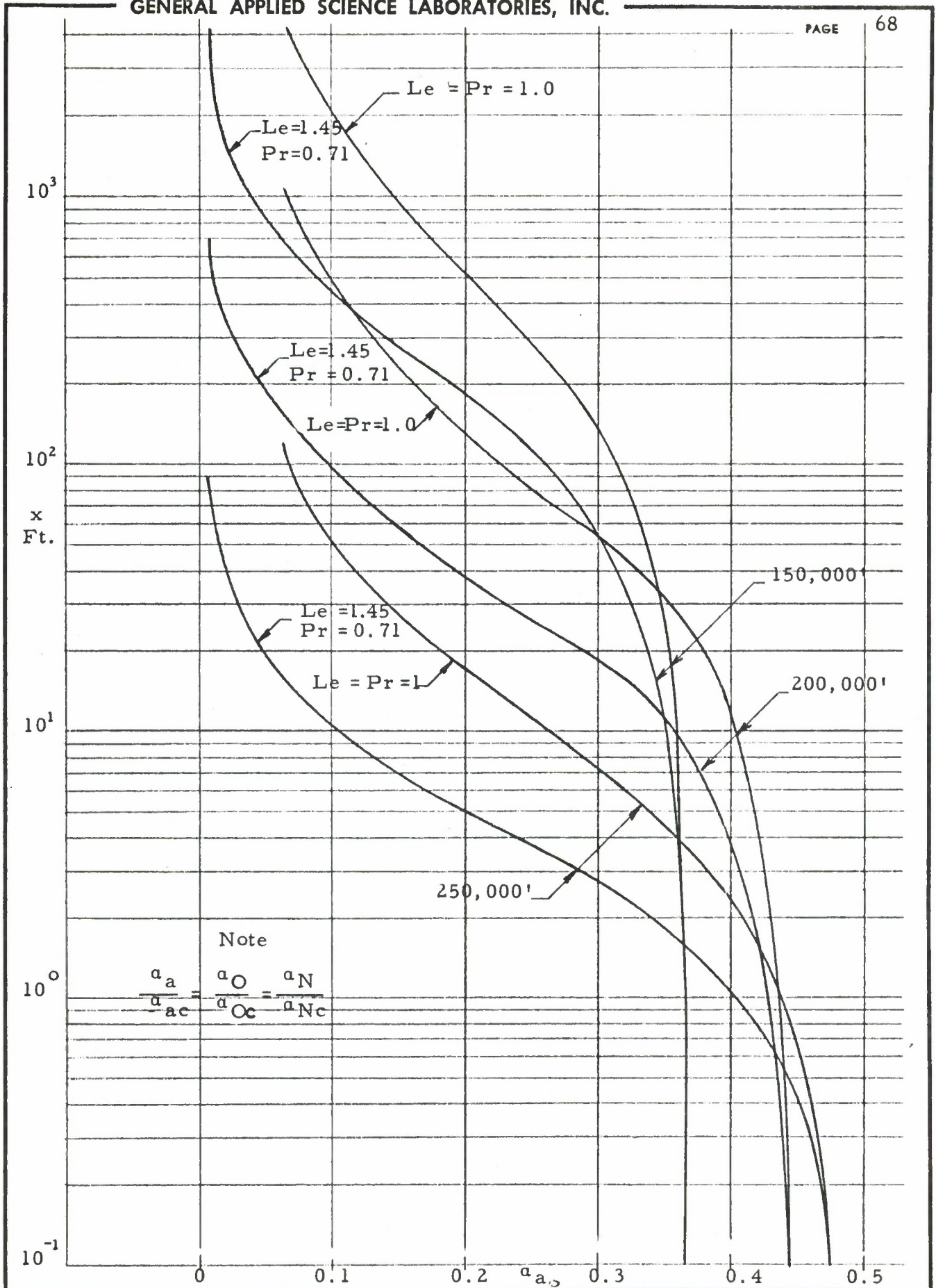


Figure 10a. Mass fraction of air, variation along the axis $\left[\bar{H}_{oc} = 1 \right]$

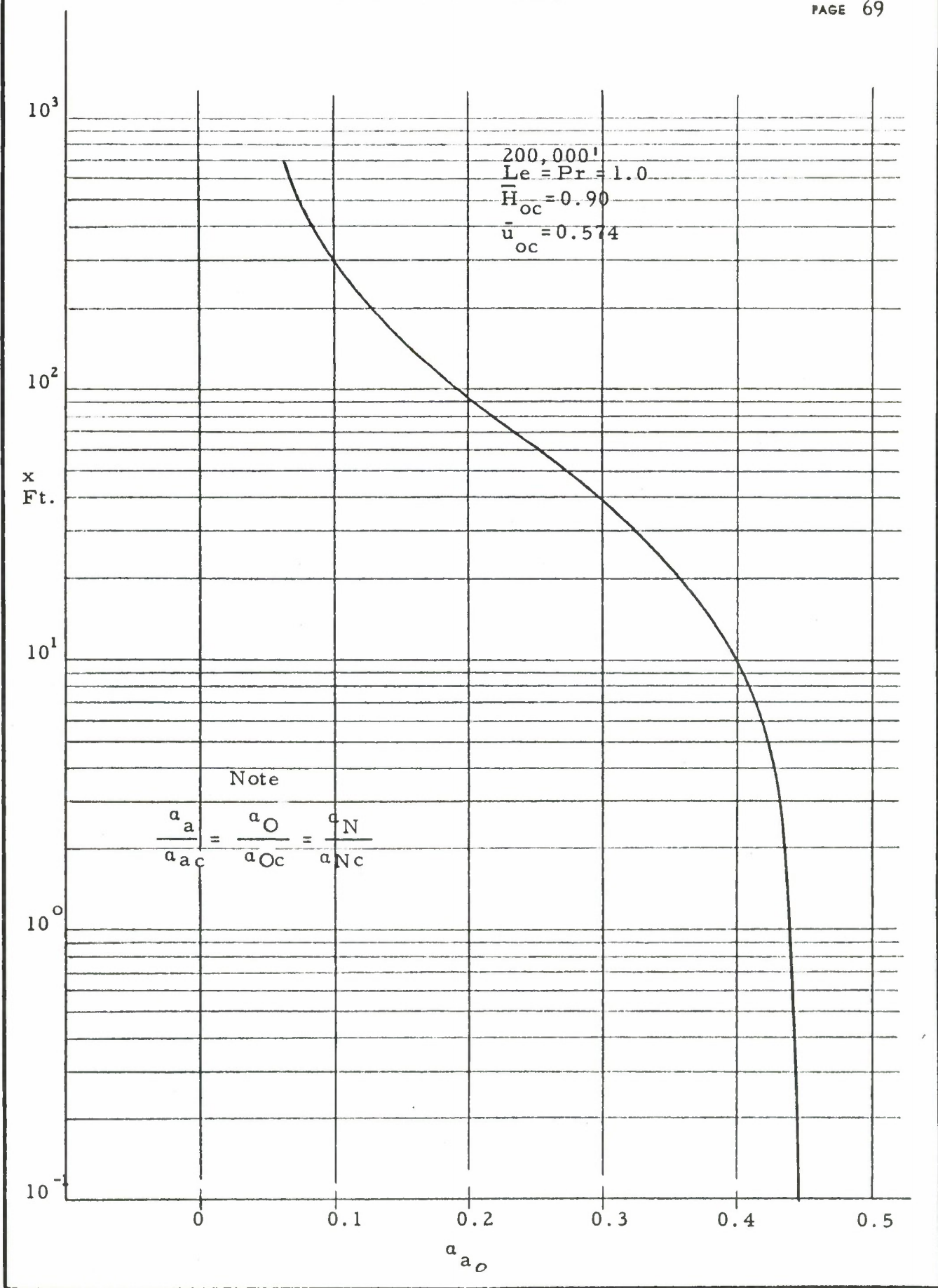


Figure 10b. Mass fraction of air, variation along the axis.

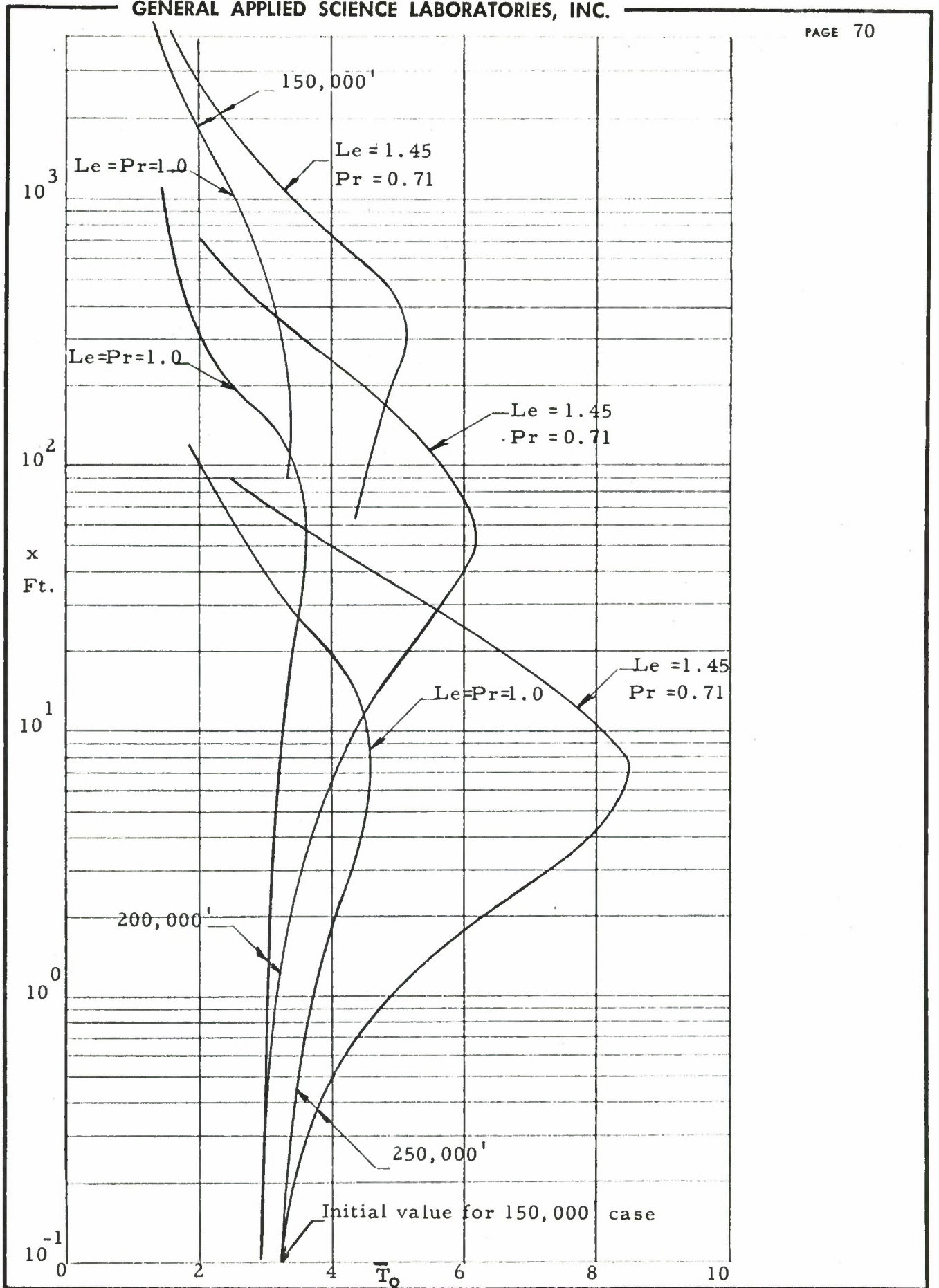


Figure 11a. Temperature of air, variation along the axis $\left[\bar{H}_{oc} = 1 \right]$

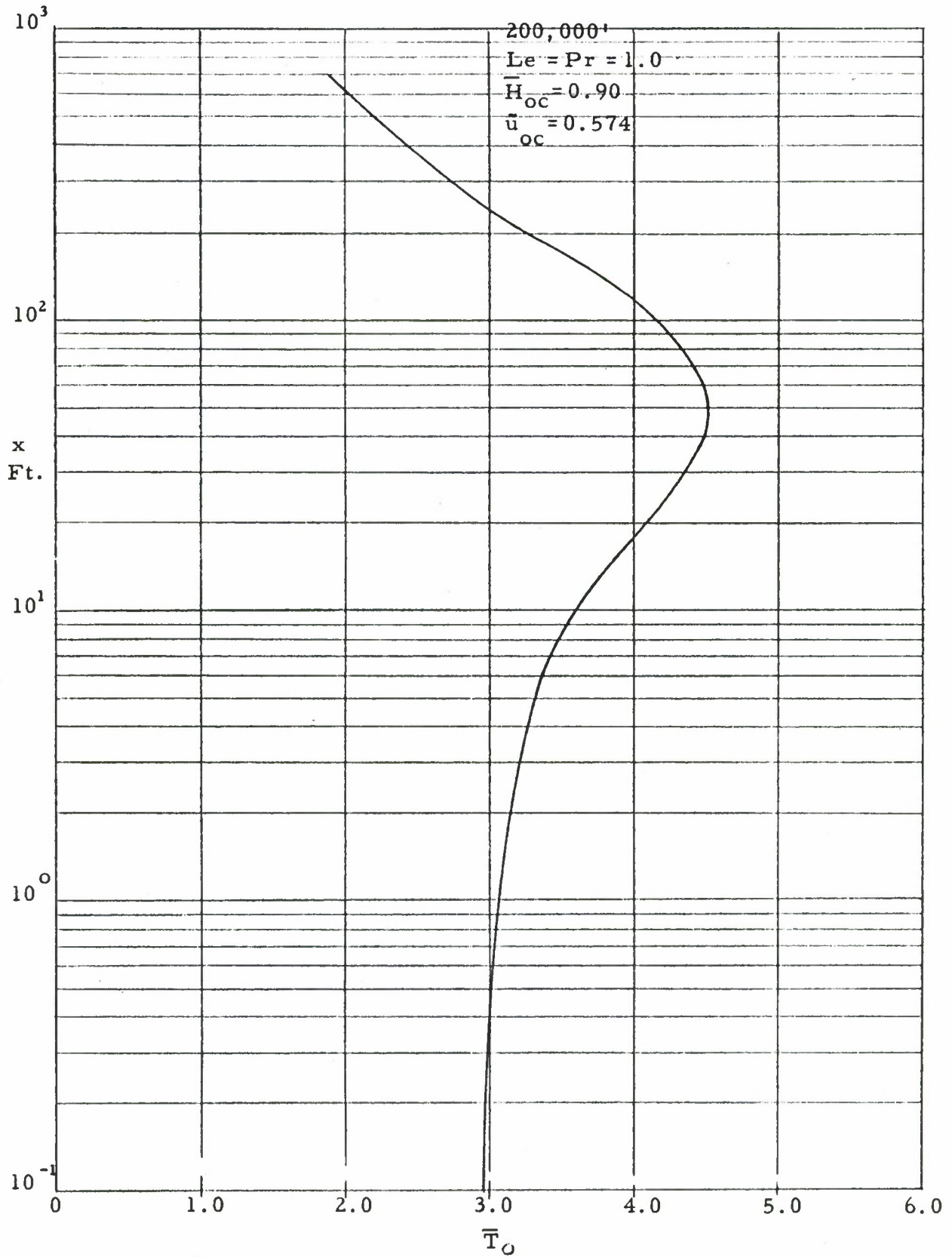


Figure 11b. Temperature of air, variation along the axis

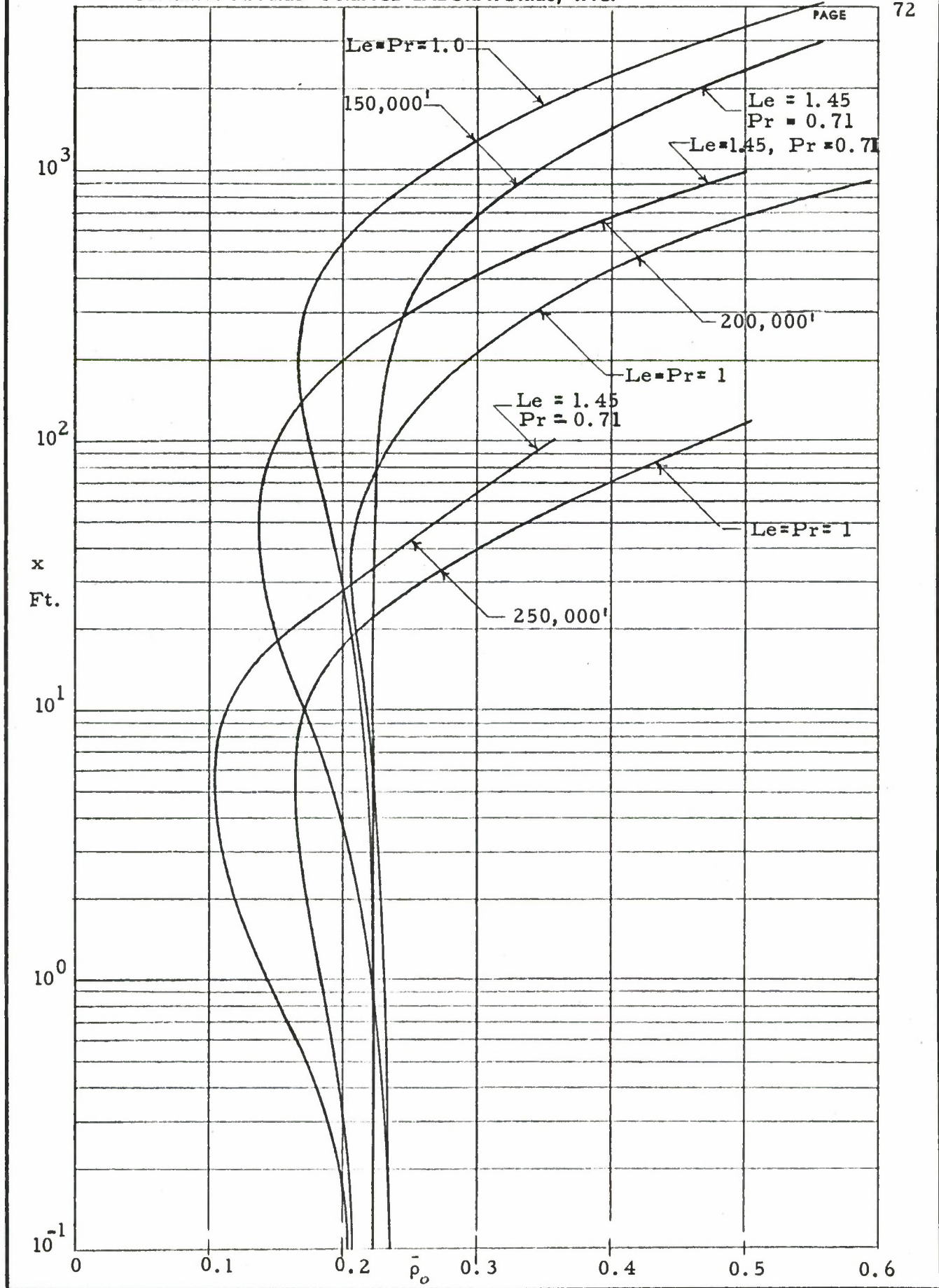


Figure 12a. Density of Air, Variation Along the Axis $[\bar{H}_{OC} = 1]$

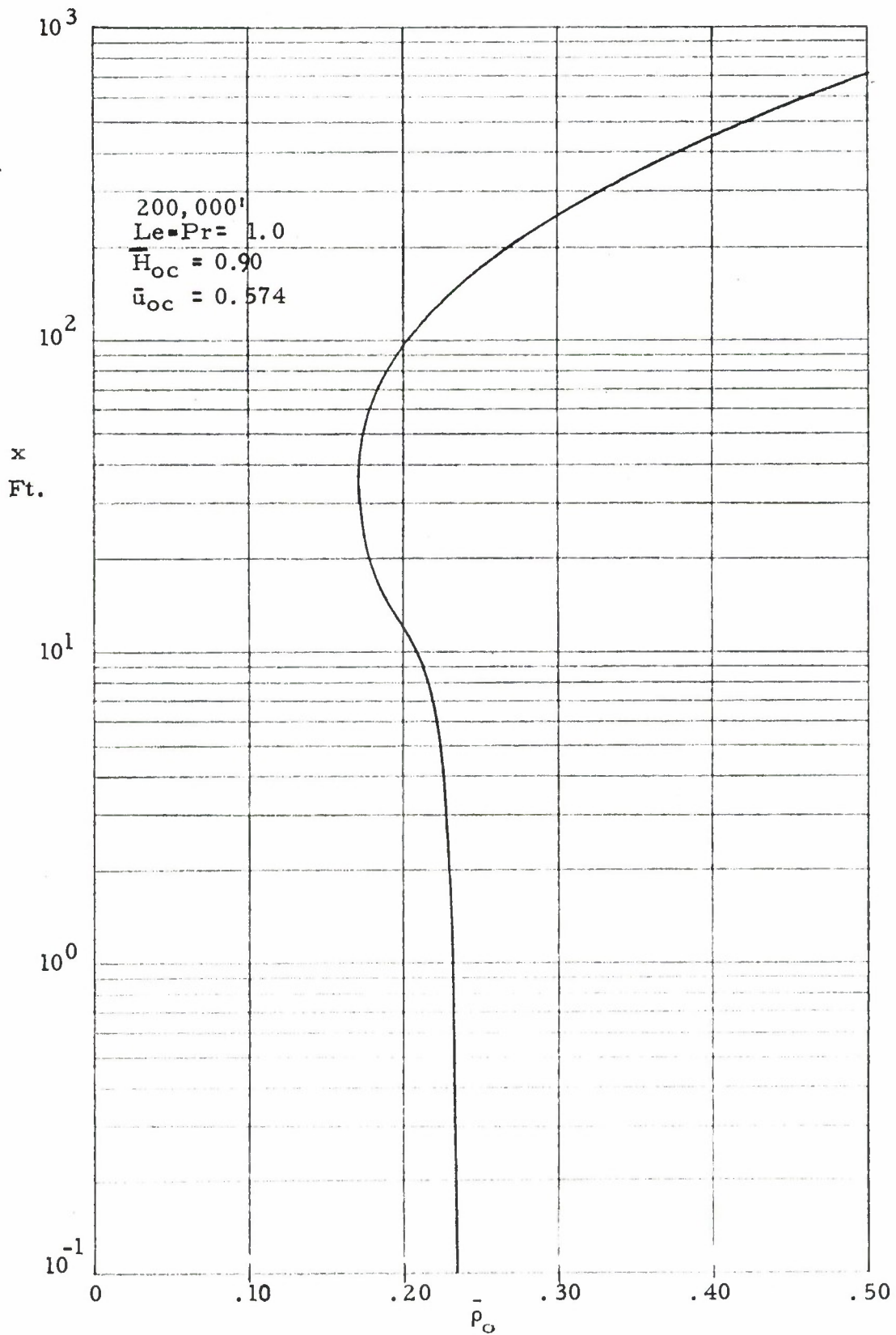


Figure 12b. Density of Air, Variation Along the Axis

Initial Condition $\alpha_{c_{NO^+}} = 5.63 \times 10^{-4}$
 150,000'

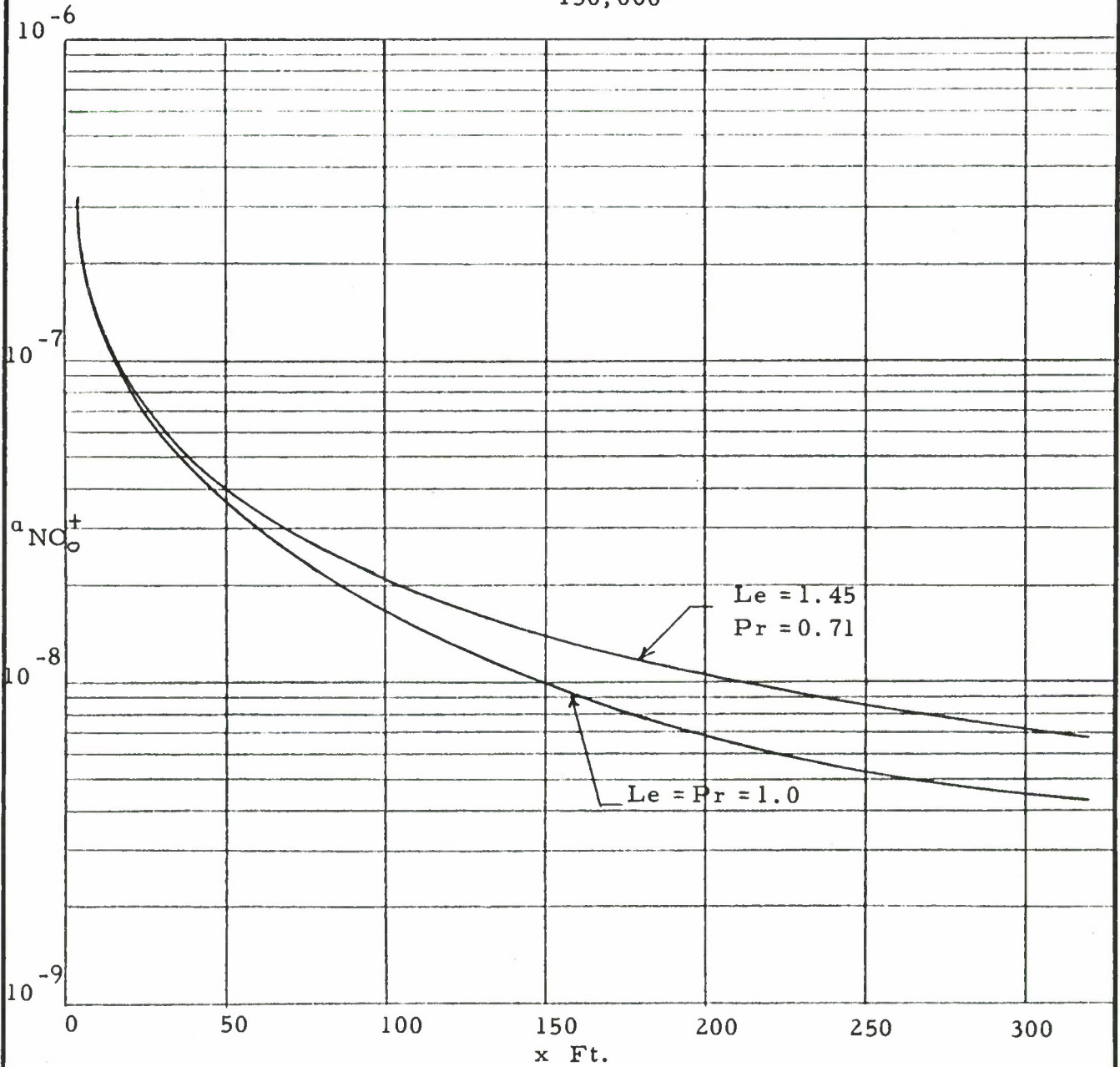


Figure 13a. Mass fraction of NO^+ along the axis $\left[\bar{H}_{oc} = 1 \right]$

Initial Condition $a_{c_{NO^+}} = 5.66 \times 10^{-4}$
 200,000'

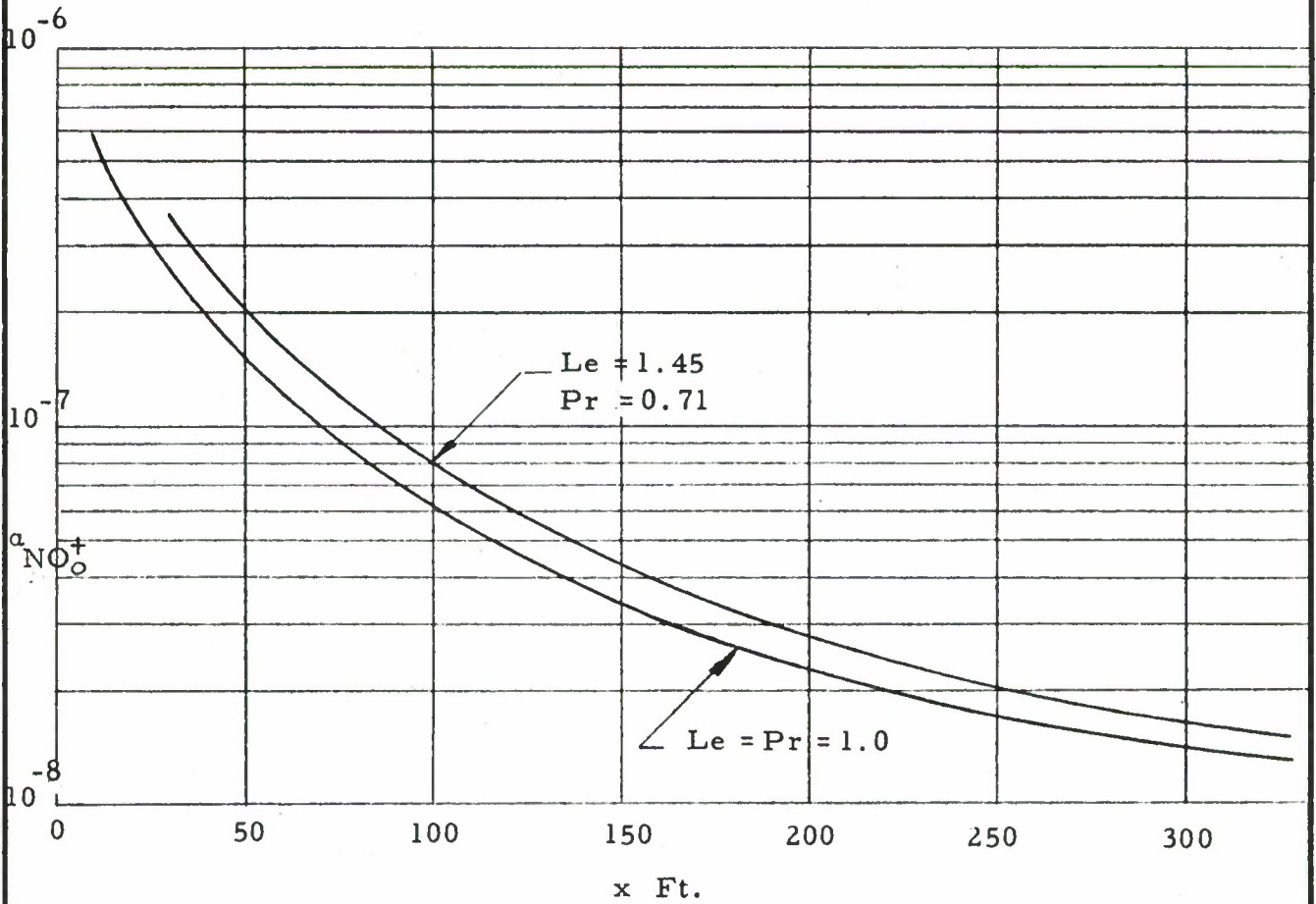


Figure 13b. Mass fraction of NO^+ along the axis $\left[\bar{H}_{oc} = 1 \right]$

Initial Condition $\alpha_{c_{NO^+}} = 4.85 \times 10^{-4}$
 250,000'

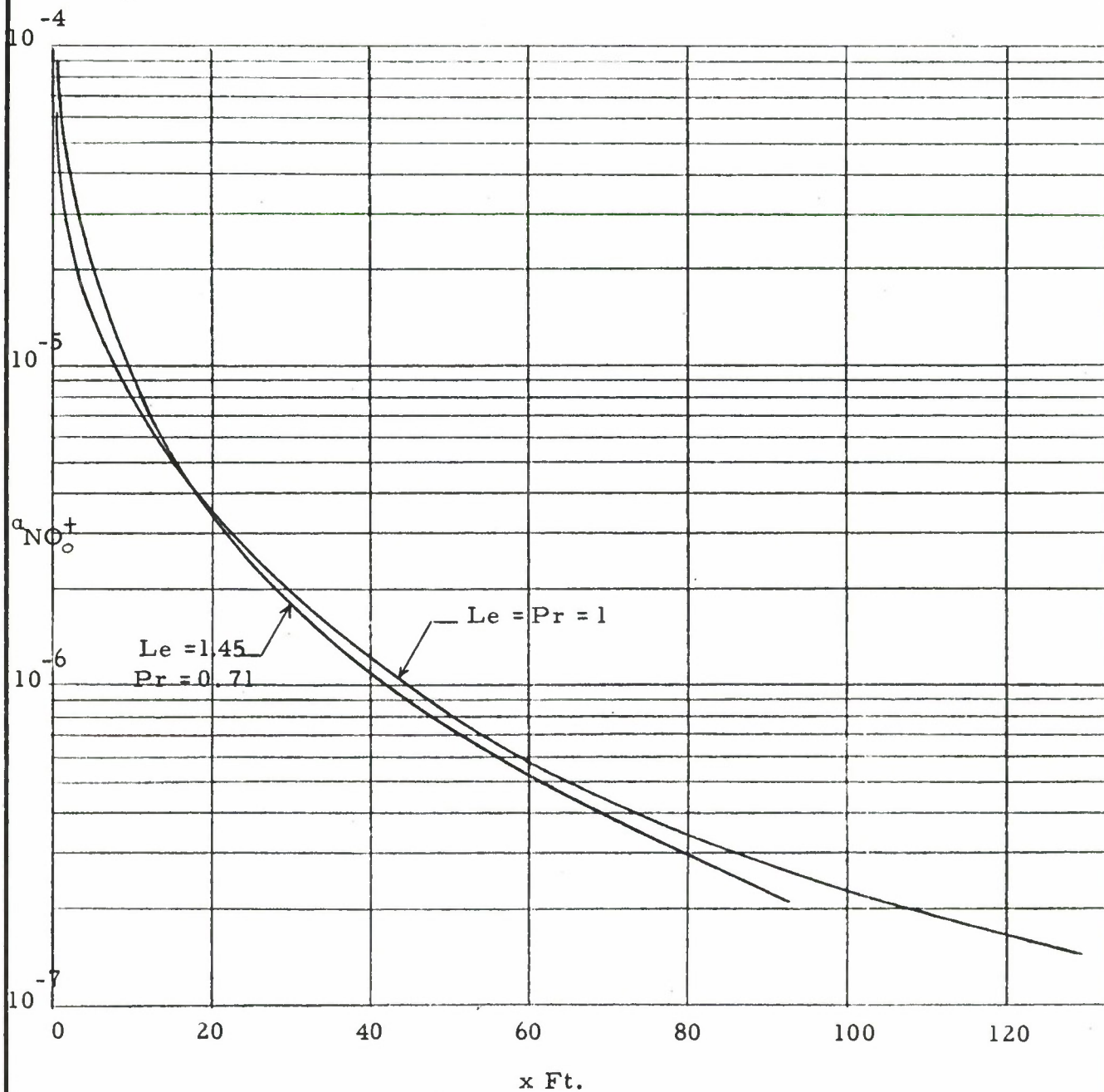


Figure 13c. Mass fraction of NO^+ along the axis $[\bar{H}_{oc} = 1]$

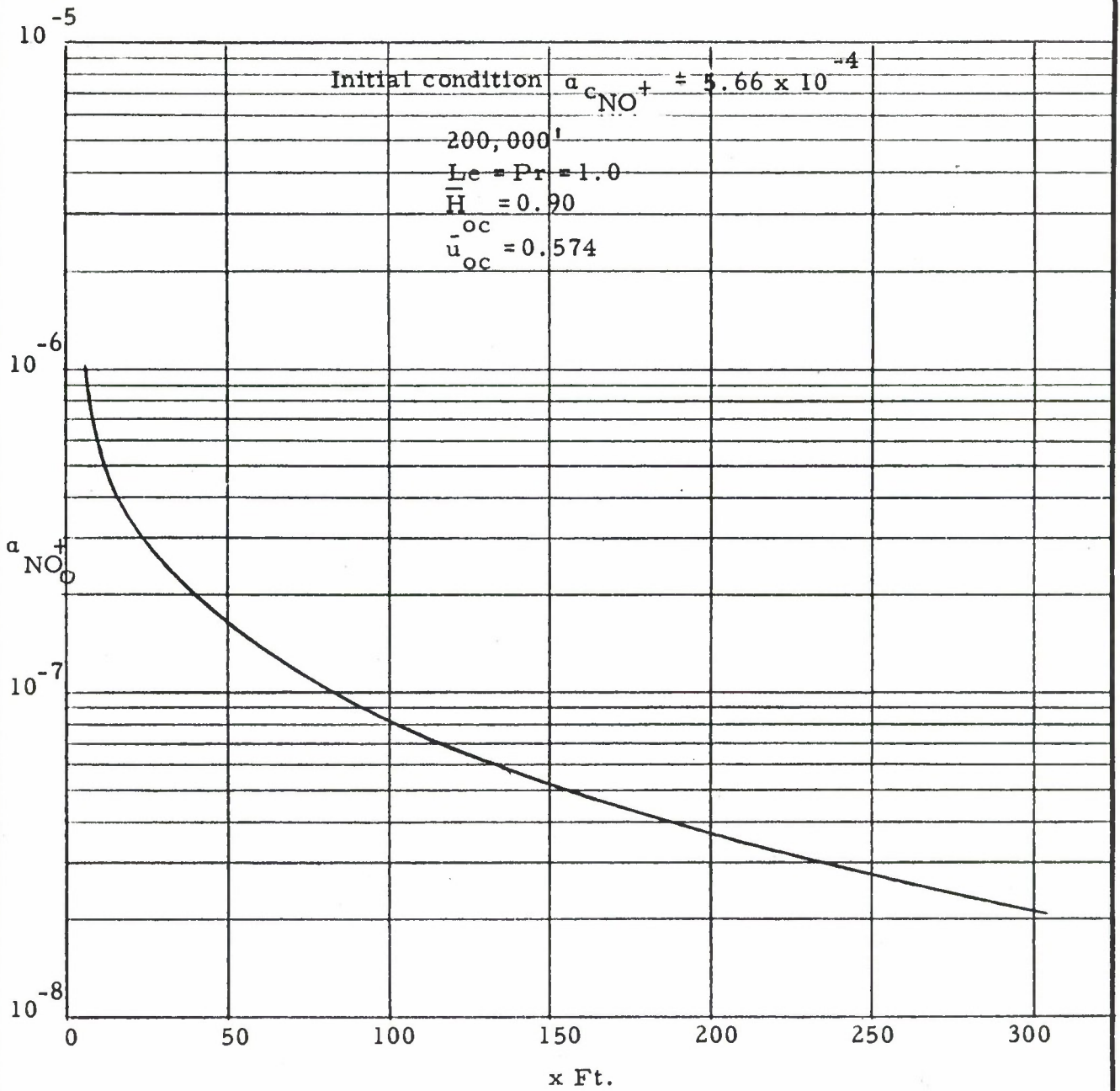


Figure 13d. Mass fraction of NO^+ along the axis.

Initial Condition $4.4 \times 10^{12} \frac{\text{Particles}}{\text{cc}}$

150,000'

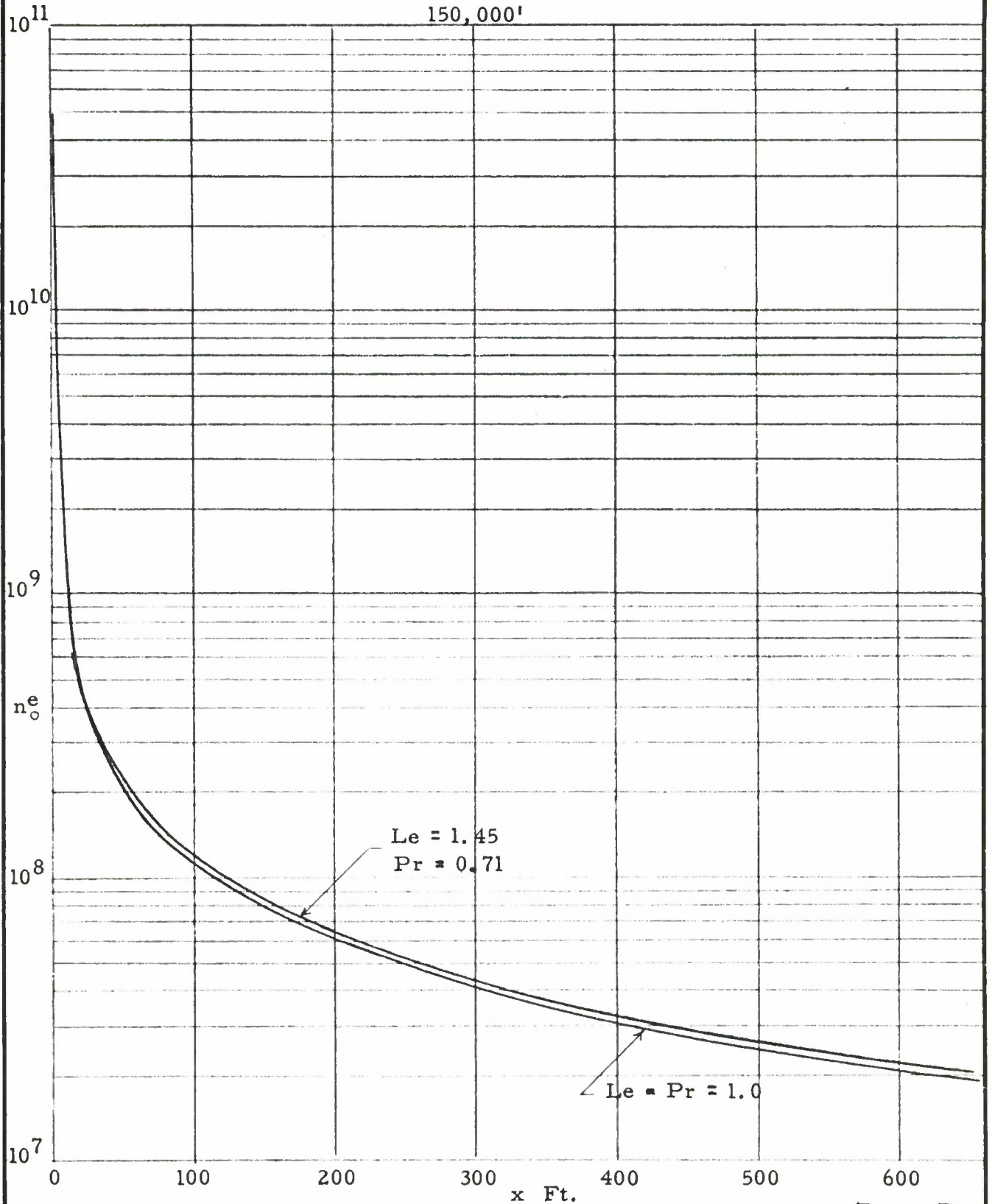


Figure 14a₁. Variation of Electron Density Along the Axis $\left[\bar{H}_{oc} = 1 \right]$

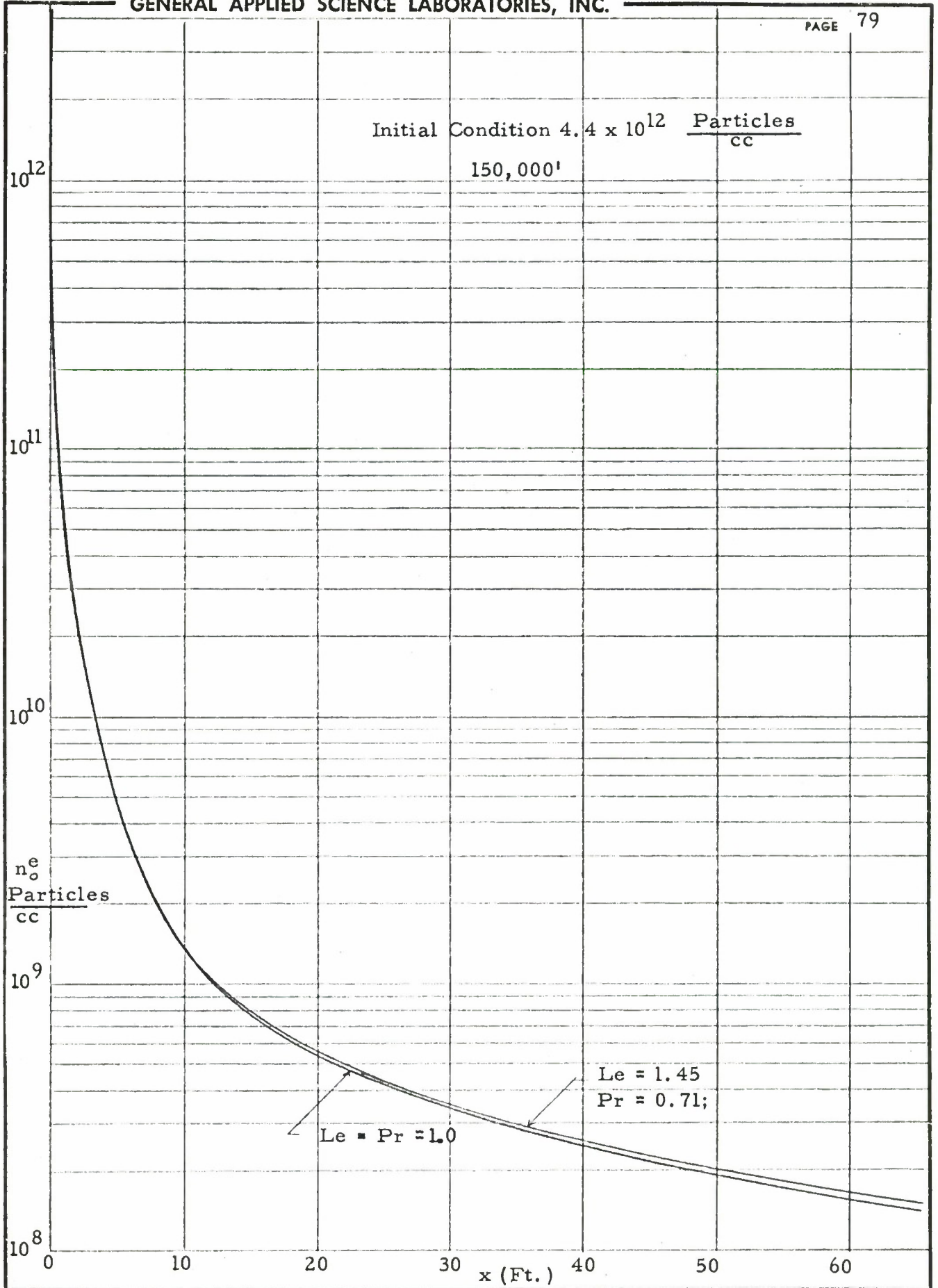


Figure 14a₂. Variation of Electron Density Along the Axis $\left[\bar{H}_{oc} = 1 \right]$

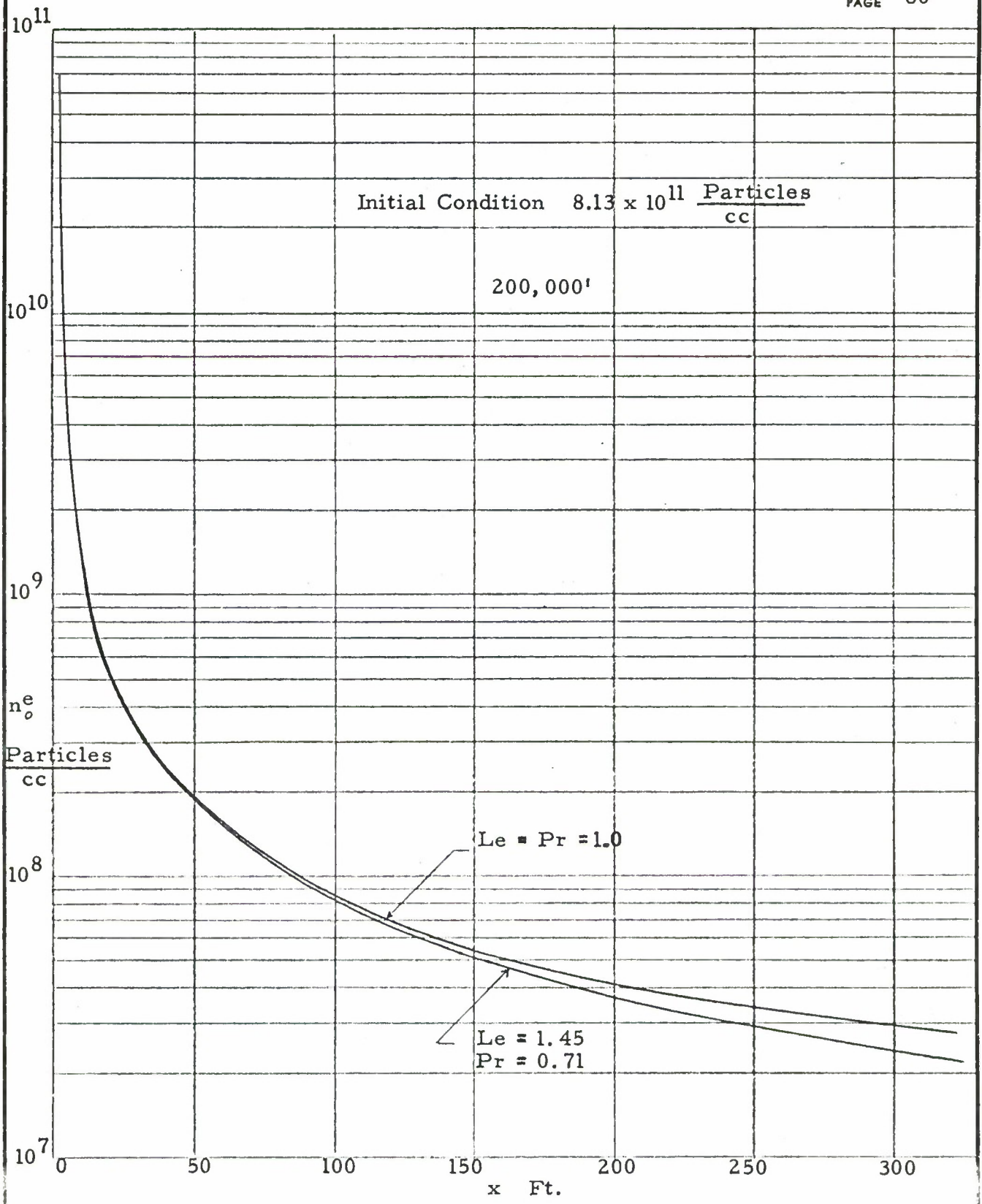


Figure 14b₁. Variation of Electron Density Along the Axis $[\bar{H}_{oc} = 1]$

Initial Condition 8.13×10^{11} $\frac{\text{Particles}}{\text{cc}}$

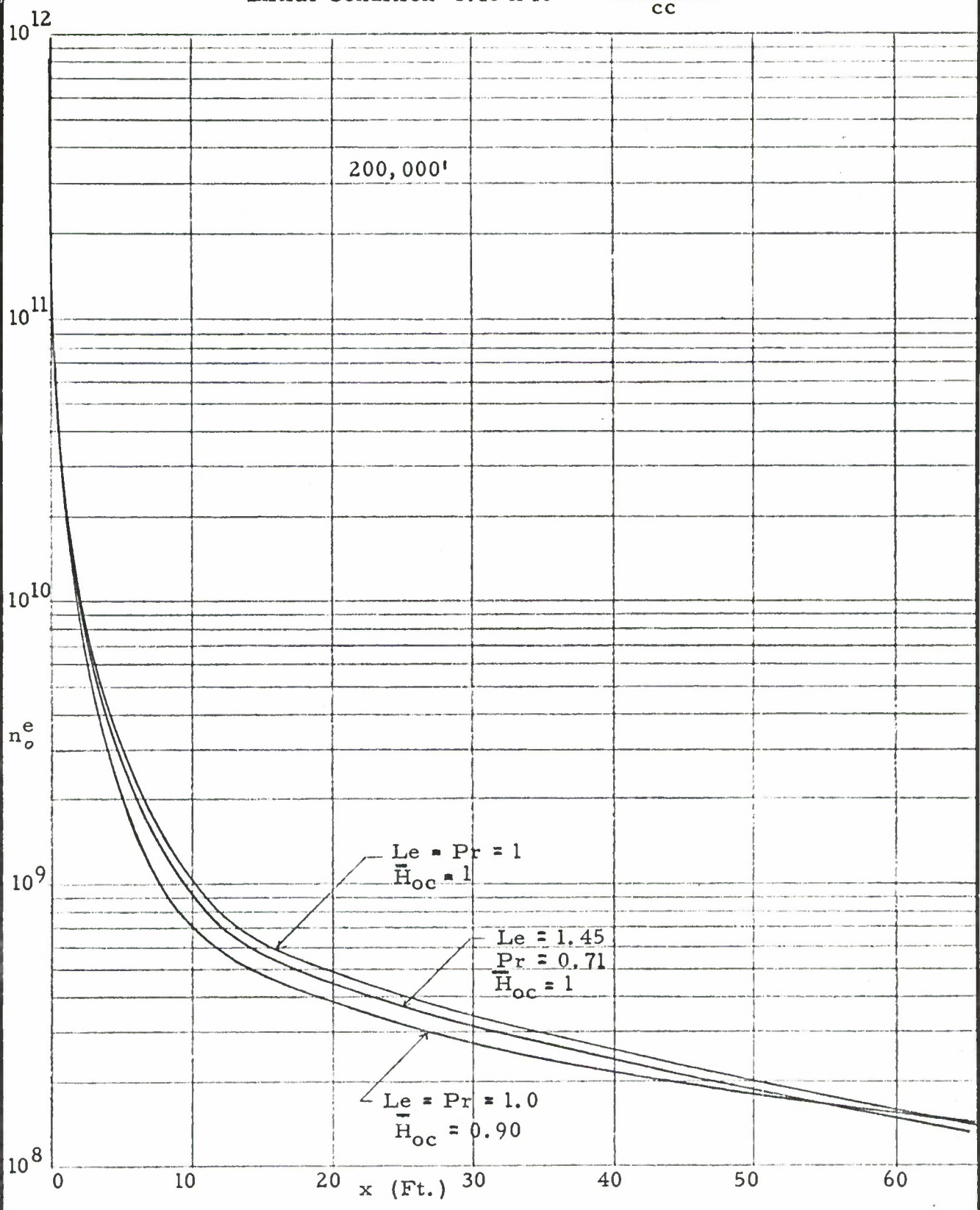


Figure 14b₂. Variation of Electron Density Along the Axis

Initial Condition 6.9×10^{10} $\frac{\text{Particles}}{\text{cc}}$

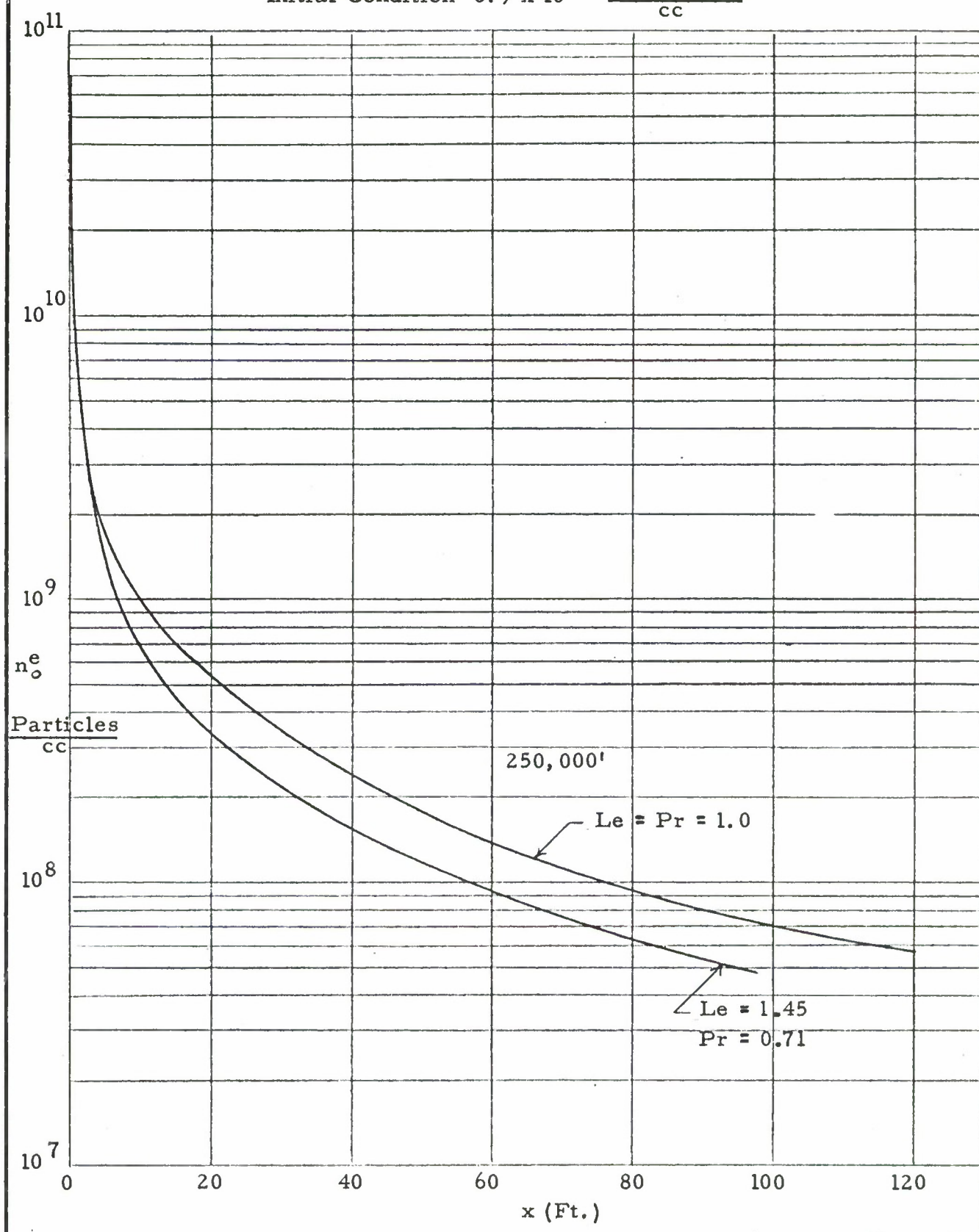


Figure 14c. Variation of Electron Density Along the Axis $[\bar{H}_{oc} = 1]$

Initial Condition 8.1×10^{11} $\frac{\text{Particles}}{\text{cc}}$

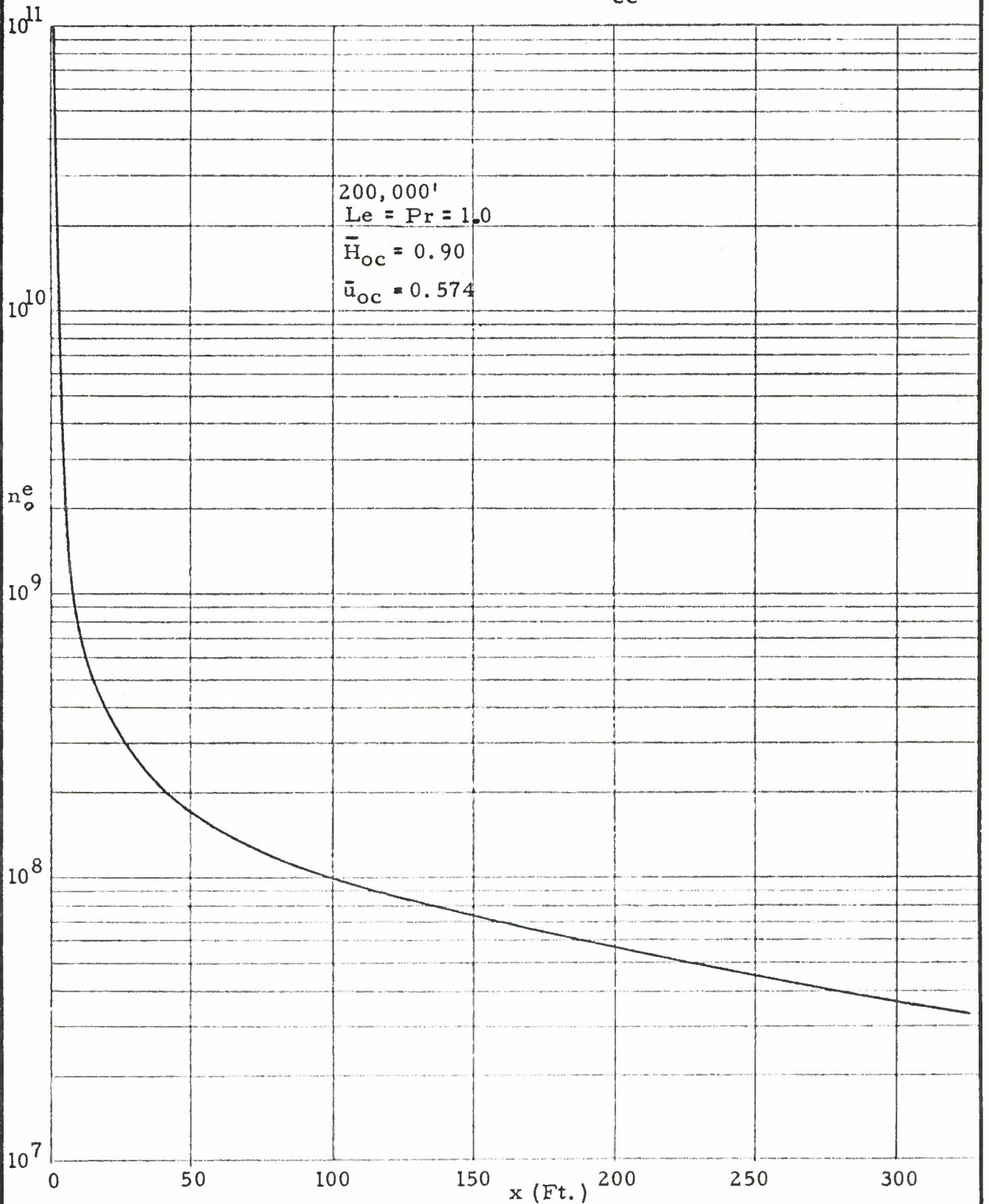


Figure 14d. Variation of Electron Density Along the Axis

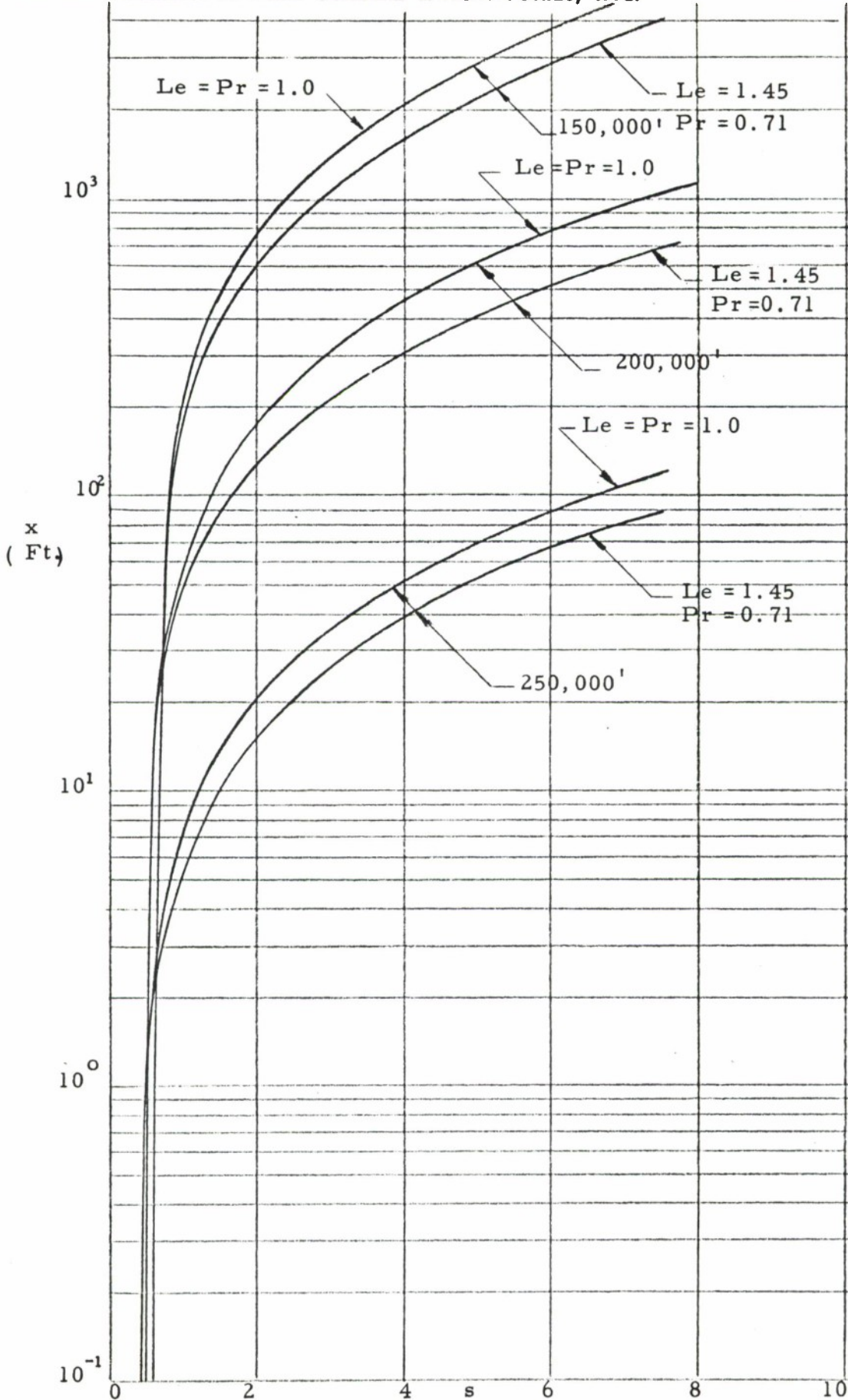


Figure 15a. Physical Versus Transform Streamwise Coordinate Along the Axis $[\bar{H}_{oc} = 1.0]$

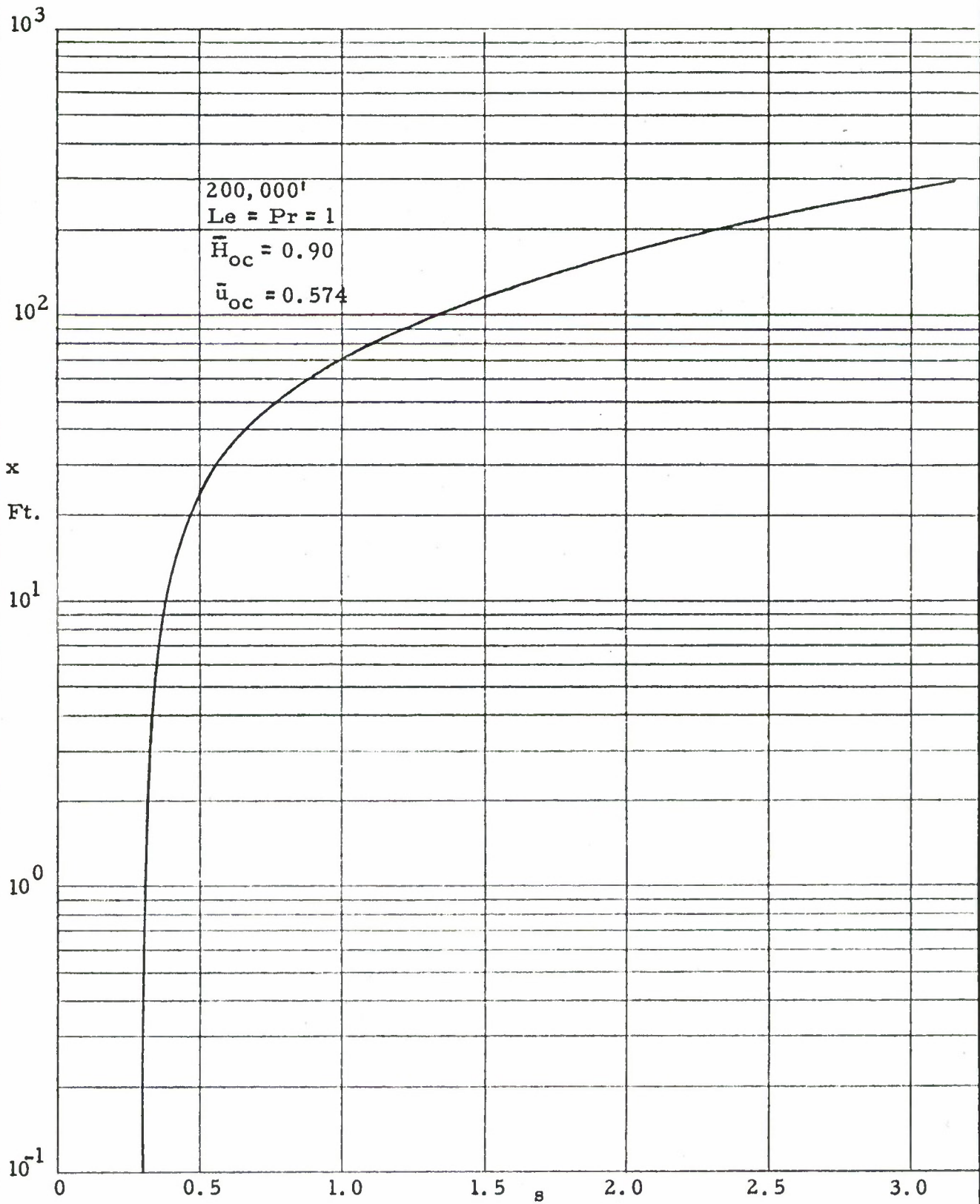


Figure 15b. Physical Versus Transform Streamwise Coordinate Along the Axis

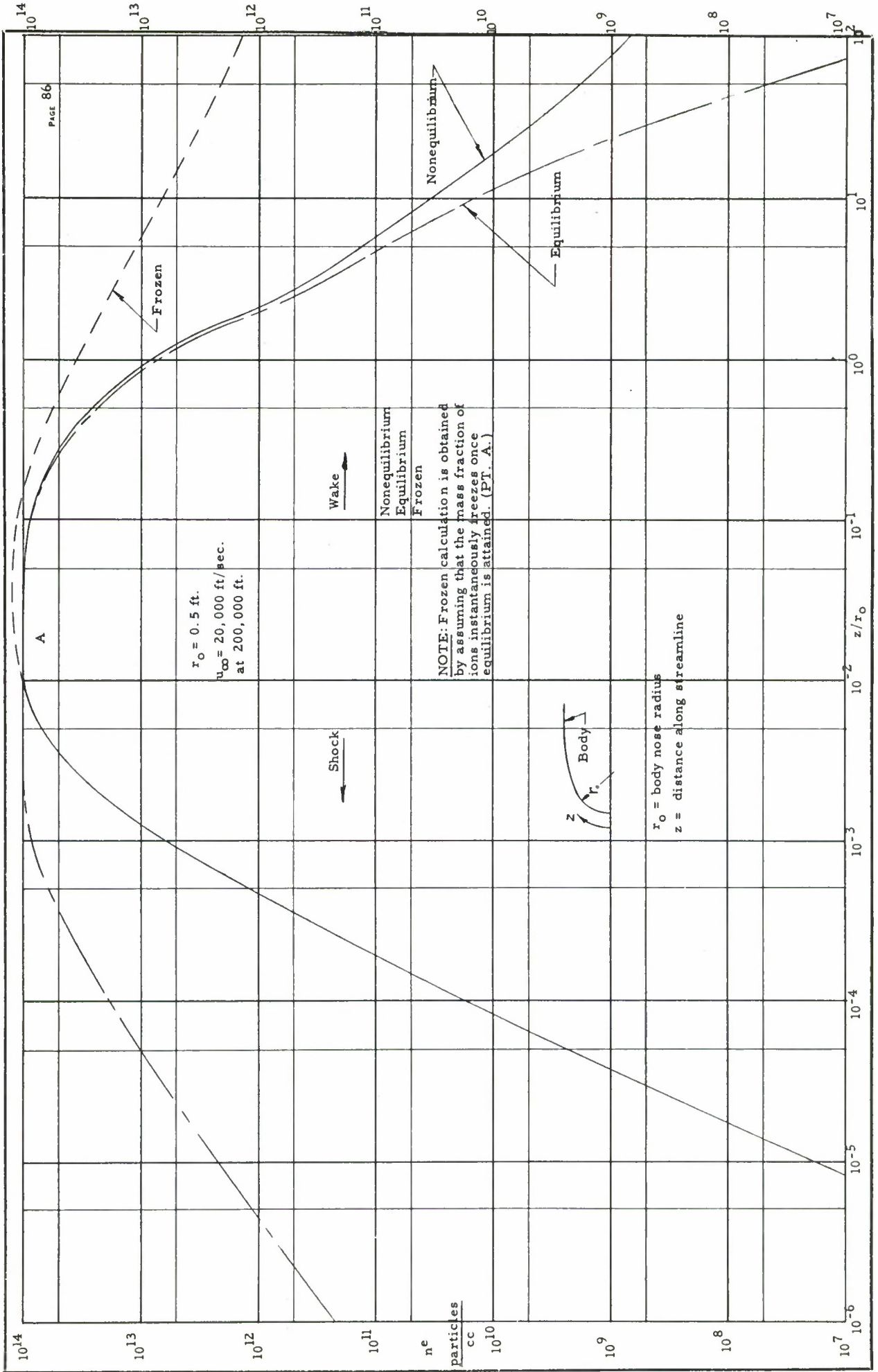


FIGURE 16 (Revised)

Figure 16. Variation of Electrons in the Inviscid Flow About a Blunt Body.

SUPPLEMENT TO GASL TECHNICAL REPORT NO. 180

HYPERSONIC AXISYMMETRIC WAKES INCLUDING EFFECTS OF

RATE CHEMISTRY

By M. H. Bloom and M. H. Steiger

Retransformation to physical coordinates by use of the approximation

$$1/\bar{\rho} \approx \bar{h}.$$

The inverse transformation is performed by means of the following equations [see (7.)] :

$$y^2 / 2 = \delta_m^2 \int_0^N (1/\bar{\rho}) NdN$$

$$\delta^2 / 2 = \delta_m^2 \int_0^1 (1/\bar{\rho}) NdN$$

We shall assume

$$1/\bar{\rho} \approx \bar{h} \quad \text{where } \bar{h} = h/h_e, \quad \bar{\rho} = \rho/\rho_e$$

Now

$$h = H - u^2 / 2$$

and from (13a)

$$H = H_o + (H_e - H_o) f$$

$$u = u_o + (u_e - u_o) f$$

where

$$f = f(N) = 6N^2 - 8N^3 + 3N^4$$

Thus

$$\bar{h} = 1 - (1 - \bar{H}_o)(1 - f) + (u_e^2 / 2h_e) \left\{ \left[2(1 - \bar{u}_o) - (1 - \bar{H}_o) \right] (1 - f) - (1 - \bar{u}_o)^2 (1 - f)^2 \right\}$$

Now define

$$I_1 = \int_0^N (1-f) NdN = \frac{N^2}{2} - \frac{3}{2} N^4 + \frac{8}{5} N^5 - \frac{1}{2} N^6$$

$$I_2 = \int_0^N (1-f)^2 NdN$$

$$= \frac{1}{2} N^2 - 3N^4 + \frac{16}{5} N^5 + 5N^6 + 8N^8 + \frac{9}{10} N^{10} - \frac{96}{7} N^7 + \frac{9}{2} N^8 - \frac{16}{3} N^9$$

$$I_{1e} = \int_0^1 (1-f) NdN = \frac{1}{10}$$

$$I_{2e} = \int_0^1 (1-f)^2 NdN = \frac{11}{210}$$

Thus

$$\left(\delta/\delta_m\right)^2 = 1 - 2I_{1e}(1-\bar{H}_o) + 2(u_e^2/2h_e) \left\{ \left[2(1-\bar{u}_o) - (1-\bar{H}_o) \right] I_{1e} - (1-\bar{u}_o)^2 I_{2e} \right\}$$

In the calculations of GASL TR-180 an initial value of

$$\delta_{mc} = 0.5 \text{ ft}$$

was used for all flight conditions.

For the special case of $\bar{H}_o = 1$, we derive

$$\left(\delta/\delta_m\right)^2 = 1 + (u_e^2/2h_e)(2/5)(1-\bar{u}_o) \left[1 - (11/42)(1-\bar{u}_o) \right]$$

where

$$\frac{\delta_m^2}{\theta_c} = \frac{21.0}{(1-\bar{u}_o)\left(1 + \frac{11}{10} \bar{u}_o\right)}$$

giving

$$\delta^2 / \left[8.4\theta_c \left(\frac{u_e^2}{2h_e} \right) \right] = \left[1 - \frac{11}{42} (1 - \bar{u}_o) + \frac{1}{\left(\frac{u_e^2}{2h_e} \right) \left(\frac{2}{5} \right) (1 - \bar{u}_o)} \right] \left[\frac{1}{1 + 1.10 \bar{u}_o} \right]$$

and

$$\frac{\delta}{\left[8.4\theta_c \left(\frac{u_e^2}{2h_e} \right) \right]^{1/2}} = \left[1 - \frac{11}{42} (1 - \bar{u}_o) + \frac{1}{\frac{u_e^2}{2h_e} \left(\frac{2}{5} \right) (1 - \bar{u}_o)} \right]^{1/2} \left[\frac{1}{1 + 1.10 \bar{u}_o} \right]^{1/2}$$

This relation is plotted in the attached figure for the typical value $(2/5)(u_e^2/2h_e) = 32$. Since $h_e = c_{pe} T_e$ at low T_e , $u_e^2/2h_e = \frac{\gamma_e^{-1}}{2} M_e^2/5$, and this corresponds to $M_e = 20$.

It is noted that δ is approximately constant for $\bar{u}_o < 0.95$. This constitutes the major portion of the wake dealt with here (see Figures 9a, b).

Moreover the factor which nondimensionalizes δ has the approximate value

$$\left[8.4\theta_c \left(\frac{u_e^2}{2h_e} \right) \right]^{1/2} \cong 0.11 M_e \text{ (ft)}$$

$$\therefore \delta \cong a(0.11 M_e) \text{ for } \bar{u}_o < 0.95$$

where "a" is a constant factor estimated from the aforementioned plot.

In this case, $a = 0.8$.

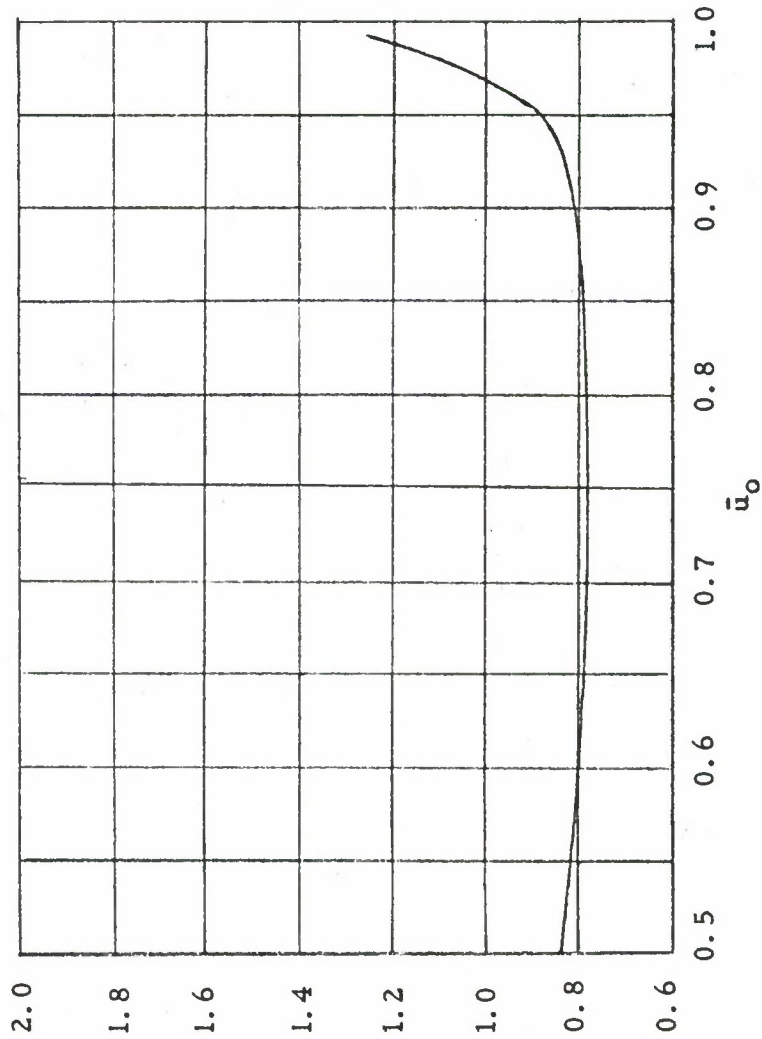
If $0.9 < \bar{H}_o < 1$ the effect on δ of deviations from unity will be small. Likewise the changes in "a" for Mach numbers M_e on the order of 20 will not be strongly influenced by deviations in M_e from 20.

M. H. Bloom
January, 1961

$$\left(8.4 \theta_c \frac{u_e^2}{2h_e} \right)^{1/2} \approx 0.108 M_e \text{ (ft)}$$

$$\delta \approx \frac{M_e}{12} \text{ (ft) for } \bar{u}_o < 0.95$$

$$M_e = 20 \text{ and } \bar{H}_o = 1$$



$$\frac{\delta \text{ (ft)}}{\left(2.1 \theta_c \frac{u_e^2}{2h_e} \right)^{1/2}}$$

$\equiv a$

ERRATA SHEET

April 11, 1961

GASL TECHNICAL REPORT NO. 180HYPERSONIC AXISYMMETRIC WAKES INCLUDING EFFECTS
OF RATE CHEMISTRY

$$\text{Eq. (17c)} \quad f(\bar{u}_0) = (5/12)(1/1-\bar{u}_0) - \left(\frac{25}{126}\right) \ln \left[(10 + 11 \bar{u}_0) / (1 - \bar{u}_0) \right]$$

$$\text{Eq. (24f)} \quad \rho_{d_i} = \left(\frac{m_i}{2h_p^3} \right) (\pi m_i kT)^{3/2} (T_i^R / T) \left(1 - e^{-T_i^V / T} \right) (f_i^E)^2 / f_{i_2}^E$$

$$\text{Eq. (25)} \quad h = RT \left[\frac{5}{2} \left(\frac{a_O}{M_O} + \frac{a_N}{M_N} \right) + \frac{a_{O_2}}{M_{O_2}} \left(\frac{7}{2} + \Lambda_{O_2} \right) + \frac{a_{N_2}}{M_{N_2}} \left(\frac{7}{2} + \Lambda_{N_2} \right) \right]$$

$$+ a_O \left(\frac{D_{O_2}}{2m_O} \right) + a_N \left(\frac{D_{N_2}}{2m_N} \right)$$

$$\text{Eq. (28b)} \quad k_{dNO^+} / k_{rNO^+} = \left[\frac{M_{NO^+} M_e}{M_N M_O} \right]^{3/2} \left[\frac{T}{10.42} \right] \left[1 - e^{-\frac{6111}{T}} \right]$$

$$\left[\frac{e^{-(I_{NO} - D_{NO}) / kT}}{5 + 3e^{-411K} + e^{-589K}} \right]$$

APPENDIX C TO GASL TECHNICAL REPORT NO. 180
HYPERSONIC AXISYMMETRIC WAKES INCLUDING EFFECTS OF
RATE CHEMISTRY

By M. H. Bloom and M. H. Steiger

The attached figures present the results of the analysis described in GASL Technical Report No. 249, Improved Hypersonic Laminar Wake Calculations Including Rate Chemistry, by Martin H. Steiger.

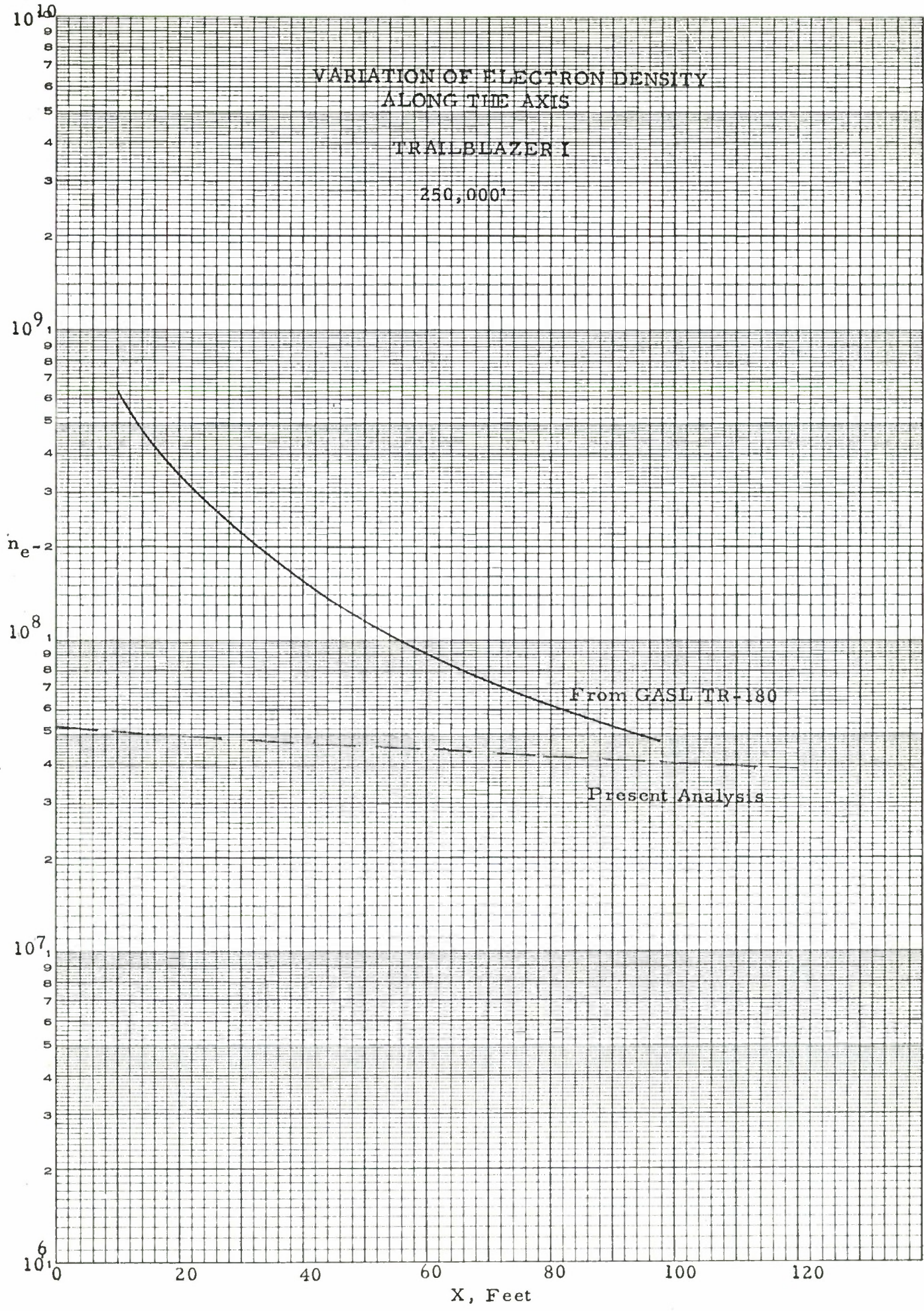
Axial variations of temperature, density, electron density and velocity deficiency are given for the flight conditions listed in Table I.

Free stream pressure, temperature and density have been revised in accordance with the Air Force Cambridge Research Center Atmospheric Model of December, 1959.

VARIATION OF ELECTRON DENSITY ALONG THE AXIS

TRAILBLAZER I

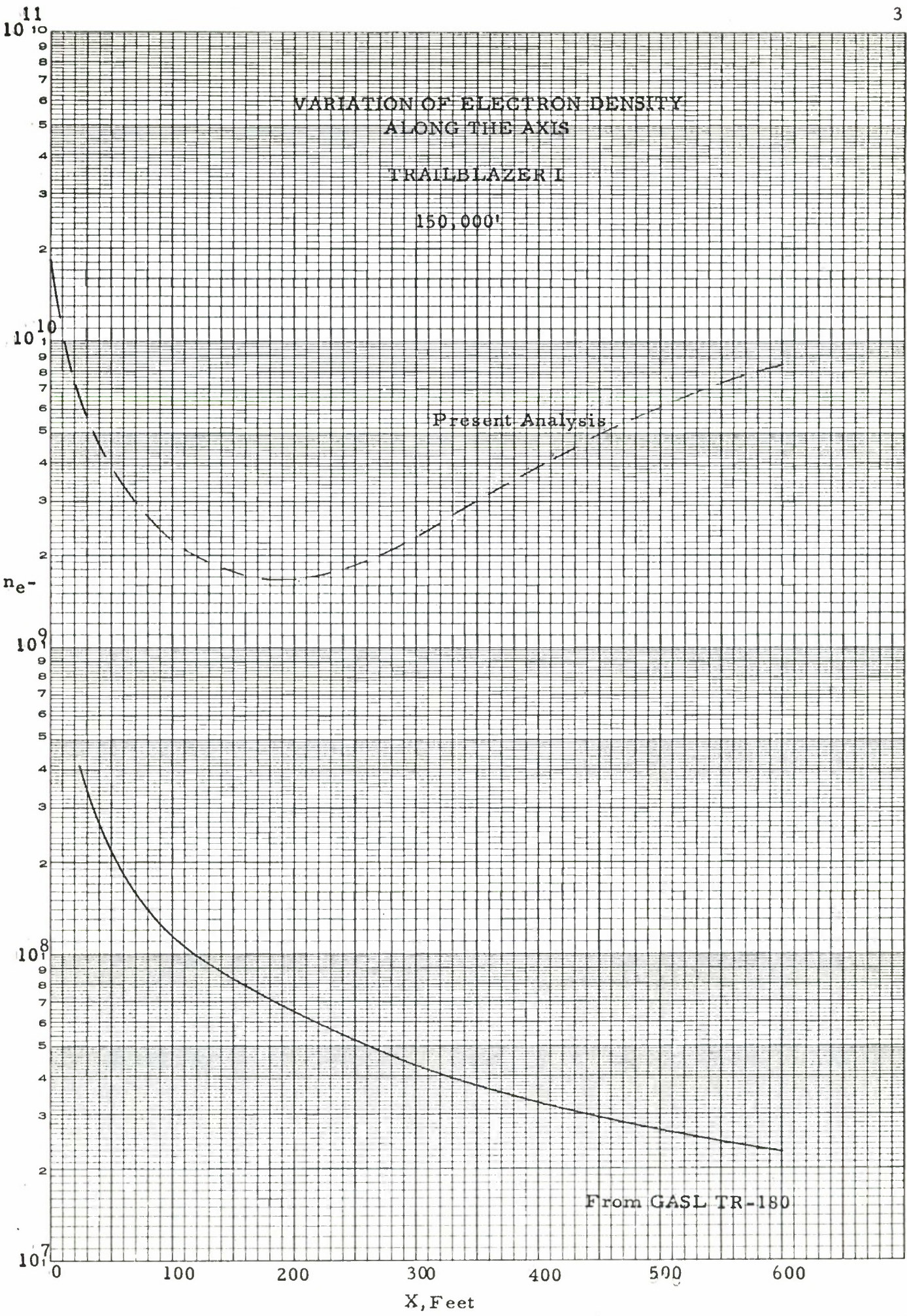
250,000'



EUGENE DIEZGEN CO.
MADE IN U. S. A.

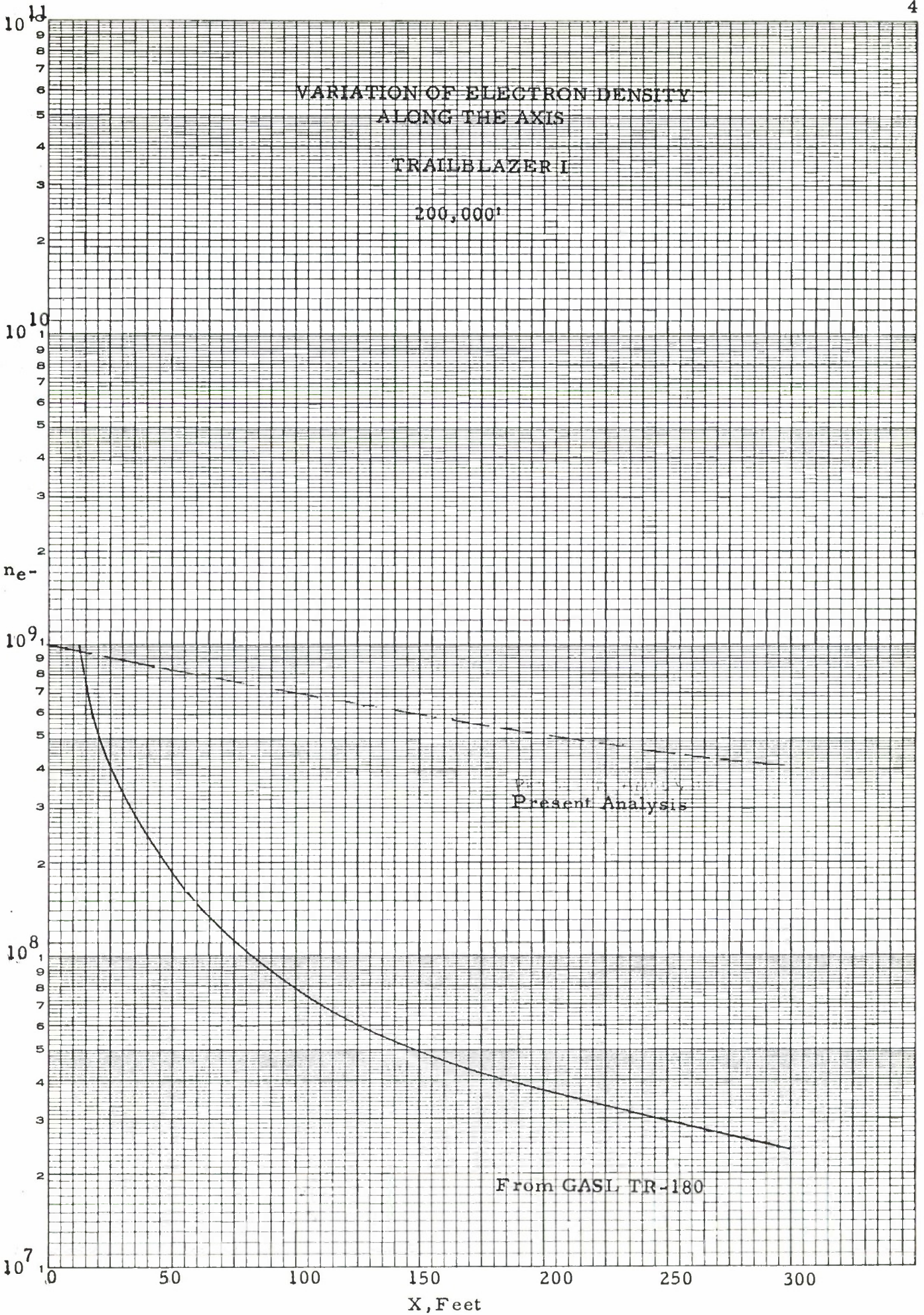
SEMI-LOGARITHMIC
4 CYCLES X 10 DIVISIONS PER INCH

X, Feet



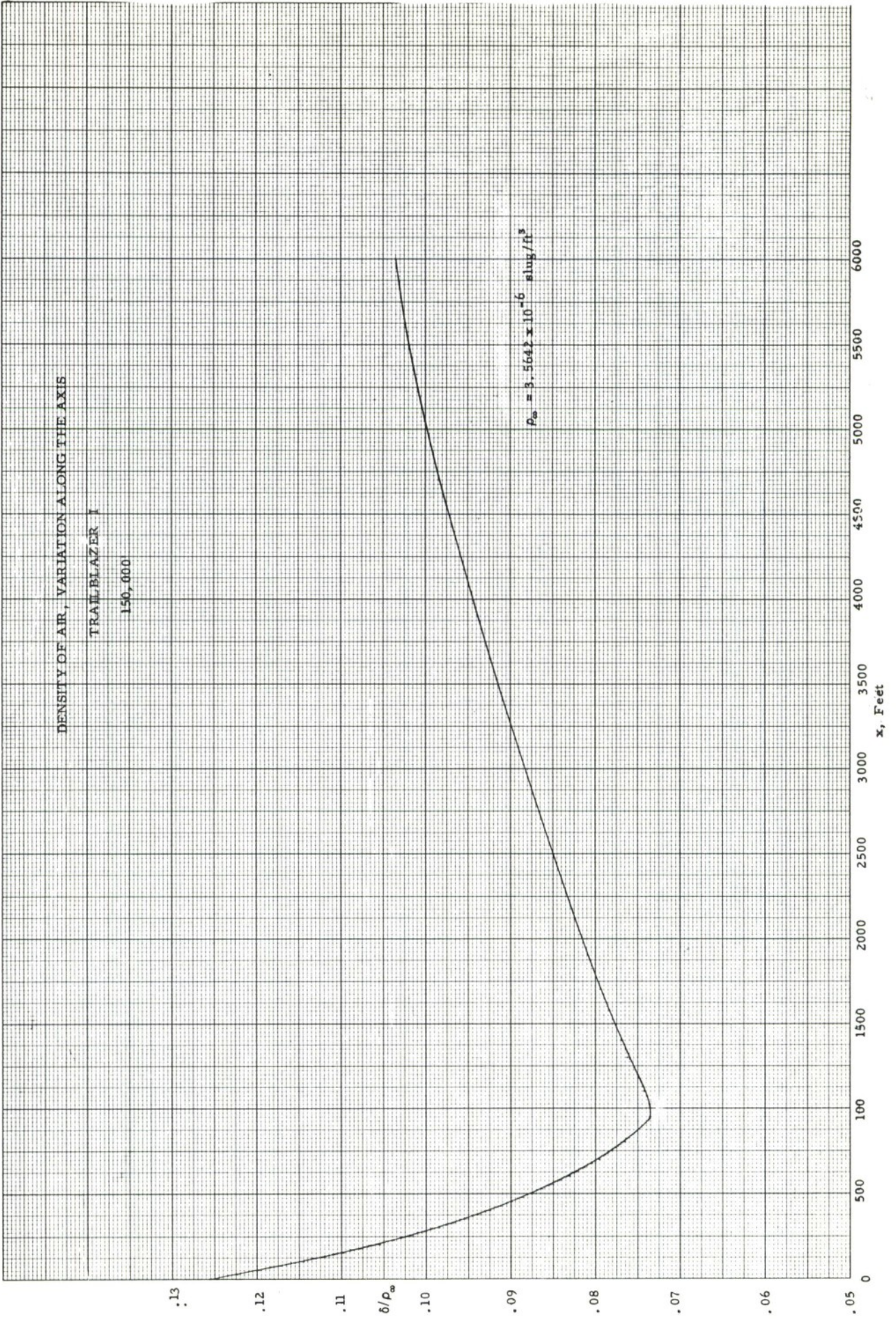
EUGENE DIETZGEN CO.
MADE IN U. S. A.

NO. 340R-L410 DIETZGEN GRAPH PAPER
SEMI-LOGARITHMIC
4 CYCLES X 10 DIVISIONS PER INCH

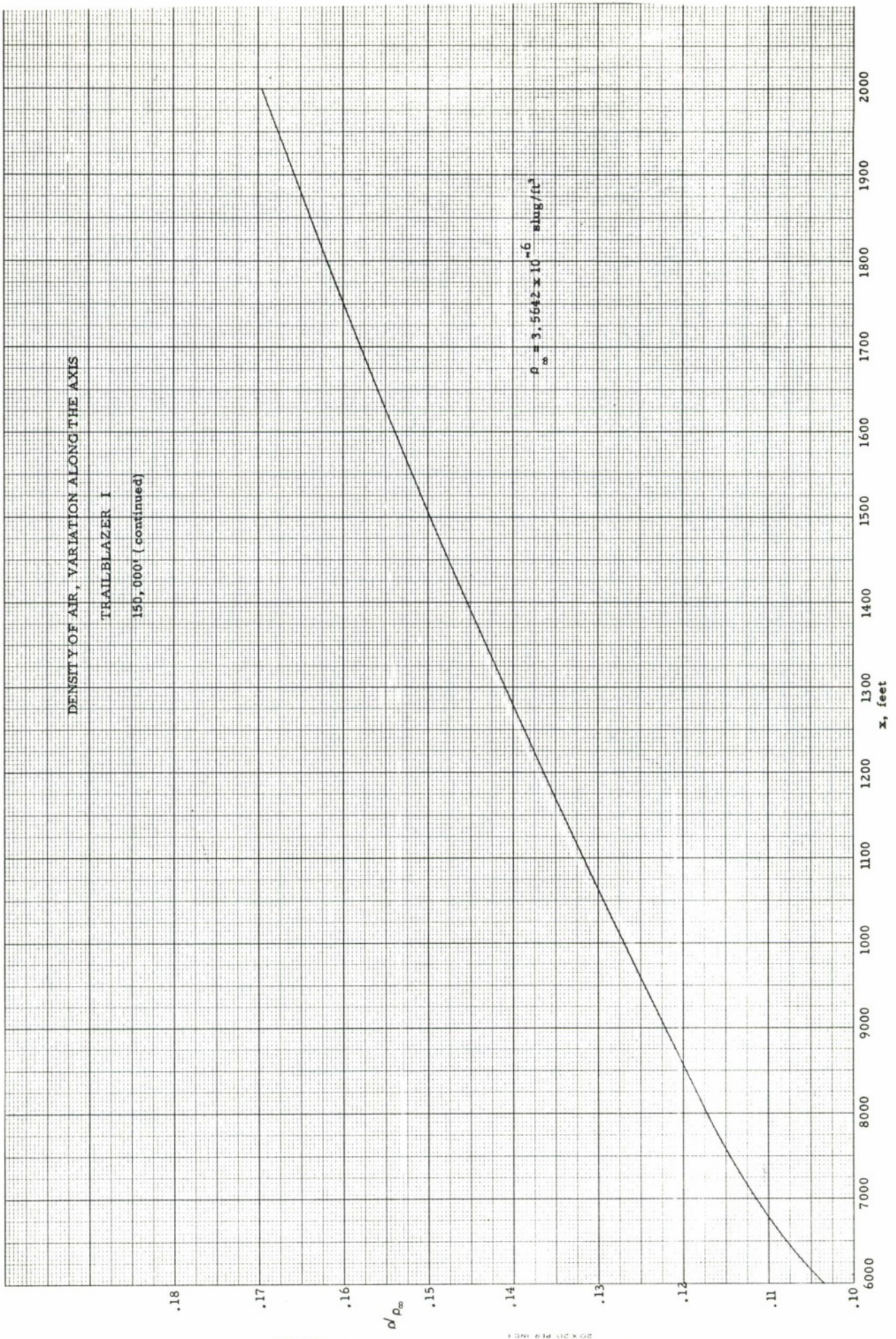


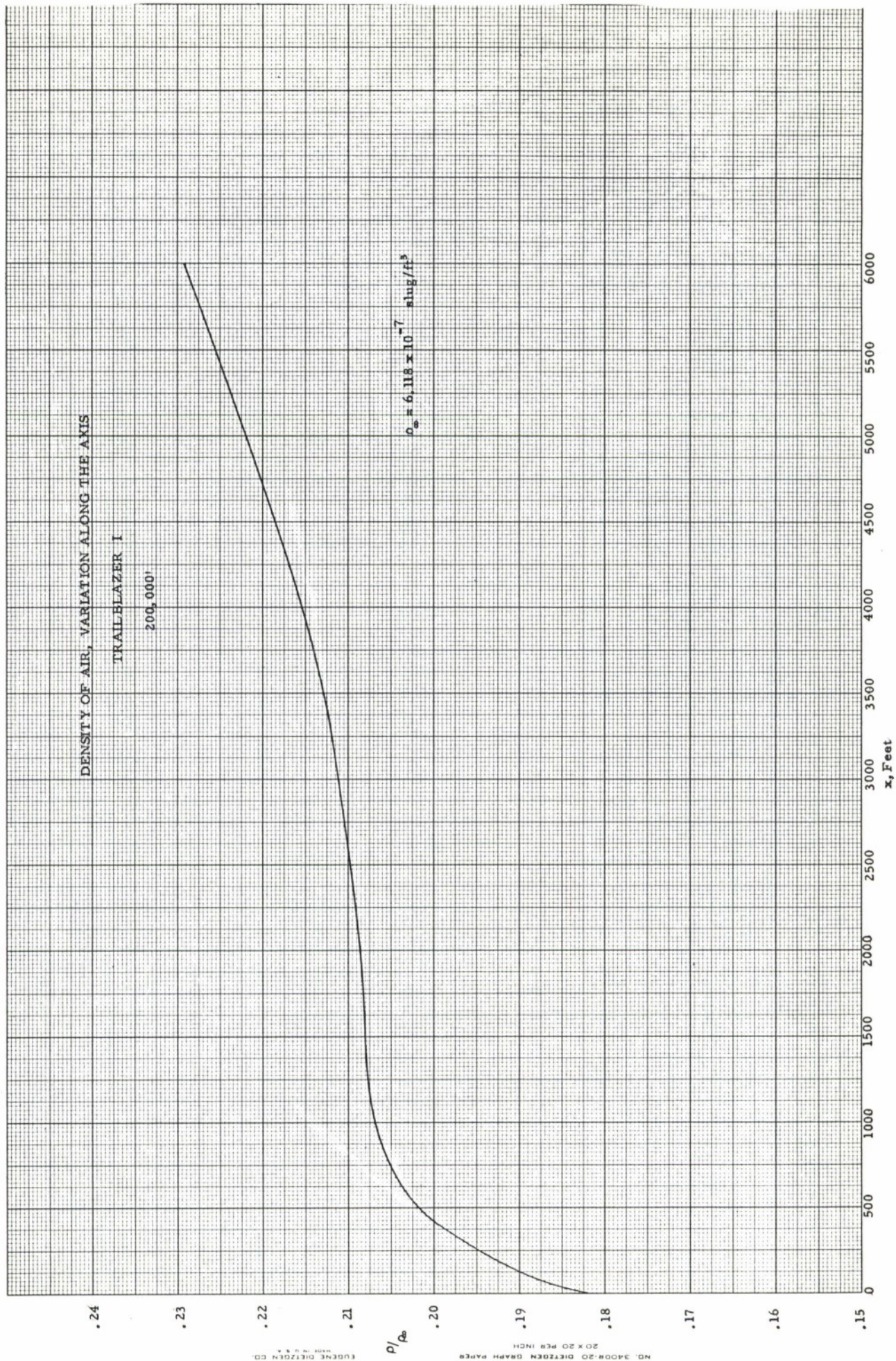
EUGENE DIETZGEN CO.
MADE IN U.S.A.

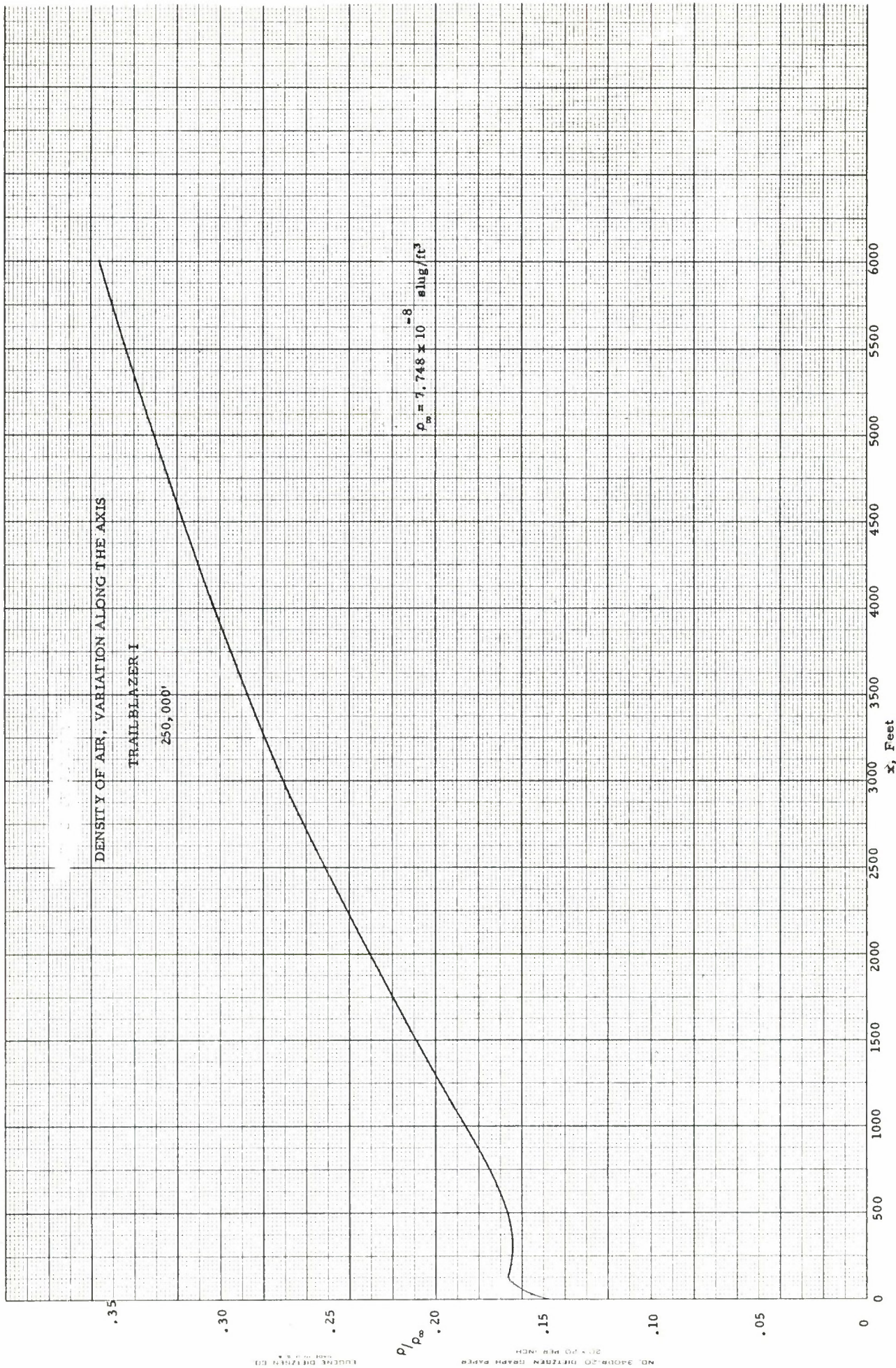
NO. 340R-L410 DIETZGEN GRAPH PAPER
SEMI-LOGARITHMIC
4 CYCLES X 10 DIVISIONS PER INCH

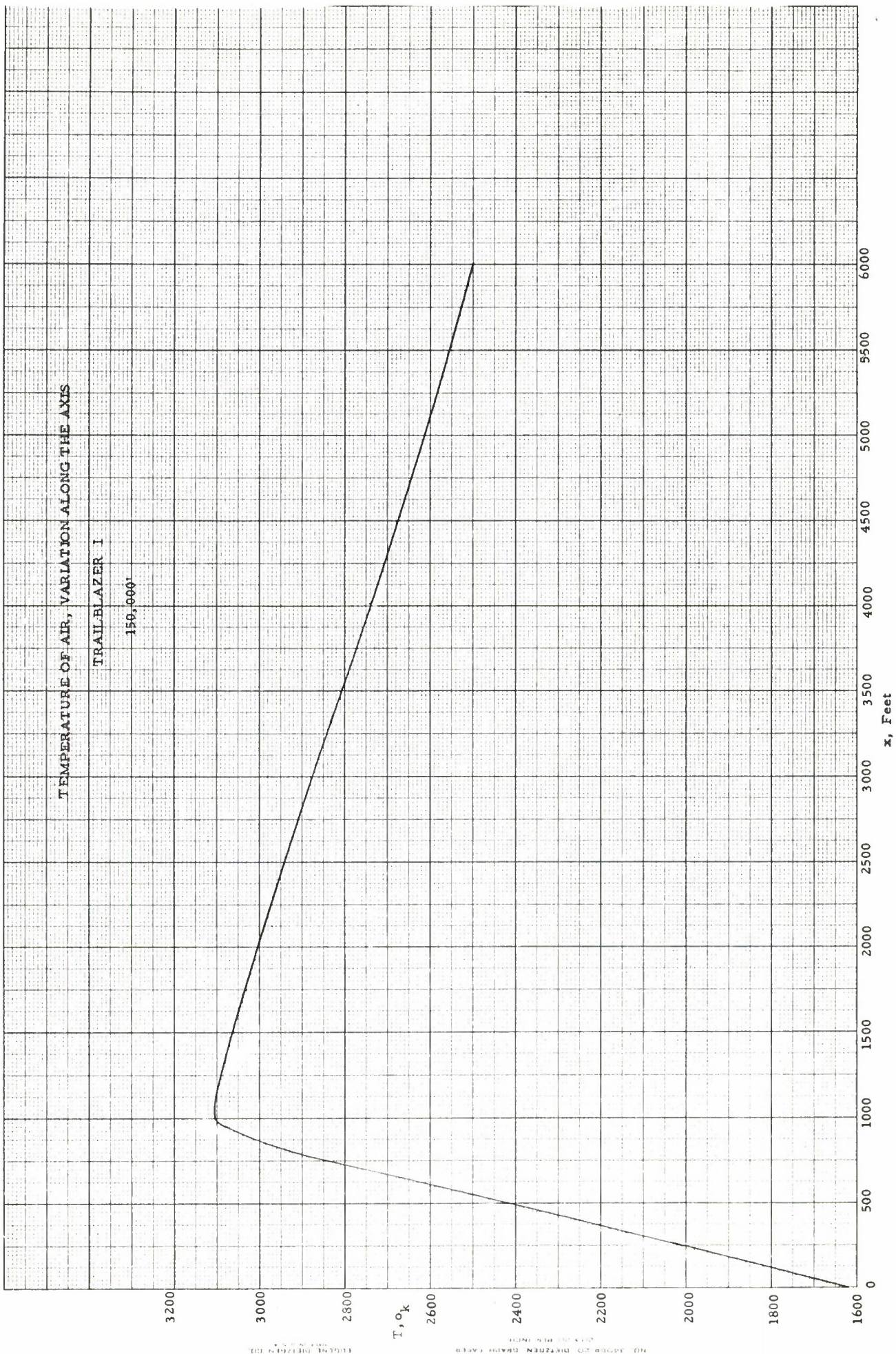


DENSITY OF AIR, VARIATION ALONG THE AXIS
TRAILBLAZER I
150,000' (continued)





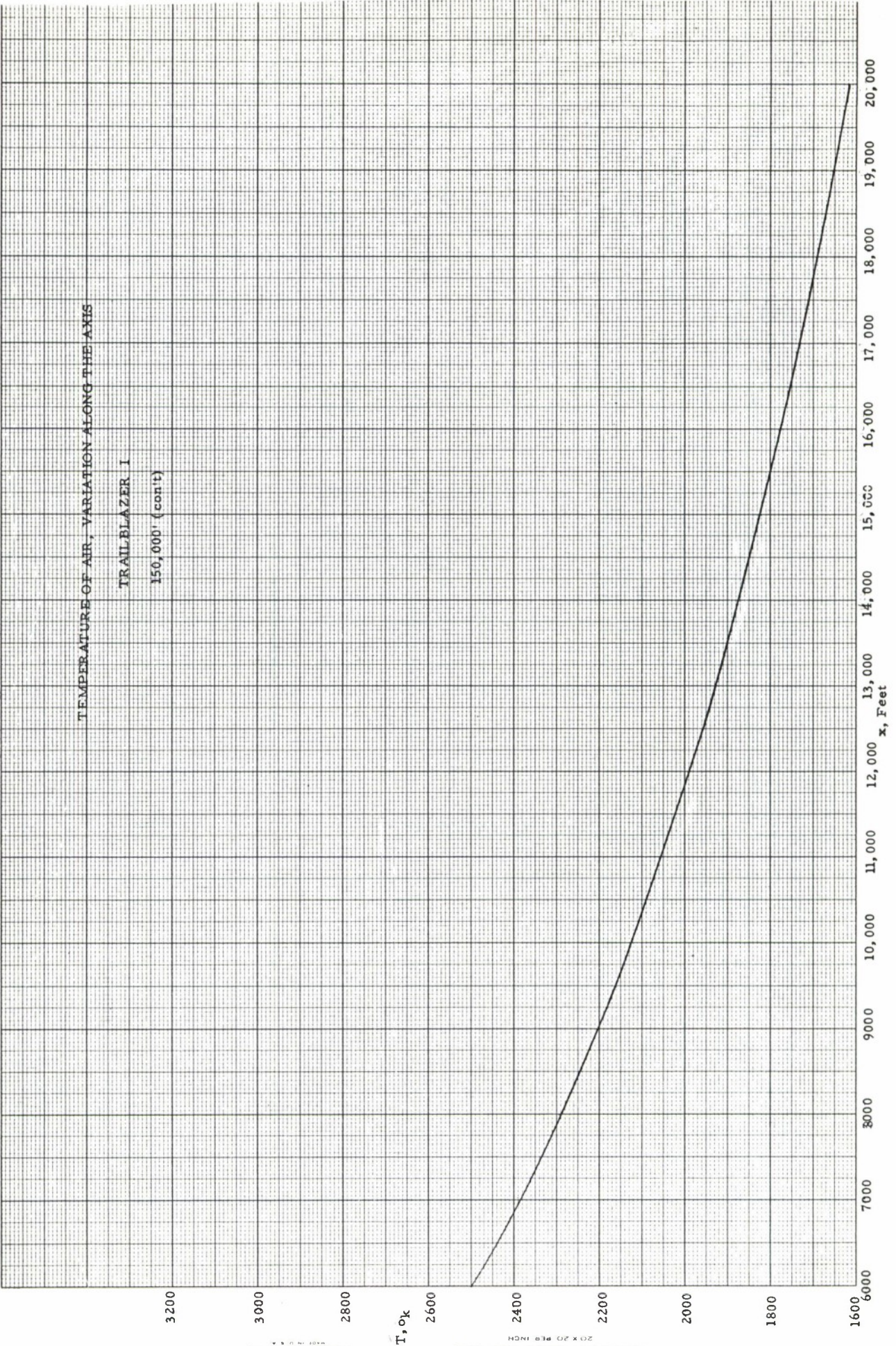




NO. 4000-20 DIEZEL ENGINE FAIR
EUGENE BERTON CO.
DALLAS, TEXAS

TEMPERATURE OF AIR, VARIATION ALONG THE AXIS

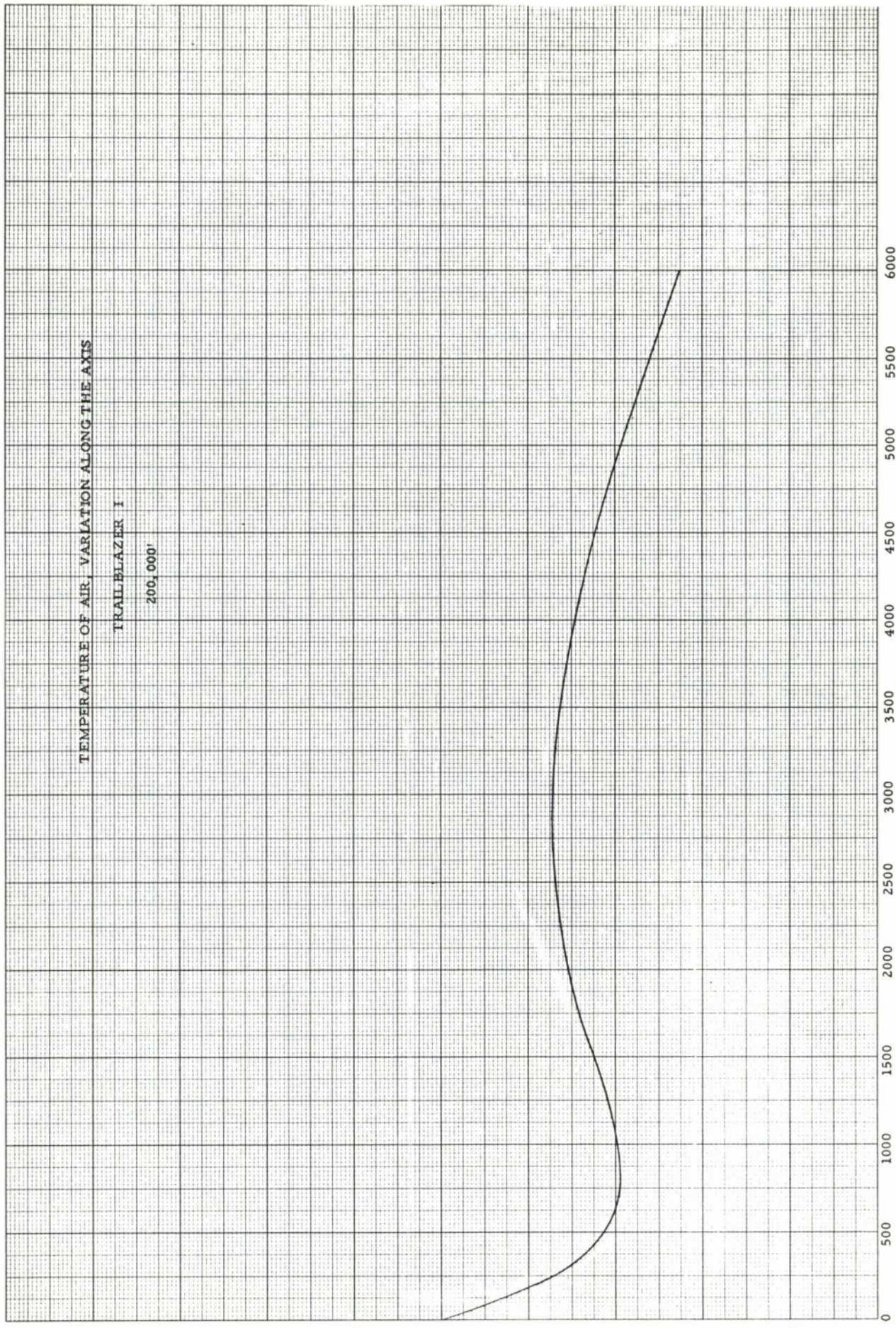
TRAILBLAZER I
150,000' (cont)



TEMPERATURE OF AIR, VARIATION ALONG THE AXIS

TRAILBLAZER I

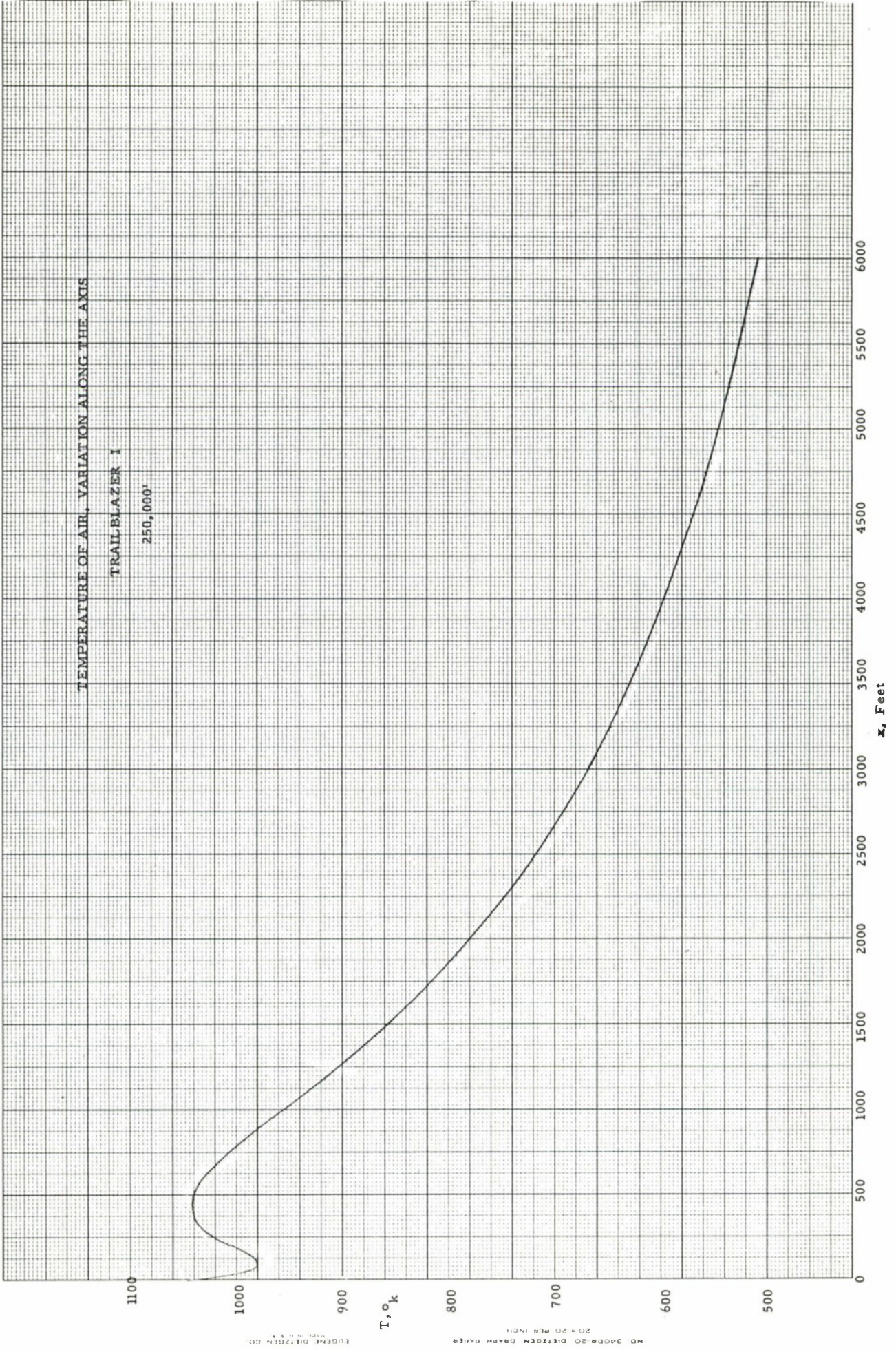
200,000'



TEMPERATURE OF AIR, VARIATION ALONG THE AXIS

TRAILBLAZER I

250,000'



VELOCITY DECAY ALONG AXIS

TRAILBLAZER I

150,000'

$u_0 = 18,900 \text{ ft/sec}$

.90

.80

.70

.60

x, Feet

6000

5500

5000

4500

4000

3500

3000

2500

2000

1500

1000

500

0

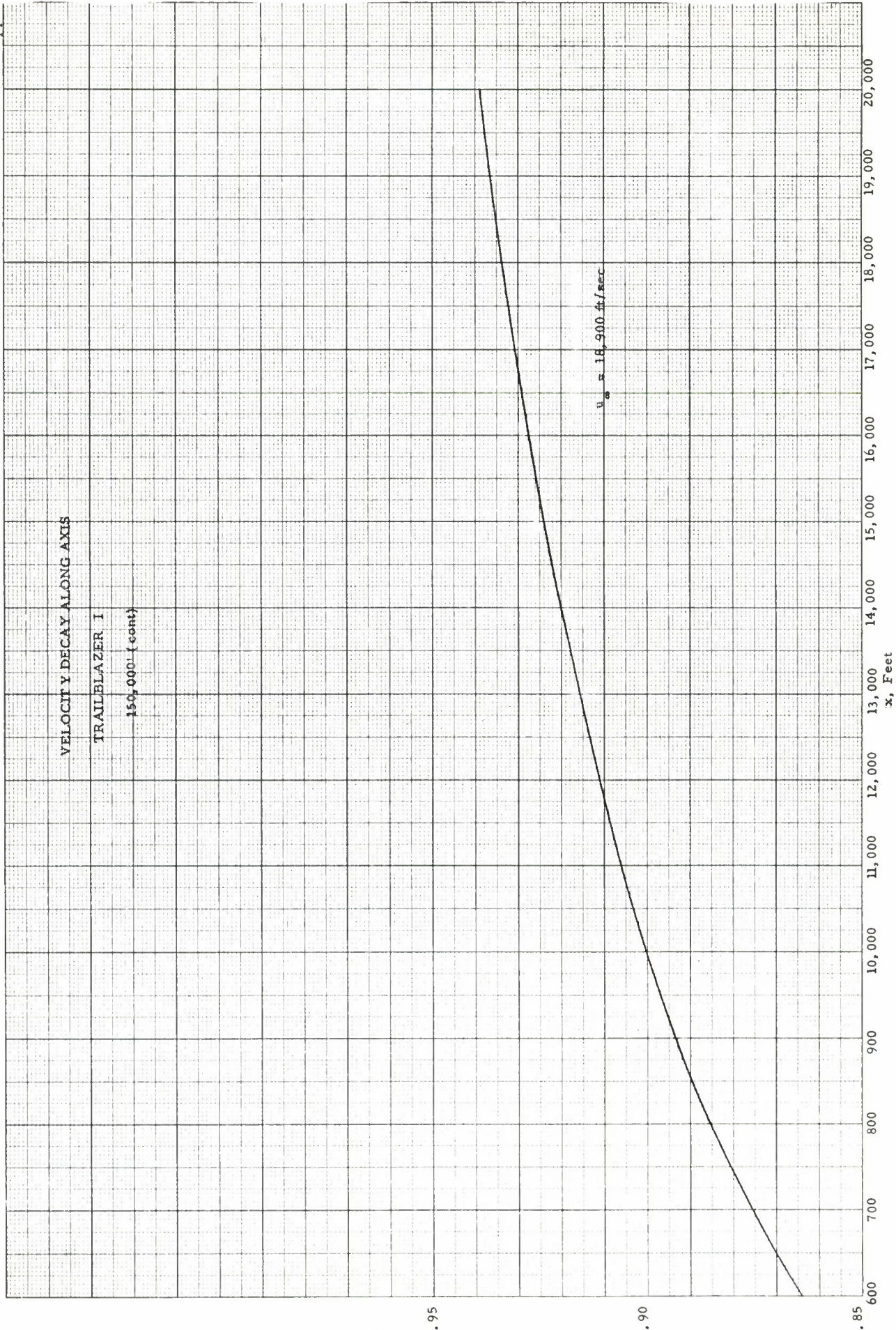
Fig 1

VELOCITY Y DECAY ALONG AXIS

TRAILBLAZER I

150,000' (cont)

$u_{\infty} = 18,900 \text{ ft/sec}$



VELOCITY DECAY ALONG AXIS
TRAILBLAZER I
200,000'

1.0

u/u_0

.95

.90

.85

$u_0 = 20,200$ ft/sec

x, Feet

6000

5500

5000

4500

4000

3500

3000

2500

2000

1500

1000

500

0

VELOCITY DECAY ALONG AXIS

TRAILBLAZER I

250,000'

$$u_m = 20,400 \text{ ft/sec}$$

1.0

$\frac{u}{u_m}$

.95

.90

.85

x, Feet

6000

5500

5000

4500

4,000

3500

3000

2500

2000

1500

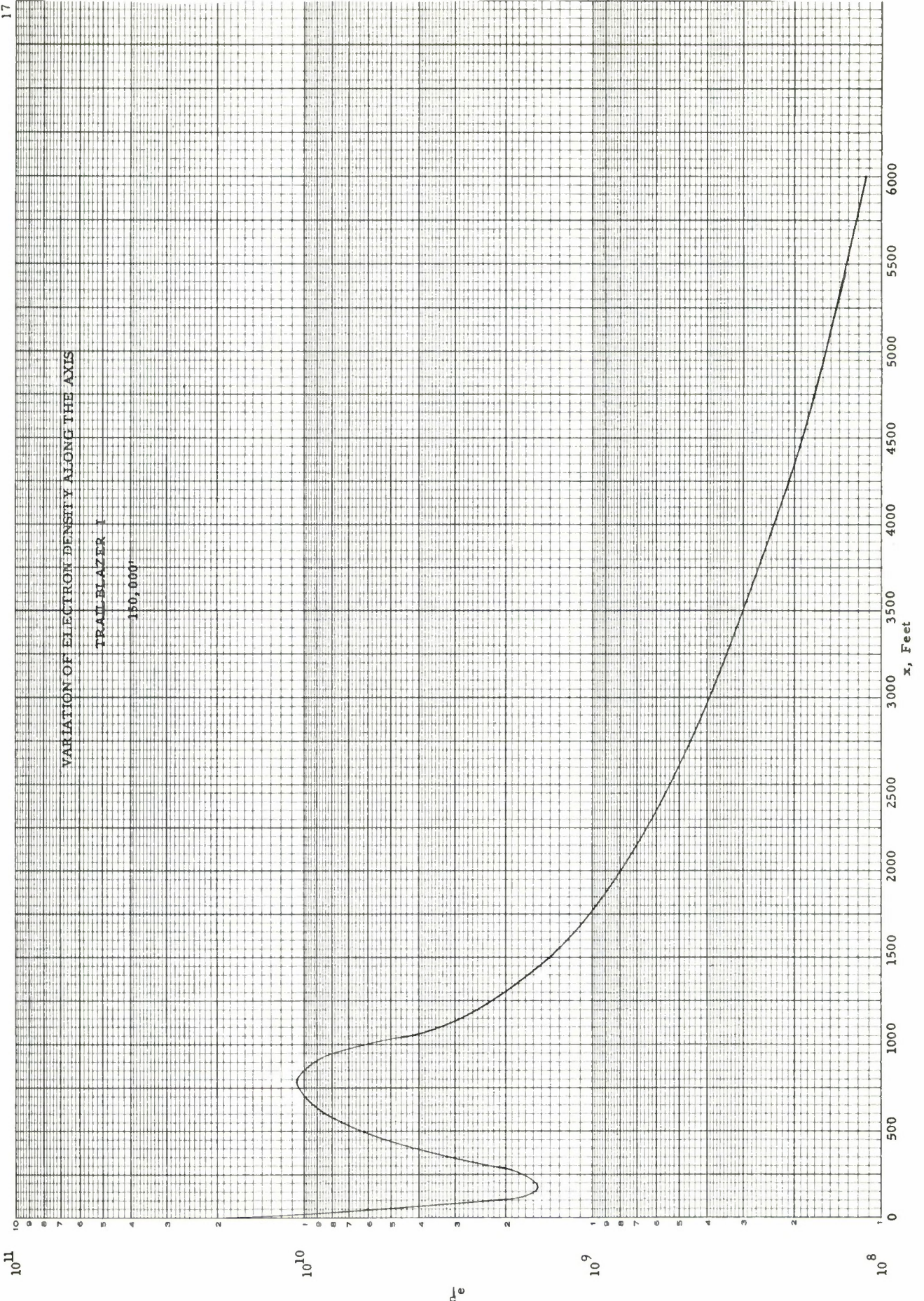
1000

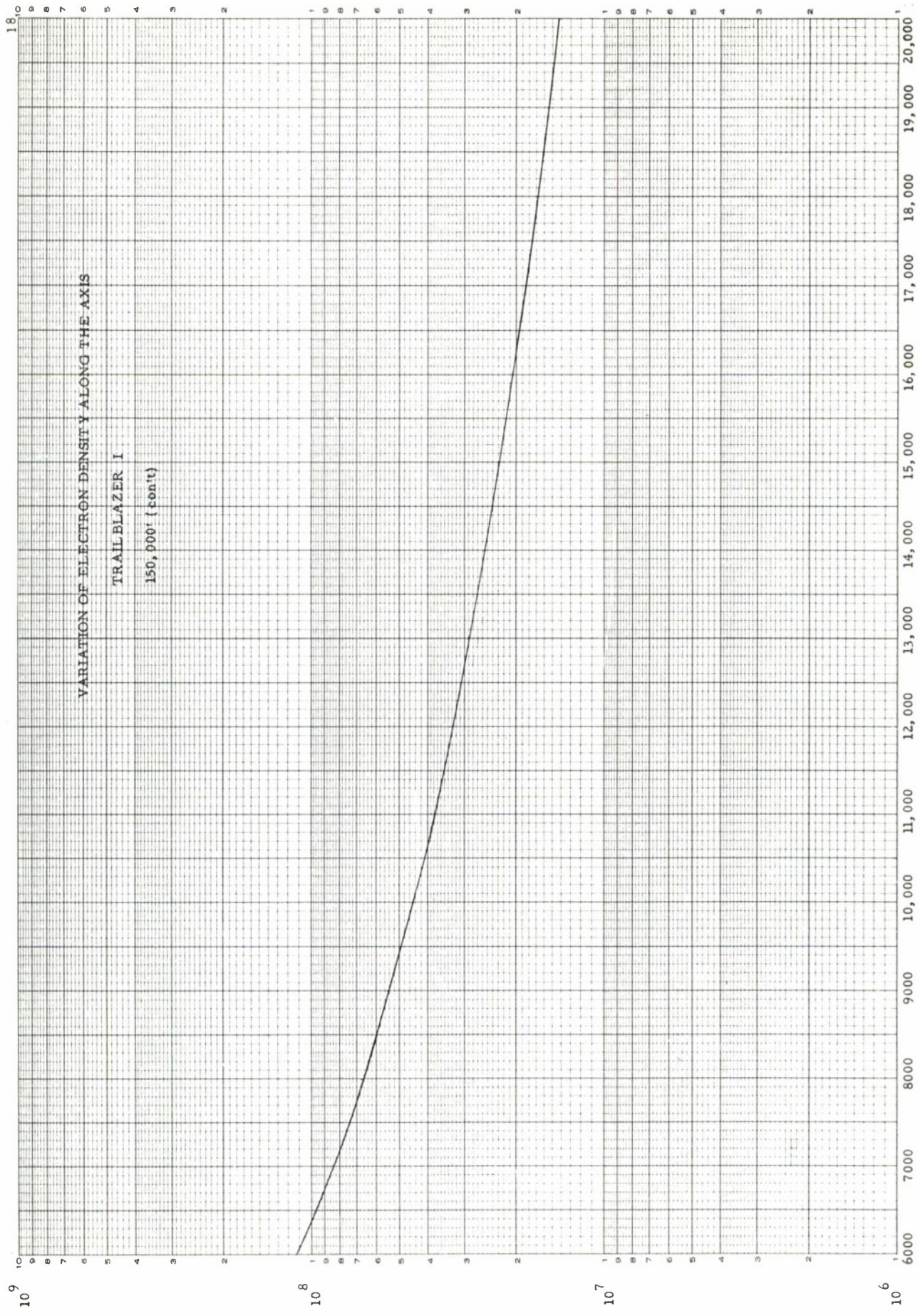
500

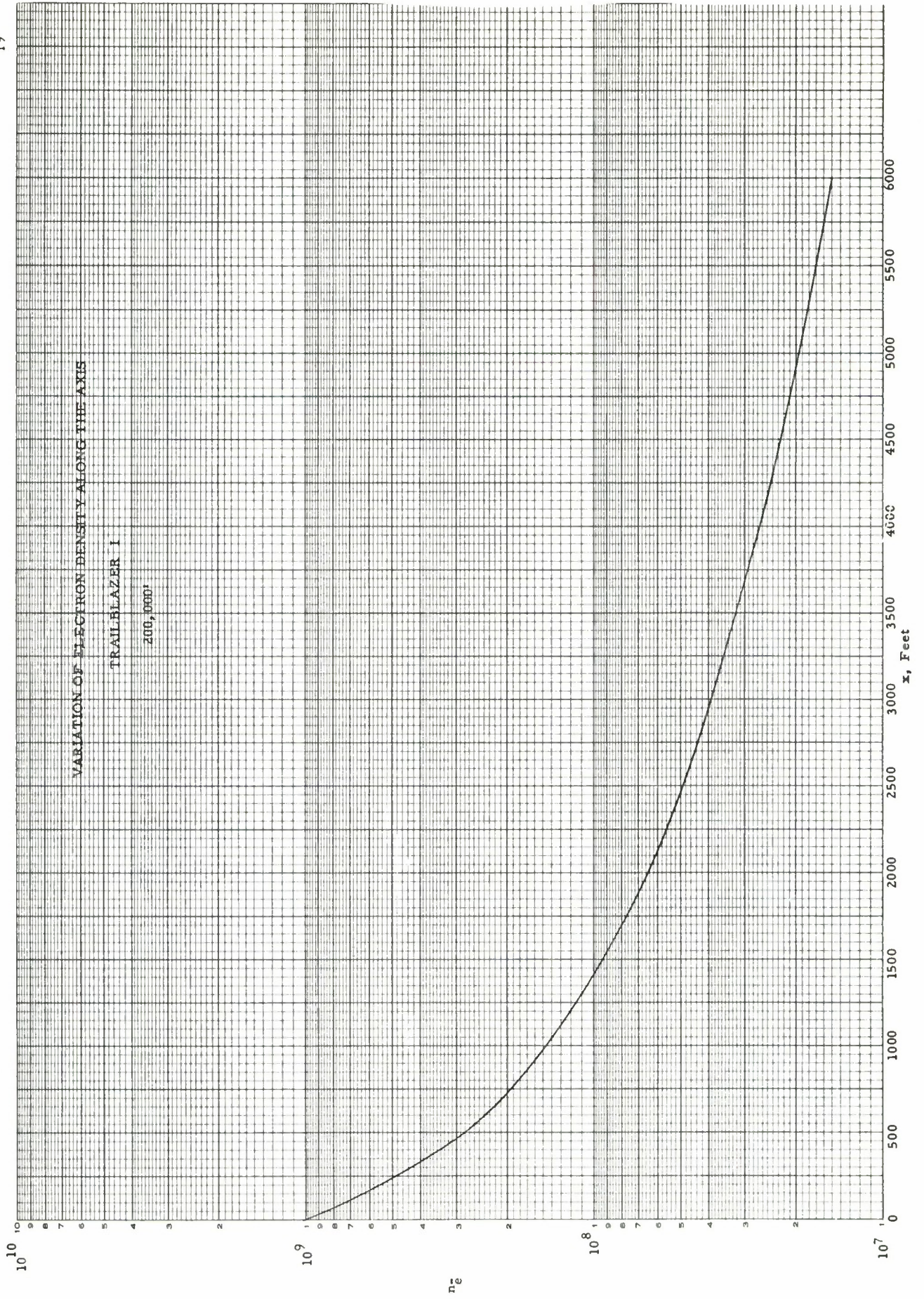
0

VARIATION OF ELECTRON DENSITY ALONG THE AXIS
TRAIL BLAZER I

150,000'







VARIATION OF ELECTRON DENSITY ALONG THE AXIS

TRAIL BLAZER I

250,000'

